12/6-14-95 (1)

PNL-10511
UC-2030

Laboratory Studies of Gas Generation and Potential for Tank Wall Corrosion During Blending of High-Level Wastes at the West Valley Demonstration Project

W.J. Gray
R.E. Westerman

May 1995

Prepared for the U.S. Department of Energy
under Contract DE-AC06-76RLO 1830

Pacific Northwest Laboratory
Richland, Washington 99352

PNL-10511

Battelle

DISCLAIMER

PACIFIC NORTHWEST LABORATORY
operated by
BATTELLE MEMORIAL INSTITUTE
for the
UNITED STATES DEPARTMENT OF ENERGY
under Contract DE-AC06-76RLO 1830

Printed in the United States of America

Available to DOE and DOE contractors from the Office of Scientific and Technical Information, P.O. Box 62, Oak Ridge, TN 37831; prices available from (615) 576-8401. FTS 626-8401.

Available to the public from the National Technical Information Service, U.S. Department of Commerce, 5285 Port Royal Rd., Springfield, VA 22161.


The contents of this report were printed on recycled paper

PNL-10511
UC-2030

Laboratory Studies of Gas Generation and Potential for Tank Wall Corrosion During Blending of High-Level Wastes at the West Valley Demonstration Project

W.J. Gray
R.E. Westerman

May 1995

Prepared for
the U.S. Department of Energy
under Contract DE-AC06-76RLO 1830

Pacific Northwest Laboratory
Richland, Washington 99352

Abstract

Laboratory experiments were conducted to simulate the transfer of acidic THOREX waste from Tank 8D-4 into the alkaline PUREX waste in Tank 8D-2 at West Valley. The purpose of the experiments was to explore means of minimizing the production of nitric oxide (NO) gas during mixing of the two wastes and to assess the potential for the gas to further react in the vapor space possibly leading to enhanced corrosion of the tank walls. Forty one THOREX/PUREX mixing tests were conducted to explore the effects of stirring rate, pH, THOREX addition rate, THOREX or PUREX dilution, and temperature. The two most important criteria for minimizing NO production were to maintain some degree of agitation and the keep the pH in the PUREX high, preferably >12.

Steel corrosion tests were performed in the presence of low partial pressures of NO_2 and liquid water or water vapor. The NO_2 (from oxidation of NO in the vapor space) concentrations were representative of those derived from the THOREX/PUREX mixing tests. It was concluded that no significant corrosion of the tank walls would be expected under the anticipated THOREX/PUREX mixing conditions if the exposure was short (<100 days).

Summary

Radioactive wastes from reprocessing of spent nuclear fuel are stored at West Valley, New York in large underground tanks. Most of the spent fuel was treated with the PUREX process, neutralized, and stored in the steel 8D-2 waste tank. A single core of mixed thorium and uranium fuel was also processed, and the waste (called THOREX) was stored as a nitric acid solution in Tank 8D-4. Before the wastes are vitrified, there are plans to transfer acidic THOREX waste from Tank 8D-4 into the alkaline PUREX waste in Tank 8D-2. During mixing, there may be some reaction between acid in the THOREX and NO_2^- in the PUREX that can result in the generation of nitric oxide (NO) gas. Once NO forms and escapes to the vapor space in Tank 8D-2, it will be quickly oxidized by air[(a)] to NO_2, which can react with the water film that coats the tank walls above the PUREX slurry and form a dilute HNO_3 solution. If the pH in the water film drops to low enough values, increased corrosion of the carbon steel tank walls could occur. To assess the magnitude of this potential problem and explore means of minimizing the production of NO gas, the Pacific Northwest Laboratory was commissioned to conduct relevant laboratory experiments.

THOREX/PUREX mixing experiments were conducted in two phases. Most of the testing was done during FY 1993 and 1994, but a few supplementary tests were conducted during FY 1995. All of the corrosion-related work was done during FY 1993 and 1994.

During the early THOREX/PUREX mixing experiments, small amounts of NO gas (plus CO_2 gas from reaction of the acidic THOREX with carbonate in the PUREX) were measured during laboratory scale tests in which simulated THOREX was added to simulated PUREX. The scale of most of the tests was 1.5 L of PUREX to which 15 to 30 mL of THOREX (same approximate ratio as the wastes in the two tanks) were typically added. A few tests were conducted with simulated waste volumes that were 10 times larger.

Because the CO_2 was of no consequence, only the generation rate and total amount of NO gas were measured during all but the first few tests. Various test parameters were changed during 41 tests to explore prospects for minimizing the amount of NO production. Test parameters that received primary emphasis included stirring rate, THOREX addition rate, incremental addition of THOREX and NaOH to maintain a high pH, effect of THOREX or PUREX dilution, and temperature. As a result of the testing, it was found that the two most important criteria for minimizing NO production were to maintain some degree of agitation and to keep the pH in the PUREX as high as possible (preferably >12) through either periodic or simultaneous addition of NaOH. These and other conclusions based on the early THOREX/PUREX mixing tests described in Section 2.0 are further described below:

- Different stirring rates had little effect on the total amount of NO that was generated, but when the stirring was stopped, the amount of NO increased by a factor of 20 to 50.

(a) The oxidation of NO to NO_2 could be practically eliminated if air were removed from Tank 8D-2 by purging with N_2 gas during the THOREX/PUREX mixing. However, this option was not explored during the course of this work.

- The nature of the testing did not allow a simple correlation to be made between the pH of the PUREX and the generation rate of NO although, in general, less NO was produced when high pH was maintained during mixing. For example, in one test where the pH was maintained at 13.3 by simultaneous addition of NaOH, the amount of NO that was generated was four times less than in other tests where the pH decreased to 10 or 11 during the THOREX addition, with all other parameters for the two test conditions being the same.

- The total amount of NO that was generated was approximately proportional to the NO_2^- concentration in the PUREX; ~0.1% of the NO_2^- was converted to NO in tests at 45°C where stirring was maintained. Thus, reducing the NO_2^- concentration in the PUREX by additional washing would reduce the amount of NO produced by a corresponding proportion.

- The activation energy for NO production between 22°C and 45°C was determined to be 12.1 kcal/mol; between 45°C and 65°C it was 5.4 kcal/mol. The nonlinearity indicates that two or more processes with different temperature dependencies were involved.

- In tests where THOREX was added to a PUREX recirculation loop, the amount of NO that was produced was very dependent on the relative flow rate in the loop compared with the THOREX addition rate. With a high ratio of loop-flow-rate to THOREX-addition rate, the amount of NO was nearly 5 times smaller than when THOREX was added directly to the reaction vessel. But with a low ratio of loop-flow-rate to THOREX-addition rate, the amount of NO was 5 times larger than when THOREX was added directly to the reaction vessel. These results are consistent with the observation that less NO was generated when the pH was kept high, i.e., a high ratio of loop-flow-rate to THOREX-addition rate kept the pH high in the mixing region of the loop.

- In the event of an accidental reversal of flow where PUREX would flow out of Tank 8D-2 into the THOREX in Tank 8D-4, tests conducted here indicated that the generation rate and total amount of NO could be much higher (perhaps a factor of 10 although a direct comparison cannot be made) than in the normal flow direction, THOREX into Tank 8D-2.

- In tests where THOREX was added directly to the PUREX and stirring was maintained, the total amount of NO that was generated was nearly independent of THOREX addition rate.

- When the acidity of the THOREX was increased ~5 times, the amount of NO increased ~50%. However, no effect on the amount of NO was observed when all constituents of the THOREX, including acidity, were diluted to 50% of their original concentrations.

- Tests conducted with 10-times larger waste volumes produced 6 to 12 times more NO gas. Thus, over this very limited volume range, these data indicate that the amount of NO that is generated may scale in direct proportion to the volume of waste involved in the mixing. It is not known whether this scaling factor can be extrapolated to the size of the actual tanks (one million times larger than the laboratory test volumes) at West Valley.

Supplemental THOREX/PUREX mixing tests described in Section 3.0 were designed to measure the effect on NO gas production caused by increasing the NO_2^- concentrations in the PUREX for the purpose of maintaining pitting corrosion control in Tank 8D-2. Sodium hydroxide was also added to the PUREX during these tests to keep the pH high during the initial THOREX addition. Because the

pH was kept higher than in most of the earlier testing described in Section 2.0, the increased NO_2^- concentrations in the present tests resulted in only modest increases in the amounts of NO gas that were observed.

In addition to the THOREX/PUREX mixing experiments, laboratory experiments were also conducted to measure the pH of water exposed to the low concentrations of NO_2 that were estimated for the Tank 8D-2 vapor space based on results from the THOREX/PUREX mixing tests. In addition, actual steel corrosion tests were performed in the presence of low partial pressures of NO_2 and liquid water or water vapor. Based on the results of these tests, it was concluded that no significant corrosion of the tank walls would be expected under the anticipated THOREX/PUREX mixing conditions if the exposure was short (< 100 days), but the steady state pH values could potentially be low enough to cause concern over long exposure periods.

An alternative to direct addition of THOREX to Tank 8D-2 would be to first neutralize the THOREX with NaOH before transferring it to Tank 8D-2. A few simple tests indicated that this could be done with no measurable gas generated during neutralization of the THOREX and subsequent mixing with the PUREX. Under these conditions, the possibility of enhanced corrosion of the tank walls would be moot. Possible engineering problems that could be encountered with this scenario were not addressed.

Acknowledgments

The authors acknowledge the many technical discussions with S.M. Barnes and M.A. Schiffhauer of West Valley Nuclear Services plus the following Pacific Northwest Laboratory personnel for setting up and running the test apparatus, for supplying some of the laboratory equipment, and for providing some analysis of the corrosion data: R.D. Bell, M.R. Elmore, S.M. Faber, W.M. Gerry, E.V. Morrey, M.R. Powell, G.L. Whiting, and R.E. Williford.

Contents

Tables

1.0 Introduction

The Western New York Nuclear Service Center at West Valley, New York was operated by Nuclear Fuel Services, Inc. from 1968 through 1972 to recover fissionable isotopes from spent nuclear reactor fuel. The waste materials from these operations were stored on the site in large underground tanks. Nearly all of the spent fuel was treated with the PUREX process, neutralized, and stored in the steel 8D-2 waste tank. A single core of mixed thorium and uranium fuel was also processed, and the waste (called THOREX) was stored as a nitric acid solution in Tank 8D-4.

Before the stored radioactive wastes are vitrified, plans are being made to transfer acidic THOREX waste (~45,000 L) from Tank 8D-4 into the alkaline PUREX waste (~2,100,000 L) in Tank 8D-2. Some options for the THOREX neutralization and transfer process were initially explored by Bray and Wise (1986). The work described in this report was performed to further explore some of those options.

Because the PUREX contains nitrite, the option of direct THOREX addition to Tank 8D-2 includes the potential for nitric oxide (NO) gas to be formed and released into the vapor space during THOREX addition. NO can be oxidized by air in the tank vapor space to form NO_2, which can diffuse into and react with the water film that coats the tank walls above the slurry. This process will ultimately lead to the formation of a dilute solution of HNO_3 in the water film, possibly leading to corrosion of the carbon steel.

West Valley Nuclear Services (WVNS) has been developing and gathering data to determine whether the THOREX addition procedure would result in significant corrosion of Tank 8D-2. The Pacific Northwest Laboratory (PNL) is supporting this effort by performing laboratory studies through the West Valley Support Program (WVSP). The PNL support activities were directed to two areas:

- Perform laboratory- and bench-scale experiments to quantify the NO_X gas release under a variety of test conditions that included variations in stirring rate, THOREX addition rate, incremental addition of THOREX and NaOH to maintain a high pH, effect of THOREX or PUREX dilution, and temperature.

- Perform laboratory experiments to determine the buildup of H^+ (decrease in pH) in water exposed to different concentrations of NO gas mixed with air and to measure the corrosion rate of carbon steel coupons suspended in the water or vapor.

Most of the THOREX/PUREX mixing tests were conducted during FY 1993 and FY 1994 as described in Section 2.0. Supplemental THOREX/PUREX mixing tests were conducted during FY 1995 as described in Section 3.0. The corrosion work, which was conducted during FY 1994, is reported in Section 4.0.

Application of the results described in this report to the actual full-scale case of transferring the THOREX from Tank 8D-4 into the PUREX in Tank 8D-2 would entail important uncertainties. Probably the greatest uncertainty is in extrapolation of the laboratory- and bench-scale results to the full scale tanks where the waste volumes are one million times larger than in the laboratory-scale tests.

A possible scaling factor is suggested as part of this report, but much larger-scale tests would be required to determine the validity of such a large extrapolation.

Another uncertainty involves the use of simulated wastes in the laboratory tests. Although the simulants were based on analyses of the actual wastes, a few mixing tests with the actual THOREX and PUREX wastes should be considered to verify the test results reported here.

This work was performed to quality assurance impact level three requirements as defined in PNL's quality assurance manual. This level ensures that the traceability, quality, and reproducibility of the results can be verified. However, if this work is the primary basis for making major project decisions, this work should be upgraded to impact level two standards. This upgrade may require additional documentation and laboratory tests.

2.0 Early THOREX/PUREX Mixing Tests

The mechanism for HNO_3 production in the condensed film on the tank wall is described by Equations (2.1) to (2.4).

$$H^+ \text{ (THOREX)} + NO_3^- + 2NO(g) \rightleftarrows HNO_2 \quad (2.1)$$

$$3HNO_2(aq) \rightleftarrows H^+ + NO_2^- + 2NO(g) + H_2O \quad (2.2)$$

$$2NO(g) + O_2(air) \rightleftarrows 2NO_2(g) \quad (2.3)$$

$$3NO_2(g) + H_2O \rightleftarrows 2HNO_3(aq) + NO(g) \quad (2.4)$$

At the point where the THOREX enters the PUREX in Tank 8D-2, the local pH is low enough to allow Equation (2.1) to proceed to the right even though in a hypothetical, instantly homogenized system, the high pH would force Equation (2.1) to the left via acid/base neutralization. Nitrous acid (HNO_2) formed by Equation (2.1) is a weak acid (dissociation constant 6.0×10^{-4} at 30°C) that rather slowly (seconds to minutes) decomposes according to Equation (2.2) (Yost and Russell 1944). Equation (2.2) must also take place in the region of localized low pH because, otherwise, the reverse of Equation (2.1) would again prevail. Once NO gas is formed and enters the vapor space, it can be oxidized by air and combine with moisture to form HNO_3 according to Equations (2.3) and (2.4).

This section describes laboratory studies performed to measure the amount of NO gas formed during THOREX neutralization and mixing with PUREX, and to investigate methods for minimizing the amount of NO.

2.1 Experimental Description

Most of the THOREX/PUREX mixing experiments were conducted with equipment similar to that shown schematically in Appendix C, Figure C.1 and described in Section 2.1.1. Simulated THOREX and PUREX wastes were prepared for these tests as described in Section 2.1.2. The simulated wastes were completely nonradioactive except for the natural ^{232}Th used in making the THOREX. System calibrations and performance checks are described in Section 2.1.3.

A few other simple laboratory mixing experiments were conducted that did not involve qualitative gas analysis equipment. The nature of these experiments are described along with the results in Section 2.2.3.

2.1.1 Apparatus

Temperature of the 2-L glass reaction vessel (Appendix C, Figure C.1) was controlled by a heating mantle and automatic temperature controller, which used a thermocouple immersed in the liquid in the vessel as a temperature sensor. In all tests unless otherwise noted, 1.5 L of PUREX was placed in the vessel to start the test.

All tests were conducted as follows. After calibration of the gas chromatograph (GC) and NO_X analyzer (see Section 2.1.3), the Ar carrier gas flow was established through the system at a rate measured by the calibrated mass flow controller (MFC). Argon was used as a carrier gas rather than air, which would simulate the conditions in Tank 8D-2, because it was desired to discover the gases formed by the reaction of THOREX with PUREX prior to oxidation by air. After allowing a few minutes to ensure that the initial concentrations of NO, CO_2, etc. in the Ar carrier gas were at or near zero, the THOREX pump was turned on and allowed to run until a predetermined amount of THOREX[(a)] had been added to the reaction vessel. Data collection normally continued until the concentrations of NO and CO_2, the only gases detected, returned to near zero. At the end of each test, the gas concentrations recorded during the test were multiplied by the Ar carrier gas flow rate to yield the generation rates of NO and CO_2. Integration of the generation rates over time gave the total amounts generated during the tests.

The system operated at a very slightly elevated pressure (< 1 psi above atmospheric). The metal bellows pump was used to raise the pressure in the off-gas line to the 5 psig required by the NO_X analyzer.

Separate computers served as both controllers and data loggers for the GC and NO_X analyzer, respectively. The computer used to control the GC also recorded pH and temperature. Gases analyzed by the GC, and their respective detection limits, are listed in Table 2.1. The NO_X analyzer was capable of detecting both NO and NO_2 at concentrations as low as ~1 part per million (ppm). Temperature, pH, and GC data were recorded approximately once every 1.5 min. Data from the NO_X analyzer were recorded once per minute; total NO_X concentrations were recorded 9 min. out of 10 and NO concentrations were recorded every 10th min. Interpretation of the NO_X data are described below.

The NO_X analyzer operates either in the NO-analysis mode or the NO_X mode, but not simultaneously. It measures NO concentrations directly, but when switched to the NO_X analysis mode, the NO_X analyzer first oxidizes all of the incoming NO_X to NO_2. Therefore, the difference between NO and NO_X represents the concentration of NO_2 originally present in the incoming gas. If the measured NO and NO_X concentrations are the same, then no NO_2 is present in the incoming gas; 100% of the incoming NO_X is NO. The clearest example of this is shown in Figure C.10 (Appendix C). The NO_X curve in that figure increases nearly uniformly up to a maximum and then decreases slowly. The NO curve increases, and then decreases, in a step-wise fashion because the NO data were recorded only once every 10 min.. However, each time the NO data were recorded, a match with the NO_X data was observed. This means that 100% of the incoming NO_X gas was NO. Similar results were observed

(a) The THOREX supply reservoir rested on a balance, and the amount added to the reaction vessel was determined by weight change.

Table 2.1. Detection Limits for Gas Chromatograph[a]

Gas	Detection Limit (ppm)
CO_2	5
CO	200
N_2O	5
H_2	10
N_2	100
O_2	100

(a) Calibrations were performed only for the first four gases listed. Even though no calibrations were performed for N_2 and O_2, the listed detection limits are expected to be approximately correct.

for all of the tests conducted in this study. Other examples are shown in Figures C.6 and C.8 (Appendix C), but they are less clear because of the erratic nature of the gas evolution in those tests. Therefore, the NO_X curves in all of the tests can be labelled "NO," and that was done in all cases except the illustrations in Figures C.6, C.8, and C.10 (Appendix C).

After the first five runs (Figures C.6 to C.10 in Appendix C and Tables 2.6 and 2.7 in Section 2.2.1), use of the GC and associated computer was discontinued because only NO and CO_2 gases were detected, and the latter was of little interest. As a result, the remaining tests did not have continuous recordings of pH and temperature. Rather, the temperature was recorded in a laboratory record book (LRB) at the beginning and two or three times during each test. The pH was measured for samples of solution (or slurry) from the reaction vessel before and after each test. In addition, a different NO_X analyzer was used that recorded data every 15 seconds instead of at one-minute intervals.

Besides the lab-scale tests conducted in the 2-L glass vessel, three large-scale tests were performed at room temperature using a 17-L polyethylene vessel. Otherwise, the setup for the large-scale tests was the same as shown schematically in Figure C.1 (Appendix C) minus the GC and the heating mantle for the reaction vessel.

2.1.2 Test Solutions/Slurries

Different batches of both THOREX and PUREX were used during the course of this work. Preparation methods and compositions are given here. In Section 2.2, the particular batches used in each test are identified along with any additional details that may be pertinent.

THOREX

The method used to prepare the THOREX was described by Bray and Wise (Appendix B, 1986). This recipe assumed the volume of THOREX in Tank 8D-4 was 45,000 L. To ensure that all components remained dissolved in solution at 25°C, Bray and Wise determined that this THOREX should be diluted to a volume representative of 59,000 L. Therefore, most of the early tests were conducted with the "diluted" THOREX.

The first batch of THOREX had been prepared for use in a related project more than a year earlier. Its composition was assumed to be represented by the nominal values listed in Table 2.2, and it was put into use at the same time that a representative sample was being analyzed. The results of the analyses given in Table 2.2 show that the actual concentrations of the more prominent components (e.g., Th and NO_3) were only about 60% of the nominal values.

Table 2.2. THOREX Composition (First Batch)

Component	Nominal[a] (mol/L)	Nominal[a] (g/L)	Nominal Diluted[b] (g/L)	Analyzed Diluted (g/L)
Th	1.48	343	262	155
Fe	0.88	49	37	27
Al	0.49	13	10	3.9
Cr	0.20	10.4	7.9	6.7
B	0.19	2.1	1.6	0.97
Ni	0.11	6.5	4.9	4.9
Na	0.18	4.2	3.2	9.3
K	0.062	2.4	1.9	ND
Mn	0.015	0.82	0.63	ND
Ba	0.0029	0.40	0.30	0.44
NO_3	11.9	739	564	362
SO_4	0.0032	3.1	2.4	1.3
Cl	0.0021	0.74	0.57	0.91
H^+	0.84		0.64 M	NA

(a) Assumes THOREX volume of 45,000 L.
(b) Assumes THOREX diluted to 59,000 L.
ND not detected.
NA not analyzed.

Table 2.3 shows that the analyzed concentrations of the major constituents in the second batch of THOREX were within the normally expected precision and bias (± 15%) of the nominal values. Therefore, the nominal values were used to calculate the amounts of THOREX to add to the PUREX in each test. The third batch of THOREX was prepared in the same manner as the second batch and was assumed to contain the nominal concentrations listed in Table 2.3, but it was not analyzed.

PUREX

At the time these tests were conducted, it was assumed that the PUREX sludge in Tank 8D-2 would be washed three times to remove sodium, cesium, nitrite, and other soluble constituents before adding the THOREX. To mimic this process, the simulated PUREX prepared for this study was also washed. The nominal composition of the original, unwashed PUREX, which was prepared according to a recipe provided by Bray and Wise (Appendix C, 1986), is listed in Table 2.4. Most of the Fe, Cr, and several other constituents precipitate as hydroxides in the high pH solution. Therefore, the PUREX was washed by allowing the solids in the original slurry to settle for a few days, which resulted in a settled solids volume equal to about one third of the total volume. Then the supernate was decanted and an equal volume of deionized water was returned. After thorough stirring, the solids were allowed to settle a second time followed by decanting the supernate and returning an equal volume of deionized water. At this point, the PUREX slurry was split into two portions. Each portion of the second-wash PUREX was washed a third time in the same manner described for the first and second washes. The total volume of the third-wash PUREX batches (solids plus supernate) was the same as the original volume of the unwashed PUREX simulant.

Table 2.3. THOREX Composition (Second Batch)

Component	Nominal[(a)]		Analyzed
	(mol/L)	(g/L)	(g/L)
Th	1.48	343	303
Fe	0.88	49	55
Al	0.49	13	12
Cr	0.20	10.4	11.2
B	0.19	2.1	2.2
Ni	0.11	6.5	7.2
Na	0.18	4.2	6.4
K	0.062	2.4	3.4
Mn	0.015	0.82	1.5
Ba	0.0029	0.40	0.52
NO_3	11.9	739	695
SO_4	0.0032	3.1	
Cl	0.0021	0.74	
H^+	0.84	NA	NA

(a) Assumes THOREX volume of 45,000 L.
ND not detected.
NA not analyzed.

Table 2.4. PUREX Sludge/Supernate Composition (g/L)[a]

Component	Nominal[b] Original	Analyzed[c] R3A	Analyzed[d] R3B	Analyzed[e] R4
Na	152	27.5[f]	21.3	10.2
Fe	17.1			
K	7.41	0.81	0.79	0.39
P	3.1	0.173		0.071
Cr	1.40			
Sm	1.2			
Mn	0.66			
Ni	0.65			
Al	0.46	0.092	0.012	0.006
Zr	0.21			
Cs	0.18			
Mo	0.14			
Ru[g]	0.14			
Ba	0.082			
Sr	0.049			
Rb	0.032			
Rh[g]	0.024			
Pd[g]	0.014			
Ag[g]	0.00031			
NO_3	214	33.1	25.6	12.4
NO_2	96	10.7	10.4	5.0
SO_4	24	3.0	2.7	1.3
CO_3	21	3.5[h]	NA	NA
Cl	1.4		0.24	0.14
F	0.025			
OH		NA	0.11 M	NA

(a) Blanks represent components not detected in the supernate analyses because they had precipitated as hydroxides or were present in very low concentrations initially.
(b) As prepared slurry, before any washing.
(c) First batch of third-wash supernate from original batch of second-wash slurry.
(d) Second batch of third-wash supernate from original batch of second-wash slurry.
(e) First batch of fourth wash supernate from second batch of third-wash slurry.
(f) Includes 7.9 g/L added as NaOH after third wash.
(g) Added after third wash.
(h) Based on inorganic carbon analysis.
NA not analyzed.

To the first batch of third-wash PUREX (designated R3A) was added 18 mL of 19 M NaOH to neutralize the acid and to precipitate, as hydroxides, the metal nitrates in the THOREX, which was to be added later as part of this testing program. In addition, the quantities of noble metals (Ru, Rh, Pd, and Ag) listed in Table 2.4 were added to the PUREX after the third washing. Although the noble metals were not expected to affect the mixing results, the desire was to make the simulated PUREX as representative of the waste in Tank 8D-2 as possible. After stirring and allowing the solids to settle, a sample of the supernate was analyzed and the results are listed under the column heading R3A in Table 2.4.

After preparation of the second batch of third-wash PUREX (designated R3B), the same quantities of noble metals listed in Table 2.4 were added, but no NaOH was added at this time. A supernate sample from this batch of PUREX was analyzed, and the results, including hydroxide, are listed under the column heading R3B in Table 2.4. For each mixing test that used a 1.5-L portion of PUREX batch R3B, an amount of NaOH was added that was calculated to increase the OH^- concentration to 0.2 M. Although the OH^- concentrations after the addition of NaOH were thought to be close to 0.2 M, the measured pH values listed for Tests 6 and 8 to 11 in Table 2.8 (Section 2.2.1) were always a little less than the expected value of 13.3. The discrepancies between expected OH^- concentrations and measured pH values were apparently due to consumption of OH^- by complex interactions with other components in the PUREX.

To determine whether there would be any potential benefit, from a NO generation standpoint, of additional washing of the PUREX, a fourth-wash PUREX was prepared from the second batch of third-wash PUREX, R3B. After decanting the supernate from R3B PUREX and adding deionized water to restore the slurry to its original volume, stirring, and allowing the solids to settle, an analysis of the supernate yielded the results listed under column R4 in Table 2.4. In the one test where this batch of PUREX was used, Test 13 (Table 2.8), an amount of NaOH was added that was calculated to increase the OH^- concentration to 0.2 M.

In addition to the "full compliment" batches of simulated PUREX described above, many of the mixing tests were performed using "simplified" PUREX. These were prepared using only NaOH, $NaNO_2$, and Na_2CO_3, which were the only components in the PUREX that were expected to react with the THOREX. The concentrations of these were chosen to provide 0.2 M OH^- plus the analyzed concentrations of NO_2^- and CO_3^{2-} listed under column R3A in Table 2.4. Thus, solutions were prepared that contained 0.20 M NaOH, 0.23 M $NaNO_2$, and 0.058 M Na_2CO_3. These solutions are represented as "S3" in Tables 2.8 and 2.9 (Sections 2.2.1 and 2.2.2).

A "simplified" PUREX representative of the fourth-wash PUREX was also prepared by assuming that the NO_2^- and CO_3^{2-} concentrations should be equal to one-third the values used for the S3 PUREX given above. In addition, the intent was to maintain the 0.2 M NaOH concentration. Therefore, PUREX batches represented as "S4" in Tables 2.8 to 2.10 (Sections 2.2.1 and 2.2.2) were prepared that contained 0.20 M NaOH, 0.077 M $NaNO_2$, and 0.019 M Na_2CO_3.

2.1.3 Calibrations and Performance Checks

The gas chromatograph and NO_X analyzer were calibrated periodically, as required by the operating procedures, using gas mixtures with known concentrations of the appropriate gases. In addition, system performance checks were conducted from time to time using known concentrations of NO gas.

This was done to ensure that nothing in the gas train of the system (condenser, drierite column, and Tygon tubing) affected the measured NO_X concentrations. In some cases, the NO-containing gas was bubbled through the PUREX in the reaction vessel to determine the response time of NO showing up at the NO_X analyzer as well as the response time for return of the NO concentration to zero.

Initially there was some concern that NO gas could diffuse from the Tygon tubing used between the reaction vessel and NO_X analyzer, or that O_2 could diffuse into the tubing from the room atmosphere and oxidize some of the NO to NO_2. To evaluate this possibility, the NO_X analyzer settings for both NO and NO_2 were set to 94 ppm using a calibration gas containing 94 ppm NO in Ar, i.e., normal calibration procedure. Then the same calibration gas was passed through ~6 ft. of 1/4in. inside diameter (ID) Tygon tubing at ~650 mL/min into the NO_X analyzer. The tubing dimensions and gas flow rates were both representative of that used in the system gas train. Readings of 98 ppm NO and 92 ppm NO_2 were obtained, which is within the expected reproducibility range of the analyzer. Thus, the Tygon tubing had no measurable effect. Figure C.2 (Appendix C) shows the results obtained when this same calibration gas was next injected below the surface of R3B PUREX in the reaction vessel. After a 1-minute delay, the measured NO concentration began to increase rapidly. Within 10 min., the measured concentration of NO approached the expected value of 94 ppm indicating that nothing within the system acted to reduce the NO concentration. Another 1-minute delay was observed after the NO was shut off. Then, the concentration fell rapidly to near zero in about 5 min. with a very small tail extending for another 5 min. or so.

Figure C.3 (Appendix C) shows results from a second performance check that was conducted somewhat differently from the first in three ways. First, simplified PUREX, rather than full-compliment PUREX was used. Thus, there were no solids in the vessel. Second, two gas streams were used because it was thought that, during the first performance check, the continued sparging of Ar through the PUREX may have contributed to the rapid decrease in NO concentration after the flow of NO was stopped. Thus, a calibration gas containing 1100 ppm NO in Ar was injected below the surface of the S4 PUREX at 410 mL/min, and a second stream of Ar entered the vessel above the surface at 1090 mL/min giving a final NO concentration of 301 ppm. Third, the temperature was 45°C, rather than 25°C as it was in the first performance check.

Figure C.3 (Appendix C) shows that the measured NO concentration stabilized at 295 ppm after about 15 min. When the Ar/NO gas was shut off, the Ar flow through the vessel was maintained at 1090 mL/min, but there was no gas bubbling through the PUREX. Again, the NO concentration returned rapidly to zero, at least as rapidly as in the first performance check, even without continued sparging of the PUREX.

Figures C.4 and C.5 (Appendix C) show results from two performance checks conducted with the large-scale system. In both cases, Ar gas containing 301 ppm NO was injected below the surface of the S4 PUREX and, after the NO was turned off, Ar continued to sparge the PUREX at 1090 mL/min. In the first test (Appendix C, Figure C.4), fresh S4 PUREX was used, so there were no solids present. The second test (Appendix C, Figure C.5) was conducted following Test 23B (Table 2.10), so solids resulting from that test were present. Steady-state concentrations of NO reached 286 ppm and 292 ppm, respectively, in the two performance checks (i.e., 5% and 3% below the expected values). The first concentration, in particular, is a little outside the range of expected reproducibility of the NO_X analyzer, which may indicate some loss of NO in the system.

However, for the purpose of this work, the observed NO concentrations were considered acceptable. Clearly, the approach to steady-state NO concentrations and the return to zero following shut-off of the NO was about the same as in the earlier tests with the 2-L vessel.

2.2 Results

This section is divided into three subsections, Primary Tests, Large-Scale Tests, and Other Mixing Tests. Primary Tests included all of the THOREX/PUREX mixing tests conducted in the 2-L test vessel using a set-up similar to that shown schematically in Figure C.1. (Appendix C).[a] Large-Scale Tests were conducted in a 17-L vessel and also used a set-up similar to that shown schematically in Figure C.1. (Appendix C).[a] Other Mixing Tests involved, primarily, some THOREX/NaOH mixing experiments conducted without qualitative gas analyses.

2.2.1 Primary Tests

Results from all of the primary THOREX/PUREX mixing tests are summarized in Tables 2.6 to 2.9 and Figures C.6 to C.39 (Appendix C). Explanations for some of the column headings in Tables 2.6 to 2.10 are given in Table 2.5, below. Other information given in the tables includes 1) corresponding figure number, 2) pH at the start and end of each test, 3) test temperature, and 4) amount of NO gas that was generated. The tests were grouped within the tables so that tests with similar parameters, or with the objective of determining the effect of changing a particular parameter, occur together. Tests in Tables 2.8 to 2.10 with nominally identical parameters were given the same number followed by a letter.

Table 2.5. Description of Column Headings in Tables 2.6 to 2.10

Ar gas carrier flow rate	Flow rate (mL/min at STP) of the Ar carrier gas sweeping through the reaction vessel, as measured by the calibrated mass flow controller (MFC). Gas generation rates were calculated from the measured concentrations multiplied by these flow rates.
Stir rate	Rotational speed, rpm, of the stirrer. In the early tests, a careful record of the exact stirrer speed setting was not made. Therefore, the rate is simply listed as medium, "med," and was probably between 300 and 400 rpm.
THOREX batch	Compositions listed in Tables 2.2 and 2.3.
PUREX batch	Compositions listed in Table 2.4 or described in Section 2.1.2.

(a) Only the first 5 tests (Tables 2.6 and 2.7) used both the GC and NOx analyzer. The remaining primary tests and all the large-scale tests used only the NOx analyzer.

Table 2.6. Comparison of Direct THOREX Addition to PUREX Versus THOREX Addition to PUREX Recirculation Loop[a]

Test	Figure	Ar Gas Carrier Flow Rate mL/min	Stir Rate rpm	THOREX				PUREX Batch	NO mL	CO_2 mL	Temp. °C
				Loop Flow mL/min	Batch	Addn Rate mL/min	Total mL Added				
1[b]	C.6	658	med	75	1	0.41	78	R3A	0.82	~0	45
2	C.7	570	med	5	2[c]	0.85	100	R3A	19[d]	18[d]	45
3[b]	C.8	662	med	NA	1	0.40	73	R3A	3.8	0.87	45

(a) See Table 2.5 for descriptions of some of the column headings.
(b) Included corrosion coupons. See schematic diagram in Figure 2.1 and Section 3.4 for results.
(c) THOREX composition listed in Table 2.3 except diluted by 59/45 with deionized water.
(d) Values could be 10 to 30% low due to loss of gas through pH holder in loop. See description in text.

Table 2.7. Back-Flow Tests of PUREX Added to THOREX[(a)]

Test	Figures	Ar gas Carrier Flow Rate mL/min	Stir Rate rpm	PUREX		THOREX Batch	NO mL	CO_2 mL	Temp. °C
				Batch	Addn Rate mL/min				
4	C.9	578	med	R3A	1.24	2	61	39	45
5	C.10	568	med	R3A	1.27	2[(b)]	66	37	25

(a) See Table 2.5 for descriptions of some of the column headings.
(b) THOREX composition listed in Table 2.3 except diluted by 59/45 with deionized water.

The in-vessel and in-loop pH probes, which were used only in Tests 1 to 3, did not accurately read pH values above about 10. Indeed, the readings were found to be one-half to one unit low at pH 13 as determined by a secondary pH probe that responded properly to the high pH values. The secondary pH probe was calibrated at pH 13.3 using a 0.2 M NaOH solution. Approximate corrections were applied to the recorded pH values obtained from the in-vessel and in-loop probes. The applied corrections were varied in a linear fashion from the measured error (one-half to one pH unit) at the beginning of the test (pH ~13) to zero correction at pH 10. The corrected values are the ones that are plotted in Figures C.6 to C.8 (Appendix C).

Test 1

A major objective of Tests 1 to 3 [Table 2.6, Figures C.6 to C.8 (Appendix C)] was to compare the amount of NO that was generated when THOREX was added directly to the reaction vessel with the amount that was generated when the PUREX was pumped through a recirculation loop and THOREX was added to the loop. The recirculation loop feature of the apparatus is not shown in the schematic representation in Figure C.1 (Appendix C). In the loop tests, a peristaltic pump was used to circulate PUREX through a 2- to 3-ft-long loop of approximately 1/8-in. ID Tygon tubing, and THOREX was pumped into a "T" in the loop. Agitation by the stirrer kept the PUREX solids in suspension in the reaction vessel, and PUREX passed through the loop as a slurry of suspended solids.

Three important points should be noted about the results from Test 1, which are shown in Figure C.6 (Appendix C) and Table 2.6. First, the spikes in the NO/NO_X data are thought to have been caused by NO bubble generation in the recirculation loop. Bubbles were not actually observed; they were merely surmised. Small bubbles are thought to have accumulated within the loop where they agglomerated into much larger bubbles, which were expelled into the reaction vessel at irregular intervals. Only after the bubbles entered the reaction vessel would they be swept away by the carrier gas into the NO_X analyzer. Thus, the spikes are thought to have been caused by irregular bursts of NO bubbles into the reaction vessel. Note the absence of large spikes when THOREX was added directly to the reaction vessel (Figure C.8 in Appendix C).

Table 2.8. Laboratory-Scale Tests of THOREX Added to Either Full-Compliment PUREX or Simplified PUREX[a]

Test	Figure	Ar Gas Carrier Flow Rate mL/min	Stir Rate rpm	THOREX[b]			PUREX Batch (1.5 L)	NO Gas		pH		Temp °C
				Batch	Addn Rate mL/min	Total mL Added		Total mL	Peak Rate μL/min	Start	End	
6	C.11	566	med	3	1.84	30	R3B[c]	5.5	290	13.1	11.3	45
7A	C.12	827	350	3	1.85	30	S3	7.6	390	13.2	10.8	45
7B	C.13	827	350	3	1.77	30	S3	6.4	380	13.2	10.8	45
8	C.14	566	med	3	0.22	30	R3B[d]	5.5	50	13.0	10.8	45
9	C.15	566	med	3[e]	1.84	30	R3B[f]	8.4	425	13.0	11.7	45
10	C.16	662	med	3[g]	1.94	60	R3B[c]	5.8	140	13.1	12.1	45
11	C.17	827	0	3	1.76	30	R3B[c]	130	5200	13.1	11.6	45
12	C.18	827	0	3	1.79	30	S3	320	4900	13.2	11.6	45
13	C.19	662	med	3	2.04	30	R4[h]	1.6	88	13.2	12.2	45
14A	C.20	827	350	3	1.88	30	S4	3.8	170	13.3	10.4	45
14B	C.21	827	350	3	1.84	30	S4	3.0	190	13.3	10.0	45
14C	C.22	827	350	3	1.73	30	S4	3.1	140	13.3	11.0	45
14D	C.23	827	350	3	1.73	30	S4	3.2	170	13.3	10.7	45

(a) See Table 2.5 for descriptions of some of the column headings.
(b) 30 mL of THOREX per 1.5 L of PUREX is approximately the same ratio as 45,000 L THOREX per 2,100,000 L PUREX.
(c) 7.12 mL 19 M NaOH added.
(d) 16 mL 19 M NaOH added to vessel following Test 6.
(e) 23.8 mL conc. HNO_3 added to 68.8 mL THOREX raising H^+ to ~4 M and diluting other constituents.
(f) 27 mL 19 M NaOH added to vessel following Test 8.
(g) THOREX diluted with deionized water to 50% of is original concentration.
(h) 12 g NaOH pellets added.

Table 2.9. Laboratory-Scale Tests of THOREX Added to Either Full-Compliment PUREX or Simplified PUREX[a]

Test	Figure	Ar Gas Carrier Flow Rate mL/min	Stir Rate rpm	THOREX[b]			PUREX Batch (1.5 L)	NO Gas		pH		Temp °C
				Batch	Addn Rate mL/min	Total mL Added		Total mL	Peak Rate μL/min	Start	End	
15	C.24	827	50	3	1.75	30	S3	13	120	13.2	10.8	45
16	C.25	827	600	3	1.83	30	S3[c]	5.6	400	13.3	12.3	45
17A	C.26	827	350	3	1.87	15	S4	1.4	110	13.3	12.9	45
17B	C.27	827	350	3	1.96	15	S4	0.80	60	13.3	12.9	45
17C	C.28	827	350	3	1.83	15	S4	0.77	60	13.3	12.9	45
18	C.29	827	50	3	1.80	15	S4[d]	1.9	40	13.3	12.9	45
19	C.30	827	350	3	1.89	30	S4[e]	2.0	95	13.3	11.3	45
20A	C.31	827	350	3	1.74	30	S4	0.63	30	13.3	11.1	22
20B	C.32	827	350	3	1.81	30	S4	0.84	34	13.3	11.1	22
21A	C.33	827	350	3	1.56	30	S4	5.1	280	13.3	11.1	65
21B	C.34	827	350	3	1.71	30	S4	5.8	320	13.3	11.0	65
22	C.36	827	350	3	1.76	30	S4[f]	0.85	43	13.26	13.25	45

(a) See Table 2.5 for descriptions of some of the column headings.
(b) 30 mL of THOREX per 1.5 L of PUREX is approximately the same ratio as 45,000 L THOREX per 2,100,000 L PUREX.
(c) 7 g NaOH pellets added to vessel following Test 7B.
(d) 8.6 g NaOH pellets added to vessel following Test 17A.
(e) 0.19 M Na_2CO_3.
(f) NaOH was added to the reaction vessel in a separate line to keep the pH constant at the same time as the THOREX was added.

Table 2.10. Large-Scale Tests of THOREX Added to Either Full-Compliment PUREX or Simplified PUREX[a]

Test	Figure	Ar Gas Carrier Flow Rate mL/min	Stir Rate rpm	THOREX[b]			PUREX Batch (1.5 L)	NO Gas		pH		Temp °C
				Batch	Addn Rate mL/min	Total mL Added		Total mL	Peak Rate μL/min	Start	End	
23A	C.40	827	350	3	1.86	321[c]	S4	4.3	25	13.3	9.3	22
23B	C.41	827	350	3	1.86	292[d]	S4	9.2	34	13.3	10.9	22
24	C.42	827	600	3[e]	1.86	290[f]	S4[g]	5.1	58	13.2	10.7	23

(a) See Table 2.5 for descriptions of some of the column headings.
(b) 300 mL of THOREX per 15 L of PUREX is approximately the same ratio as 45,000 L THOREX per 2,100,000 L PUREX.
(c) The intended amount of THOREX (300 mL) was inadvertently exceeded.
(d) The intended amount of THOREX (300 mL) was stopped slightly short due to a clogged line caused by solids that crystallized from solution.
(e) THOREX was diluted about 10% with deionized water to prevent solids from crystallizing from solution.
(f) The amount of "full strength" THOREX is somewhat uncertain because of the dilution noted in (e).
(g) 120 g of NaOH pellets were added to vessel following Test 23B.

Secondly, the curve labelled "NO_X" in Figure C.6 (Appendix C) actually represents the NO gas. Both curves, NO and NO_X, were included in this figure for illustrative purposes as described in Section 2.1.1.

The third point about the data in Figure C.6 (Appendix C) is that, at the time this test was run, it was assumed that the THOREX composition corresponded to the "Nominal Diluted" values listed in the fourth column of Table 2.2. This would correspond to a THOREX/PUREX ratio of 42 mL THOREX per 1.5 L PUREX. Had that been true, the amount of THOREX added in this test (78 mL) would have nearly doubled the representative amount. However, the as-analyzed concentrations of the major constituents in this batch of THOREX simulant were only about 60% of the expected values (Table 2.2). Therefore, 70 mL of this THOREX simulant was required to add the appropriate amounts of Th, HNO_3, and other constituents. At the point where 70 mL of THOREX had been added in this test, the amount of NO generated was 0.82 mL. This point is shown by Figure C.6 (Appendix C) to have occurred 175 min. into the test.

There are a few other points to be made about the results from this first test: 1) Figure C.6 (Appendix C) shows no obvious effect of increasing the stir speed at 180 min.; 2) the NO/NO_X concentrations returned to zero about an hour after the THOREX addition was stopped at 195 min.. This slow return to zero was common to all the tests (much slower in some cases than others) and is discussed in detail in Section 2.3; 3) Table 2.6 indicates that little CO_2 was generated during this test. An error in setting up the computer for this run resulted in loss of the chromatograms containing the CO_2 data. However, personal observations of the GC data "on-the-fly" indicated the presence of only a very little CO_2 in this test; and 4) corrosion coupons were placed in the reaction vessel during this test as described in Section 3.1.1.

Test 2

Figure C.7 (Appendix C) and Table 2.6 show results from the second recirculation loop test, which used a lower ratio of loop-flow-rate to THOREX-addition-rate than Test 1. The main purpose of this test was to reduce that ratio to one that was more representative of anticipated full-scale conditions. Also in this test, a device for holding a pH probe was placed within the PUREX recirculation loop downstream from the "T" where THOREX was introduced into the loop.

The most notable results from this second loop test were the rapid drop in pH within the recirculation loop and the observation of large volumes of bubbles within the loop. Some of the bubbles lodged within the pH probe holder and displaced the PUREX/THOREX slurry enough to uncover the sensing portion of the probe. To resubmerge the probe within the slurry, the gas bubbles had to be released from the holder every 5 min. or so. This unexpected problem with the bubbles is thought not to have had more than a transient effect on the in-loop pH measurements. However, gas released from the pH probe holder obviously did not get swept into the gas analyzers and, therefore, was not included in the rates and amounts shown in Figure C.7 (Appendix C) and Table 2.6. The fraction of the gas that was lost through the pH probe holder is hard to judge, but may have been 10 to 30% of the total gas volume.

The volume of bubbles within the recirculation loop was much greater in Test 2 than in Test 1, apparently because of the much lower ratio of loop-flow-rate to THOREX-addition-rate. This probably allowed more bubbles to accumulate because they were not being carried away by the loop flow as rapidly. A more important cause of the greater bubble volume in the second loop test was probably

that the pH within the loop dropped to lower values. Although in-loop pH measurements were not made in the first test, the pH was unlikely to have dropped so low as that shown for Test 2 in Figure C.7 (Appendix C). Lower in-loop pH values in the second test are an expected result of the lower ratio of loop-flow-rate to THOREX-addition-rate simply because of the greater proportion of the acidic THOREX within the loop.

Four other features of the second loop test deserve mention. First, the second batch of THOREX was used, and the measured concentrations were close to the expected values (see Table 2.3). Second, the test was continued until more than double the full-scale ratio of 28 mL THOREX per L of PUREX (42 mL THOREX per 1.5 L PUREX) was added. At the point where 42 mL of THOREX had been added, 19 mL of NO and 18 mL of CO_2 had been generated. Third, as more THOREX beyond 42 mL was added, the pH within the reaction vessel eventually dropped sharply to about 5, which is far below the value that would be allowed in the full-scale case. The sharp rise in NO and CO_2 generation rates about 100 min. into the test may be associated with the pH drop, but the abrupt nature of the rise suggests that the irregular passage of gas bubbles from the loop into the vessel may also have been involved. Fourth, after the in-flow of THOREX was stopped, the NO concentration returned to near zero within about 30 min., but the CO_2 concentration remained high. Perhaps CO_2 gas continued to slowly evolve from solution due to the low pH.

Test 3

Results from the first test where THOREX was added directly to PUREX are shown in Figure C.8 (Appendix C) and Table 2.6. The first batch of THOREX, which had only about 60% of the expected concentrations of Th, HNO_3, etc., was used. By the time 70 mL of this THOREX had been added, which is representative of the full-scale case, 3.8 mL NO and 0.87 mL CO_2 had been generated. Again, as was described for Test 1, the NO_X curve is actually representative of the NO data. After the THOREX addition was stopped, the CO_2 curve dropped rapidly to zero while the NO and NO_X curves tailed off rather slowly. This is the reverse of what happened in Test 2 and probably reflects the very different final pH values in the two tests ($\sim$5 in Test 2 and $\sim$11.6 in Test 3).

Test 4

This test was run to evaluate the consequences of an accidental backflow of PUREX from Tank 8D-2 into the THOREX in Tank 8D-4. The potential for this to happen might exist if THOREX were pumped into a PUREX recirculation loop, such as was evaluated in Tests 1 and 2. The potential might also exist if THOREX were pumped directly into Tank 8D-2 and if the end of the inlet pipe were below the surface of the slurry in the tank. If the inlet pipe were above the slurry surface, accidental backflow would suck only air, not PUREX slurry.

The test was run by placing one liter of undiluted THOREX (Table 2.3) in the reaction vessel and pumping PUREX into the vessel. The total amount of PUREX added was purely arbitrary since there was no specified amount of accidental backflow. Because of the high acidity of the THOREX (initially 0.8 M HNO_3), large amounts of NO and CO_2 were generated in this test as shown in Figure C.9 (Appendix C) and Table 2.7. After stopping the PUREX addition, the generation rates of NO and CO_2 dropped rapidly at first but thereafter tailed off extremely slowly.

Test 5

This test [Table 2.7, Figure C.10 (Appendix C)] was a repeat of Test 4 except that it used diluted THOREX and was run at 25°C rather than 45°C. The results from these two backflow tests were similar. Because of the method of data recording, as was described in the Section 2.1.1, the NO and NO_X curves show that there was no NO_2 present. Therefore, the generation rate of NO is actually represented by the NO_X curve. Both curves are shown here, as they were in Figures C.6 and C.8 (Appendix C), for illustrative purposes.

Tests 6, 7A, and 7B

Results from these tests, which were run under similar conditions, are presented in Table 2.8 and Figures C.11 to C.13 (Appendix C). Test 6 used PUREX containing the full complement of constituents whereas Tests 7A and 7B used simplified PUREX. Slightly higher peak generation rates of NO, as well as higher total NO, were observed with the simplified PUREX (Tests 7A and 7B), but otherwise the results from all three tests were quite similar.

Test 8

The THOREX addition rate in this test (Figure C.14 in Appendix C) was nearly 10 times slower than in Tests 6, 7A and 7B, but the total amount of THOREX was the same. About the same amount of NO was generated as in Tests 6, 7A, and 7B, but the peak generation rate was six to eight times lower in Test 8 because of the lower THOREX addition rate.

Test 9

The acidity of the THOREX used in this test was raised to ~4 M by adding concentrated HNO_3. This resulted in dilution of the other constituents to about two-thirds of their normal concentrations. However, the total OH^- equivalent of this THOREX (i.e., the amount of OH^- in the PUREX required to neutralize the acid in the THOREX and also to precipitate the Th, Fe, and other components in the THOREX as hydroxides) changed very little from the normal THOREX. The results in Table 2.8 and Figure C.15 (Appendix C) show that the total NO increased by about 50% compared to Tests 6 and 8. Clearly, the higher acidity of Test 9, compared to Tests 6 and 8, resulted in the production and decomposition of more HNO_2.

Test 10

Rather than *increasing* the acidity of the THOREX as in Test 9, this test explored *decreased* acidity by using THOREX that had been diluted by deionized water to 50% of its nominal concentration. To compensate for the reduced concentrations, double the volume (60 mL) of THOREX was added so that the same total amount of active ingredients were involved. Table 2.8 and Figure C.16 (Appendix C) show that about the same total amount of NO was generated as in Tests 6 and 8. The peak generation rate in Test 10 was about half that in Test 6. Thus, diluting the THOREX in Test 10 had an effect similar to reducing the THOREX addition rate as in Test 8.

Tests 11 and 12

These tests, one with full-compliment PUREX and one with simplified PUREX, were conducted with no stirring. Table 2.8 and Figures C.17 and C.18 (Appendix C) show that the total amount of NO increased by a factor of 24 to 46 compared with Tests 6 to 8, which had medium stirring rates. Not only were the peak rates high in Tests 11 and 12, but the return to zero was very slow. Turning on the stirrer after a time resulted in another peak in the NO generation rate and, thereafter, a more rapid return to zero, particularly in Figure C.18 (Appendix C). Test 12, with simplified PUREX, generated more NO than Test 11, which used full-compliment PUREX. The larger amount of NO with simplified PUREX, compared to full-compliment PUREX, is similar to the difference observed between Test 6 and Tests 7A and 7B.

Test 13

Table 2.8 and Figure C.19 (Appendix C) show the results of this test, which was the only test run with fourth-wash PUREX that contained the full compliment of components. Less than one-third as much NO was generated in Test 13 as in Tests 6 and 8, which used third-wash PUREX, even though Table 2.4 shows that the difference in NO_2^- concentrations between third- and fourth-wash PUREX was a factor of only about two. Note, however, that the pH drop in Test 13 was less than in Tests 6 and 8 and also less than in Tests 14A to 14D, which used simplified PUREX.

Tests 14A to 14D

These four tests [Table 2.8, Figures C.20 to C.23 (Appendix C)] with simplified PUREX generated about twice as much NO as did Test 13 with full-compliment PUREX. The difference between Test 13 and Tests 14A to 14D may be related to the pH difference noted above. Perhaps the additional components, primarily solids, present in the full-compliment PUREX (Test 13) reacted with acid from the THOREX to prevent such a large change in pH.

Tests 15 and 16

Results from these two tests, which were performed to investigate the effect of stirring rate, are shown in Table 2.9 and Figures C.24 and C.25 (Appendix C). The effect of stirring rate on total NO was small, but the shapes of the curves were quite different. With slow stirring (Test 15), the total amount of NO was roughly double that generated with medium stirring (Tests 7A and 7B) but not nearly so much as with no stirring (Test 12). However, the peak rate in Test 15 was over three times lower (until the stirrer speed was increased) than in Tests 7A and 7B, and the return to zero was very slow. Increasing the stirrer speed (Figure C.24, Appendix C) after nearly 4 h caused a large immediate increase in the NO generation rate followed by a more normal rate of return to zero. The peak rate and total amount of NO generated during fast stirring [Test 16, Figure C.25 (Appendix C)] were about the same as with medium stirring (Tests 7A and 7B). However, the return to zero was faster in Test 16. Table 2.9 also shows that the final pH was higher with fast stirring (Test 16) than with slow or medium stirring (Tests 7A, 7B, or 15). This pH difference was unexpected and, without repeating the fast-stir test, it is hard to judge how much faith to place in this single pH measurement.

Tests 17A to 17C

These tests [Table 2.9, Figures C.26 to C.28 (Appendix C)] were conducted to determine the effect of adding only half as much THOREX, which was intended to lower the OH^- concentration only to 0.1 M (pH 13.0). Clearly, halving the amount of THOREX reduced the amount of NO by more than a factor of two (compare Tests 17A to 17C with Tests 7A and 7B).

The difference in peak rate and total NO between Test 17A and Tests 17B and 17C apparently can be attributed to random differences. Examination of other replicate test results (7A and 7B, 14A to 14D, 20A and 20B, and 21A and 21B) indicates that the overall reproducibility between tests was approximately ± 0.5 mL, almost independent of the total amount of NO generated.

Test 18

Table 2.9 and Figure C.29 (Appendix C) show that the effect of slow stirring on fourth-wash PUREX was about the same as on third-wash PUREX (Test 15). That is, there was a small increase in the amount of NO compared to similar tests with medium stirring (Tests 17A to 17C), and the return to zero was very slow.

Test 19

This test [Table 2.9, Figure C.30 (Appendix C)] was conducted to investigate the effect of a ten-fold increase in Na_2CO_3 concentration. Compared to Tests 14A to 14D, the peak rate and total NO were somewhat smaller here. This result makes sense because some of the acid from the THOREX will have reacted with the increased Na_2CO_3 in Test 19 (see Equation 2.11 in Section 2.3), resulting in the formation of less HNO_2 and its NO decomposition product.

Tests 20A to 21B

These tests [Table 2.9, Figures C.31 to C.34 (Appendix C)] were conducted, along with Tests 14A to 14D [Table 2.8, Figures C.20 to C.23 (Appendix C)], to investigate the temperature dependence of NO production during THOREX/PUREX mixing. An Arrhenius plot of all eight test results is shown in Figure C.35 (Appendix C). Calculated activation energies were 12.1 kcal/mol between 22°C and 45°C and 5.4 kcal/mol between 45°C and 65°C. The nonlinearity indicates that two or more processes with different temperature dependencies are involved.

Test 22

Table 2.9 and Figure C.36 (Appendix C) show results from simultaneous addition of THOREX and 5.4 M NaOH in separate lines to S4 PUREX. The relative addition rates of THOREX and NaOH were selected with the objective of maintaining a nearly constant pH in the reaction vessel. The start and end pH values cited in the figure indicate that this objective was accomplished. However, it is suspected that the NaOH got slightly ahead of the THOREX, despite the pH measurements to the contrary, because the NO generation rate started to decrease slightly just before the THOREX and NaOH pumps were turned off. This decrease in NO generation rate may indicate that the effective pH of the slurry was actually beginning to increase. The total amount of NO was only about one fourth the amount generated under conditions (Tests 14A to 14D) that were similar except for the simultaneous addition of NaOH.

Other Laboratory-Scale Mixing Tests

In an effort to understand the reason(s) for the rather slow tail-off in NO generation rates observed in many of the tests described above, two tests were conducted using pure HNO_3 so that no solids would be generated. Figure C.37 (Appendix C) shows results from adding pure HNO_3 to pure $NaNO_2$. No pH measurements were made. The starting $NaNO_2$ solution would have had a near-neutral pH, and addition of the HNO_3 would have lowered the pH somewhat. However, most of the added HNO_3 (0.0052 moles) would have reacted with a portion of the 0.12 moles of NO_2^-, which was originally present, to form HNO_2. Seventy milliliters (0.0031 moles) of NO gas was generated from decomposition of the HNO_2. Thus, about 60% of the added HNO_3 reacted to form HNO_2 with subsequent decomposition to generate NO. This is a far higher percentage of HNO_3 reacting with the NO_2^- than in the THOREX/PUREX mixing tests. In those tests, almost all of the HNO_3 from the THOREX reacted with OH^- from the PUREX and only a small percentage reacted with NO_2^- from the PUREX. For example, 1.2% of the HNO_3 in Tests 7A and 7B reacted to form NO gas.

Figure C.38 (Appendix C) shows results from adding pure HNO_3 to S4 PUREX in step-wise fashion and measuring the pH after each step. The first three steps were conducted one day and the last two steps the next day. With the exception of the first run on the second day, the total amount of NO in each step increased as the pH decreased. Figure C.39 (Appendix C) is an expansion of the data from Figure C.38 (Appendix C) between 240 and 330 min.; the small offset from zero near 300 min. in Figure C.38 (Appendix C) was subtracted from the data to produce Figure C.39 (Appendix C). This zero-correction allowed for better comparison of the NO tail-off with tests where THOREX was added to S4 PUREX (Figures C.31 to C.34 in Appendix C). Although the NO tail-off shown in Figure C.39 (Appendix C) was somewhat faster in this test where no solids were generated, it was still not as fast as in the performance checks (Figures C.2 to C.5 in Appendix C where NO gas was simply bubbled through the PUREX).

2.2.2 Large-Scale Tests

Large-scale tests were conducted with THOREX and PUREX volumes 10 times larger than in the Primary Tests described above, i.e., 300 mL of THOREX and 15 L of simplified fourth-wash PUREX (0.20 M NaOH, 0.077 M $NaNO_2$, and 0.019 M Na_2CO_3). The reaction vessel was made of polyethylene and was ~17 L in size, the same stirrer that was used in the Primary Tests was also used here, and the tests were conducted at ambient temperature. The test setup was the same as shown in Figure C.1 (Appendix C) minus the GC, temperature controller, and pH probe inside the reaction vessel, i.e., the same setup as in Tests 6 to 21B except for size. The purpose of these tests was to help determine the scaling factor that should be used to extrapolate the results described in this report to the actual addition of THOREX from Tank 8D-4 into the PUREX in Tank 8D-2. Results from these large-scale tests are summarized in Table 2.10 and Figures C.40 to C.42 (Appendix C). Descriptions of some of the column headings in Table 2.10 are listed in Table 2.5 (Section 2.2.1).

Test 23A

Table 2.10 and Figure C.40 (Appendix C) show results from the first large-scale test. The stir rate, which was the same as in most of the Primary Tests, was enough to create a slight vortex in the reaction vessel. Slightly more than the intended amount of THOREX was inadvertently added, which apparently caused the pH to drop more than was desired.

The most notable feature of the data in Figure C.40 (Appendix C), however, was the very slow return of the NO generation rate toward zero. The total amount of NO generated by the time the test was terminated was ~6 times the amount generated in Tests 20A and 20B, which were conducted under similar conditions but employed 10 times less THOREX and PUREX.

Test 23B

This test [Table 2.10, Figure C.41 (Appendix C)] was essentially a repeat of Test 23A. However, it was allowed to continue longer; after the test was terminated, the zero setting on the NO_X analyzer was checked to ensure that part of the reason for the persistent tail in the NO data was not caused by a zero shift of the analyzer. More than double the amount of NO was generated, compared to Test 23A, despite the slightly higher final pH, which was due to the slightly smaller quantity of THOREX that was added. Only a small part of the additional NO can be attributed to the longer duration of the test that allowed more of the NO in the tail to be measured and included in the total. Apparently the different amounts of NO simply represent random variations between tests. The average amount of NO generated in Tests 23A and 23B (6.8 mL) was ~9 times the average amount generated in Tests 20A and 20B (0.74 mL), a difference approximately equal to the ten-fold difference in solution volumes.

Test 24

The conditions for this test were the same as for Tests 23A and 23B except that the stirring rate was faster, which resulted in a large vortex. Also, the end of the THOREX addition line was moved closed to the center of the reaction vessel such that it was in, or near, the vortex created by the fast stirring. Table 2.10 and Figure C.42 (Appendix C) show that the peak NO generation rate was higher and the NO tail-off was much faster, but the total amount of NO was in the range of Tests 23A and 23B. The dip in the curve happened when the THOREX was inadvertently drawn down below the level of the pump intake line in the supply reservoir. This appears not to have had much effect on the test results, particularly not in the rate of NO tail-off. Clearly, the faster tail-off rate was caused by the faster stirring rate.

2.2.3 Other Mixing Tests

A possible alternative to direct addition of THOREX from Tank 8D-4 to the PUREX in Tank 8D-2 would be to neutralize the THOREX prior to transferring it into Tank 8D-2. Bray and Wise (1986) recommended against this alternative because a sticky, viscous precipitate formed when 19 M NaOH was added to THOREX. They believed that this precipitate could not be easily broken up to the point where it would form a pumpable slurry. To explore the prior neutralization alternative further, it was decided to perform a few simple THOREX/NaOH mixing experiments using a variety of NaOH concentrations. These experiments were performed using "dilute" THOREX equivalent to 59,000 L in Tank 8D-4 (second THOREX batch; see Table 2.3 for undiluted composition).

Several simple mixing experiments were performed where NaOH was mixed in a beaker with the dilute THOREX in the ratio of 8.9 moles of NaOH per liter of THOREX. This is the approximate amount of NaOH needed to neutralize the HNO_3, precipitate the Th, Fe, and Cr as hydroxides, and complex with the Al. The NaOH concentrations varied from one to 19 moles/liter. Sometimes the THOREX was added to the NaOH solution, but more often NaOH was added to the THOREX. The mixing order seemed not to make much difference.

With NaOH concentrations of 1 to 5 M, readily pumpable slurries were formed. Rheology and particle-size-distribution measurements were performed on two of these slurries; the results are summarized in the two following subsections.

The highest NaOH concentration tried was 19 M. When this was combined with THOREX with no stirring, a viscous precipitate formed that tended to stick to the container surfaces, in agreement with the observations of Bray and Wise (1986). However, it was possible to use vigorous prodding and stirring to break up this sticky precipitate to the point where it appeared to be a pumpable slurry, albeit a stiff one because of the high solids/liquid ratio. When the 19 M NaOH and THOREX were combined and stirred vigorously at the same time, a seemingly pumpable slurry was produced to begin with.

No matter what NaOH concentration was used, combining and simultaneous vigorous stirring, as opposed to combining first and then stirring, gave better results in terms of producing a readily pumpable slurry. Combining with no stirring produced a gelatinous precipitate that took considerable effort to break up into a pumpable form. The more concentrated the NaOH, the more important it became to combine and stir at the same time.

In another experiment shown schematically in Figure C.43 (Appendix C), 1 M NaOH was pumped at 6.5 mL/min through 1/16 in. ID Tygon tubing while diluted THOREX was pumped at 0.7 mL/min into a "T" in the line. This ratio of THOREX to NaOH was about the same as in the THOREX/NaOH mixing tests described above. The Tygon tubing downstream from the "T" extended into an inverted graduated cylinder that was nearly full of water. Any gas bubbles coming through the Tygon tubing would have escaped to the vapor space in the graduated cylinder and allowed the volume of gas generated by the mixing to be measured to within approximately ± 0.1 mL. The precipitate, which formed immediately inside the "T," could be seen passing readily through the Tygon tubing downstream from the "T" with no tendency to stick to the tubing. After exiting the Tygon tubing, the precipitate piled up in the bottom of the beaker and could be readily broken up by gentle stirring. This experiment was continued for about an hour during which time ~ 45 mL of THOREX was combined with ~ 400 mL of 1 M NaOH. Within the limit of detection (~ 0.1 mL), no gas evolved during this time.

An attempt was made to repeat the above experiment using 5 M NaOH instead of 1 M. However, the precipitate that formed in the "T" could not be pumped. Either the Tygon tubing came loose from the stainless steel "T," or the peristaltic pumps stalled.

In one last experiment, a previously-prepared mixture of diluted THOREX plus 1 M NaOH (same ratio as above) was pumped at 1.3 mL/min into a beaker containing an inverted graduated cylinder filled with second-wash PUREX,[a] using an arrangement similar to that shown in Figure C.43 (Appendix C). The experiment was continued for 20 min. during which time no gas collected in the inverted cylinder. Again, the minimum detectable amount of gas was ~ 0.1 mL.

(a) This PUREX had been washed only twice. Therefore, its NO_2^- concentration was expected to be about three times higher than that listed for the 3rd-wash supernate in Table 2.4.

Rheology Results

Measurements were made on two slurries produced by mixing dilute THOREX with 1 M NaOH (designated NT-1) and with 5 M NaOH (designated NT-5). Both slurries were determined to be readily pumpable through 2- or 3-in.-diameter pipes. Critical flow velocities necessary to ensure the particles remained in suspension were calculated to be 2.3 ft/s or less for NT-5 at 25° to 65°C. Even lower critical flow velocities would apply to the NT-1 slurry. Details of the rheology measurements are described in Appendix A.

Particle-Size Distribution

Measurements were made on the same two slurries used for the rheology measurements, NT-1 and NT-5. The Brinkman particle-size analyzer used for these measurements was set to cover the size range 0.5 to 150 μm.

Particle-size distribution results can be represented either on the basis of the total *number* of particles or on the basis of the total *volume* of particles. The mean particle diameters listed in Table 2.11 show that there is a big difference between the particle number and particle volume basis of representation. This difference occurs because most distributions, including the two shown here, include a very large number of very small particles that brings the average size down when particle numbers are used as the basis for averaging. However, the total volume of these small particles is insignificant when compared to the total volume of all the particles. Therefore, the particle-size distributions based on volume are probably most useful.

There is some evidence that many of the particles smaller than ~3 μm detected by the Brinkman instrument are erroneous. However, even if this were true, it has almost no effect on the total volume of particles or on the mean diameter based on the volume of particles. This is another reason for putting more faith in the volume-based distribution. Details of the particle-size distribution measurements are described in Appendix B.

2.3 Discussion

The major results of the THOREX/PUREX mixing studies can be summarized as follows:

1. Small amounts of CO_2 and NO gases were generated; no other gases were detected. Because the amounts of CO_2 were small and inconsequential to the process, analysis of CO_2 was discontinued after the first five tests.

Table 2.11. Mean Particle Diameters Based on Number or Volume of Particles

Test	Mean Diameter, Number (μm)	Mean Diameter, Volume (μm)
NT-1	2.3	77
NT-5	2.0	95

2. During initial testing, a comparison was made between the amount of NO that was generated when THOREX was added directly to the reaction vessel with the amount that was generated when the PUREX was pumped through a recirculation loop and THOREX was added to the loop. Results from the two loop tests varied considerably. With a high ratio of loop-flow-rate to THOREX-addition rate, the amount of NO was nearly 5 times smaller than when THOREX was added directly to the reaction vessel. With a low ratio of loop-flow-rate to THOREX-addition rate, the amount of NO was 5 times larger than when THOREX was added directly to the reaction vessel.

3. Only a small fraction of the NO_2^- in the PUREX was converted to NO gas during THOREX addition. For example, the amounts of NO generated in Tests 6 and 8 represent the conversion of 0.072% of the NO_2^- in the full-compliment, third-wash, PUREX to NO gas. In Test 13, 0.066% of the NO_2^- in the full-compliment, fourth-wash, PUREX was converted to NO gas. Thus, about the same fraction of NO_2^- was converted to NO gas with both third-wash and fourth-wash PUREX batches despite the different initial concentrations of NO_2^-.

4. Somewhat more NO gas was generated in tests using simplified PUREX compared to those using full-compliment PUREX. Thus, the average of Tests 7A and 7B represent the conversion of 0.091% of the NO_2^- in the simplified, third-wash, PUREX to NO gas. In Tests 14A to 14D, an average of 0.13% of the NO_2^- in the simplified, fourth-wash, PUREX was converted to NO gas.

5. The activation energy for NO production between 22°C and 45°C was determined to be 12.1 kcal/mol; between 45°C and 65°C it was 5.4 kcal/mol. The nonlinearity indicates that two or more processes with different temperature dependencies were involved.

6. Different stirring rates had little effect on the total amounts of NO generated, but the NO generation tail-off was very dependent on stirring rate (much slower at slow stirring rates). However, when the stirring was stopped, the amount of NO generated was very much greater. Thus, 1.7% of the NO_2^- in the full-compliment, third-wash, PUREX (Test 11) was converted to NO gas and 4.2% of the NO_2^- in the simplified, third-wash, PUREX (Test 12) was converted to NO gas.

7. The total amount of NO that was generated was nearly independent of THOREX addition rate.

8. When the acidity of the THOREX was increased ~5 times, the amount of NO increased ~50%. However, no effect on the amount of NO was observed when all constituents of the THOREX, including acidity, were diluted to 50% of their original concentrations.

9. In the event of an accidental reversal of flow where PUREX would flow out of Tank 8D-2 into the THOREX in Tank 8D-4, tests conducted here indicated that the generation rate and total amount of NO could be much higher (perhaps a factor of 10 although a direct comparison cannot be made) than in the normal flow direction, THOREX into Tank 8D-2.

10. Tests conducted with 10-times larger waste volumes produced 6 to 12 times more NO gas. Thus, over this very limited volume range, these data indicate that the amount of NO that is generated may scale in direct proportion to the volume of waste involved in the mixing. It is not known whether this scaling factor can be extrapolated to the size of the actual tanks at West Valley.

11. In all cases, it took anywhere from several minutes to a few hours after the THOREX addition was stopped for the NO gas generation rate to tail off to zero. Testing performed to date has not been able to identify a specific reason for this result.

Some of these observations are readily explained while, in other cases, the chemistry and kinetics are imperfectly understood, as indicated by the following discussion.

The major chemical reactions involved with mixing the acidic THOREX with the alkaline PUREX are summarized by Equations (2.5) to (2.12).

$$HNO_3(aq) + NaOH(aq) \rightarrow NaNO_3(aq) + H_2O \quad (2.5)$$

$$Th(NO_3)_4(aq) + 4NaOH(aq) \rightarrow Th(OH)_4(s) + 3NaNO_3(aq) \quad (2.6)$$

$$Fe(NO_3)_3(aq) + 3NaOH(aq) \rightarrow Fe(OH)_3(s) + 3NaNO_3(aq) \quad (2.7)$$

$$Cr(NO_3)_3(aq) + 3NaOH(aq) \rightarrow Cr(OH)_3(s) + 3NaNO_3(aq) \quad (2.8)$$

$$Ni(NO_3)_2(aq) + 2NaOH(aq) \rightarrow Ni(OH)_2(s) + 2NaNO_3(aq) \quad (2.9)$$

$$Al(NO_3)_3(aq) + 4NaOH(aq) \rightarrow NaAl(OH)_4(aq) + 3NaNO_3(aq) \quad (2.10)$$

$$2HNO_3(aq) + Na_2CO_3(aq) \rightarrow CO_2(g) + 2NaNO_3(aq) + H_2O \quad (2.11)$$

$$HNO_3(aq) + NaNO_2(aq) \rightarrow NaNO_3(aq) + HNO_2(aq) \quad (2.12)$$

In all cases where the component is listed as (aq), the aqueous species are actually ionic with the exception of HNO_2, which is one of the products in Equation (2.12). HNO_2 is a weak acid with an ionization coefficient of 6.0×10^{-4} at 30°C (Yost and Russell 1944).

In the mixing tests, the relative amounts of THOREX and PUREX were such that the final pH of the mixture was generally 10 or higher. Under these alkaline conditions, the acidic THOREX is neutralized [Equation (2.5)] and most of the constituents are precipitated from solution as hydroxides [Equations (2.6 to 2.9)], forming a slurry. At these high pH values, the aluminum probably remains in solution as a hydroxide complex as indicated by Equation (2.10). As indicated by Result 1 above, the production of CO_2 gas, which is represented by Equation (2.11), is of little consequence.

Equation (2.12) shows HNO_2 as a reaction product. Under well stirred equilibrium conditions, molecular HNO_2 would not exist because it would be neutralized by the excess hydroxide. However, it obviously does form because HNO_2 is the source of NO gas observed in these mixing tests. Apparently, localized acidic conditions exist at the point where THOREX enters the PUREX thereby allowing HNO_2 to form according to Equation (2.12) and decompose according to Equation (2.13).

$$3HNO_2(aq) \rightleftarrows H^+ + NO_3^- + 2NO(g) + H_2O \qquad (2.13)$$

When THOREX is added to PUREX, there is competition for reaction with the HNO_3 between Equations (2.5), (2.11), and (2.12). It is clear that Equation (2.5) is favored because so little NO (from the decomposition of HNO_2) and CO_2 gases are formed.

The kinetics and equilibrium constant for Equation (2.13) are given by Equations (2.14) and (2.15), respectively (Yost and Russell 1944), where the concentrations are expressed in moles/L, the pressure, P_{NO}, in atmospheres, and the time in minutes. Values for the rate and equilibrium constants as functions of temperature are plotted in Figures C.44 and C.45 (Appendix C).

$$\frac{-d(HNO_2)}{dt} = \frac{k(HNO_2)^4}{(P_{NO})^2} \qquad (2.14)$$

$$K = \frac{(H^+)(NO_3^-)(P_{NO})^2}{(HNO_2)^3} \qquad (2.15)$$

It would be possible to calculate the generation rate of NO gas during and after THOREX/PUREX mixing if the process were controlled entirely by the partitioning between Equations (2.5), (2.11), and (2.12) together with the decomposition of HNO_2 according to Equations (2.13), (2.14), and (2.15). In fact, the calculation would be simple if the partition coefficients for Equations (2.5), (2.11), and (2.12) were known. However, the situation is complicated by two things. First, and most important, the concentration of HNO_2 in the alkaline THOREX/PUREX mixture should be extremely small. That is, there should be essentially no HNO_2 left to decompose into NO gas once a homogeneous mixture has been achieved, a process that should require no more than a minute or two under the stirring conditions used in these tests. Second, the proton that is generated as part of Equation (2.13) has the potential to react with excess NO_2^- to generate more HNO_2 which, in turn, can decompose to produce more NO gas. This second mechanism has the potential to contribute to the tail-off in NO generation rates that was a common feature of the experimental mixing results.

An approximate decomposition rate of HNO_2 in the absence of these two complicating factors can be obtained from a very simple calculation. The instantaneous rate of decomposition of HNO_2 in the THOREX/PUREX mixtures can be approximated by substituting appropriate values into Equation (2.14) based on experimentally observed parameters.

- The concentration of NO_2^- in third-wash PUREX is ~ 0.23 M. Less than 0.1% of that is converted to NO gas (Item 3 above). A reasonable maximum concentration to assume for HNO_2, therefore, might be 2×10^{-4} M.

- Concentrations of NO gas in the vapor space of the reaction vessel were commonly on the order of 100 ppm. Therefore, assume a pressure of 10^{-4} atm.

- The rate constant at 45°C is about 1000 $L^3 \cdot atm^2/(moles^3 \cdot min)$.

- Using these values in Equation (2.14) gives an instantaneous decomposition rate of 1.6×10^{-4} mol/(L•min).

At this rate of reaction, it would take just over one minute for all of the HNO_2 to decompose. However, by the time the HNO_2 concentration is halved, the decomposition rate would be cut by a factor of 16, assuming no change in NO partial pressure. Thus, it is easy to visualize a tail-off in NO generation rate that extends over 30 min., which is the approximate time period observed in many of the tests. However, for this mechanism to operate requires the persistence of molecular HNO_2 in a high pH solution, which is an unreasonable supposition.

As was noted in Section 2.2.1, a few tests were performed with the objective of explaining the cause for the slow tail-off in NO generation rates. The relevant observations are reiterated here.

1. The tail-off was very strongly influenced by stirring rate. Slow stirring, or no stirring, resulted in a slow tail-off (Figures C.17, C.18, C.24 and C.29 in Appendix C).

2. When pure HNO_3 was added to pure $NaNO_2$ (Figure C.37 in Appendix C), there was a very slow tail-off. In this test, the pH remained low because there was no hydroxide present. Therefore, molecular HNO_2 would be expected to persist and decompose according to Equations (2.13) to (2.15). This is in contrast to the THOREX/PUREX mixing tests where the pH remained high and molecular HNO_2 would not be expected to persist.

3. In the high pH THOREX/PUREX mixtures where HNO_2 would not persist, it would be only in the localized low pH region near the THOREX entry point where HNO_2 would exist and could decompose according to Equation (2.13). It was thought that the NO gas generated by this localized decomposition of HNO_2 might dissolve in the mixture and then slowly evolve from solution into the vapor space. To evaluate this possibility, low concentrations of NO gas were bubbled through both full-compliment and simplified PUREX. However, Figures C.2 to C.5 (Appendix C) show that the NO tail-off was fast after NO was eliminated from the incoming gas stream. Thus, NO dissolution followed by slow evolution did not appear to offer the sought-for explanation for the

slow NO tail-off. However, in retrospect, the gas bubbles in these tests were large, and NO was only a small percentage of the gas in the bubbles. As a result, the mixtures may never have become truly saturated with dissolved NO gas. Therefore, the possibility that the slow NO tail-off might be caused by the slow evolution of dissolved NO gas from solution has not been entirely discounted.

4. It was felt that the solids present in the THOREX/PUREX mixtures might play a role in the slow NO tail-off. For example, very small bubbles of NO gas might adhere to solid particles in the slurry where they would be slow to dislodge and escape into the vapor space. This mechanism could also explain the dependence of the NO tail-off on stirring rate (faster stirring would dislodge the bubbles from the solids faster). To assess the effect of solids, a test (Figures C.38 and C.39 in Appendix C) was run in which pure HNO_3 was added to S4 PUREX so that no solids were generated. Figures C.38 and C.39 (Appendix C) show that the NO tail-off was somewhat faster than in tests that included solids, but not nearly so fast as when NO gas was simply bubbled through either full-compliment or simplified PUREX (Figures C.2 to C.5 in Appendix C). Therefore, the results presented in Figures C.38 and C.39 (Appendix C) show that the presence of solids is also not the complete explanation for the slow tail-off in the NO gas generation rates.

In summary, the slow tail-off in NO generation rates after the THOREX addition was stopped has at least four possible contributing mechanisms: 1) the slow decomposition of HNO_2 given by kinetic Equation (2.14); 2) the reaction of the proton from Equation (2.13) to produce more HNO_2; 3) attachment of small bubbles of NO gas to solids and their subsequent slow release; and 4) slow evolution of dissolved NO gas from solution. All four mechanisms may operate, thus making the phenomenon very difficult to model with any confidence. Because of the strong dependence of the NO tail-off on stirring rate, it seems clear that there must be more involved than the strictly chemical mechanisms given in 1 and 2, above. The stirring rate effect strongly suggests that there is some dependence on physical mechanisms such as 3 and 4, above.

Although the slow tail-off in NO generation rates is of academic interest, it may be relatively unimportant from an operations standpoint. Even though the tail-off was strongly dependent on stirring rate, the total amount of NO that was generated in the tests described here was nearly independent of stirring rate as long as the stirring was not stopped entirely. Thus, the total amount of NO that was generated in these tests, which seems to be the more important parameter, appears not to be very dependent on the tail-off.

3.0 Supplemental THOREX/PUREX Mixing Tests

Following completion of the mixing tests described in Section 2.0, WVNS requested additional tests, which are described in Table 3.1. The motivations for the additional tests were:

- Recent analyses of the wastes in Tanks 8D-4 and 8D-2 indicated that the acidity of the THOREX was less than suggested by historical records, as was the nitrite concentration of the PUREX.

- To maintain pitting corrosion control during THOREX addition, the NO_2^-/NO_3^- ratio in Tank 8D-2 must be kept above a minimum value. Compensation for the addition of NO_3^-, which is a major component of the THOREX, requires the simultaneous or periodic addition of $NaNO_2$ during THOREX addition.

- There were also some minor adjustments to the relative volumes of Tanks 8D-4 and 8D-2 compared to the values assumed for the testing described in Section 2.0.

The test conditions listed in Table 3.1 were designed to explore the effect that these differences would have on the amount of NO gas produced during the transfer of THOREX into Tank 8D-2.

3.1 Experimental

3.1.1 Apparatus

In the period between the testing described in Section 2.0 and before the supplemental testing described in this section, all the equipment had been dispersed to other projects or confined by temporary closure of the building for safety and operational upgrading. Therefore, the entire experimental setup had to be reassembled using mostly different equipment that was acquired by purchasing, borrowing, or fabrication.

The new equipment setup was the same as shown schematically in Figure C.1 (Appendix C) with the following exceptions:

- There was no gas chromatograph and associated computer; the reaction vessel contained no corrosion coupons, pH probe, or thermocouple; i.e., the configuration was the same as it was following the first five runs as described in Section 2.1.1.

- A second peristaltic pump was used to allow the simultaneous addition of NaOH during Batch #1 as described in Table 3.1.

- Because the earlier tests showed that NO was the only gas produced, aside from a little CO_2, the NO_X analyzer was set up to analyze only NO, rather than both NO and NO_2, and it was programmed to analyze the NO concentration at 10 second intervals.

Table 3.1. Test Conditions Requested by WVNS for Supplemental Runs [a,b]

Test 26	Batch #1	Add 17.8 mL of THOREX (0.039 M H^+) while simultaneously adding 7.5 mL of 19 M NaOH to maintain pH at 13.3.
	Batch #2	Dilute the THOREX from 0.039 M H^+ to 0.027 M H^+. Add 37.3 mL of the diluted THOREX and allow the pH to drop.
	Batch #3	Dilute the THOREX from 0.027 M H^+ to 0.0078 M H^+. Add 14 mL of the diluted THOREX and continue to allow the pH to drop.
Test 27		Same as Test 26 with the following exceptions:
		At the start of both Batches #2 and #3, add $NaNO_2$ to the reaction vessel to bring the concentration up to the requirement for pitting corrosion control. $C_1 = 0.11(C_2)^{0.72} \times 10^{0.02T}$ where C_1 = $NaNO_2$ concentration C_2 = NO_3^- concentration T = temperature (°C)
		Based on this equation and the calculated concentrations of NO_3^-, 13.5 g of $NaNO_2$ was added at the start of Batch #2 bringing the total NO_2^- concentration to 0.18 M, and 16.4 g of $NaNO_2$ was added at the start of Batch #3 bringing the total NO_2^- concentration to 0.34 M.
Test 28		Same as Test 26 with the following exceptions:
		Do not add NaOH during Batch #1, i.e., allow the pH to drop from the starting value of 13.3.

(a) All volumes are based on 1,600,000 L of PUREX in Tank 8D-2 and 50,600 L of THOREX in Tank 8D-4; volume of PUREX in laboratory reaction vessel was 1.5 L in all cases.
(b) All tests were performed at 45°C.

3.1.2 Test Solutions

THOREX

The THOREX used in these tests had the same nominal composition listed in Table 2.1 except that it was diluted with deionized water by a factor of 11.1/9.1 so that the total NO_3^- concentration was reduced from 11.1 M to 9.1 M, and the final H^+ concentration was reduced to 0.039 M (see Table 3.2).

Table 3.2. Nominal THOREX Composition for Supplemental Mixing Tests

Component	Concentration (mol/L)
Th	1.21
Fe	0.72
Al	0.40
Cr	0.16
B	0.16
Ni	0.090
Na	0.15
K	0.051
Mn	0.012
Ba	0.0024
NO_3	9.1
SO_4	0.0026
Cl	0.0017
H^+	0.039

PUREX

The nominal PUREX composition used in these tests was similar to the simplified batch "S4" described in Section 2.1.2 except that the $NaNO_2$ and Na_2CO_3 concentrations were reduced somewhat. Thus, the simplified PUREX composition used in these supplemental tests was 0.20 M NaOH, 0.049 M $NaNO_2$, and 0.005 M Na_2CO_3.

3.1.3 Calibrations and Performance Checks

The NO_X analyzer was calibrated according to instructions in the equipment manual before testing began. Calibration involved establishing gas flow conditions approximately equal to those to be used during testing. Then, with pure Ar gas flowing through the instrument, the "zero" knob was adjusted to give a null reading on the computer that served both to control the NO_X analyzer and as the data acquisition system. Next, a certified calibration gas consisting of Ar containing 274 ppm NO was passed through the instrument, and the "span" was adjusted to give a reading of 274 ppm on the computer. Thereafter, readings within $\pm 5\%$ of the actual value were expected for NO concentrations

ranging from zero to a few thousand ppm. When a second calibration gas consisting of Ar containing 1040 ppm NO was passed through the instrument, a reading of 1020 ppm was observed. This was considered to be an acceptable demonstration of the linearity of the instrument.

To check the entire gas-train system (see Figure C.1, Appendix C), the 274 ppm NO in Ar calibration gas was connected to the mass flow controller (MFC) so that it passed through the reaction vessel before entering the NO_X analyzer. Again, a reading of 274 ppm was registered on the computer thereby confirming the integrity of the system.

Six weeks after the initial calibration described above and immediately before the last two runs, the instrument calibration was rechecked. Pure Ar gave a reading of 0.10 ppm and the 274 ppm NO in Ar calibration gas gave a reading of 273 ppm. Both were considered acceptable and no calibration readjustment was made.

Because the entire experimental setup had to be reestablished as described in Section 3.1.1, a determination was made to try to reproduce the results obtained with Tests 7A and 7B (Table 2.8). This would provide a measure of any differences caused by uncontrolled experimental variables and allow them to be factored into comparisons between the supplemental test results and results from the earlier tests.

To reproduce the Test 7A/7B conditions, a new batch of THOREX was prepared with the same nominal composition listed in Table 2.3, and a new batch of simplified PUREX containing 0.20 M NaOH, 0.077 M $NaNO_2$, and 0.019 M Na_2CO_3 (the same composition as in Tests 7A/7B) was made. Two different runs were conducted (Tests 25A and 25B), and the results are given in Table 3.3 and Figures C.46 and C.47 (Appendix C).

The amounts of NO generated by Tests 25A and 25B (9.8 and 9.3 mL, see Table 3.3) were somewhat higher than for Tests 7A and 7B (7.6 and 6.4 mL, see Table 2.8). Since the source of $Th(NO_3)_4$ was different from that used in the earlier tests, a chemical analysis of the THOREX seemed in order to determine whether more or less than the nominal hydration water might be associated with the $Th(NO_3)_4 \cdot 4H_2O$ that was used. In addition, a dilute solution of the $Th(NO_3)_4 \cdot 4H_2O$, by itself, was prepared and analyzed. The results of both analyses are listed in Table 3.4. Except for the Al, the analyzed values are within the uncertainty of the analyses ($\pm 10\%$ for Al and Cr, $\pm 15\%$ for Th, Fe, and Ni). Thus, the difference between the results for Tests 25A/25B and Tests 7A/7B does not appear to be attributable to an error in the makeup of the THOREX.

Two other possible reasons for the slightly different results of Test 25A/25B and Tests 7A/7B were considered. One potential reason is the slightly lower final pH values listed for Tests 25A/25B. If this difference were real, it might explain a slight excess of NO generation in Tests 25A/25B because, typically, more NO is generated as the pH decreases. However, the pH difference cannot be ensured. All pH measurements in the current set of tests were performed at a controlled temperature of 25 ± 1°C whereas those in the previous test series were done at room temperature, which may have differed from 25°C by ± 3 to 4°C. Such temperature differences could account for the observed pH differences, which were not temperature-corrected.

Table 3.3. Laboratory-Scale Test of THOREX Added to Simplified PUREX[a]

Test	Figure	Ar Gas Carrier Flow Rate mL/min	Stir Rate rpm	THOREX		NO Gas		pH		Temp. °C
				Addn Rate mL/min	Total mL Added	Total mL	Peak Rate μL/min	Start	End	
25A	C.46	700	350	1.6	36	9.8	290	13.2	10.6	45
25B	C.47	700	350	1.4	36	9.3	270	13.3	10.3	45

(a) See text (Section 3.1.3) for descriptions of the THOREX and PUREX used in these tests.

Table 3.4. Composition of Th Solutions (mol/L)

Element	THOREX		Th Solution	
	Nominal	Measured	Nominal	Measured
Th	1.48	1.33	1.48×10^{-5}	1.44×10^{-5}
Fe	0.88	0.90		
Al	0.49	0.39		
Cr	0.20	0.18		
Ni	0.11	0.095		

The second potential reason considered for the noted differences in NO generation was the stirring conditions. A precise record of the configuration of the propellers attached to the stirrer shaft during the earlier testing was not made. Therefore, it is known only that the configuration was similar during the current tests, but it may not have been exact. Also, a new stir motor (same brand and model) was used, but its rotational speed was not measured as it was in the earlier tests. Earlier, a speed of 350 rpm was measured for a motor setting of "3," the setting used for most tests. Literature that accompanied the new stir motor indicated a speed of 350 rpm at a motor setting of "3," which was also used for the recent tests. However, it cannot be guaranteed that the rotational speeds were indeed the same for the two sets of tests.

The fact that the "tail-off" in the NO generation curves (Figures C.46 and C.47 in Appendix C) had a slightly longer duration than was observed earlier (Figures C.12 and C.13 in Appendix C) suggests that the stirring in the current test series may have been slightly less vigorous than it was in the earlier tests. It was found in the earlier testing that slower stirring led not only to a longer NO tail-off but also to slightly more total NO generation. All of this suggests that the slightly longer tail-off and the slightly larger amounts of NO in the current tests *might* have been caused by somewhat less vigorous stirring.

Although the difference in results between Tests 25A/25B and Tests 7A/7B was reproducible, it was decided that the magnitude of the difference did not warrant further investigation. Rather, the reader should simply be cognizant of this small difference when comparing the results from the current test series with those from the earlier testing.

3.2 Results and Discussion

Initial results for Tests 26, 27, and 28 are shown in Table 3.5 and Figures C.48 to C.51 (Appendix C). Figures C.50 and C.51 (Appendix C) are two different plots of the same data for Test 28. The pH dropped dramatically in Test 28 because all of the available hydroxide precipitated, primarily as $Th(OH)_4$ and $Fe(OH)_3$, upon addition of the THOREX, and no NaOH was added during Batch #1 to compensate as was done in Tests 26 and 27. A large volume of NO was generated during

Table 3.5. Supplementary Tests of THOREX Added to Simplified PUREX[a,b]

Test	Figure	THOREX Addn Rate mL/min[c]	Moles NaOH added in Batch 1[d]	$NaNO_2$ Added at start of Batches 2 and 3	Batch #1[e]		Batch #2[e]		Batch #3[e]		Total NO mL	Temp. °C
					Total NO mL	End pH	Total NO mL	End pH	Total NO mL	End pH		
26	C.48	1.6	0.145	No	0.16	13.23	1.2	12.41	0.22	12.06	1.6	45
27	C.49	1.6	0.139	Yes	0.32	13.18	5.4	11.21	2.0	9.03	7.7	45
28	C.50, C.51	1.6	none	Yes	0.10	12.92	690	4.3	--	--	690	45
26½	C.52	1.6	0.146	Yes[f]	0.26	13.26	1.5	12.34	0.88	11.85	2.6	45
27A	C.53	1.5	0.143	Yes	0.47	13.26	3.0	12.36	1.4	11.93	4.9	45
29	C.54	1.4	0.148	No	0.53	13.26	1.3	12.37	0.25	11.94	2.1	45

(a) Ar carrier gas flow rate was the same for all tests, 700 mL/min
(b) The stir rate was the same for all tests, 350 rpm
(c) These addition rates are slightly less than for most of the tests listed in Tables 2.6 to 2.10. However, results from the earlier tests showed that THOREX addition rate, by itself, was not an important parameter.
(d) Measured by before-and-after weighing of the supply container
(e) See Table 2.12 for description of batch numbers
(f) Only half as much $NaNO_2$ added as in Tests 27, 27A, and 28

Batch #2 of Test 28 because of the large pH decrease. Because the pH dropped so low during Test 28, those test conditions clearly do not represent viable conditions for the addition of Tank 8D-4 waste to Tank 8D-2 waste. Therefore, Batch #3 was not run for Test 28 and no further consideration was given to Test 28.

There was a marked difference between Tests 26 and 27 with respect to the ending pH values observed at the ends of Batches #2 and #3 [Table 3.5, Figures C.48 and C.49 (Appendix C)]. This difference seemed questionable because the addition of $NaNO_2$ in Test 27 at the beginnings of Batches #2 and #3 was not expected to have a significant effect on the pH of this slurry at such a high initial pH. Therefore, to explore further any possible effect of $NaNO_2$ on the pH, Test 26½ was conducted with only half as much $NaNO_2$ added at the beginnings of Batches #2 and #3 (Figure C.52 in Appendix C). In addition, Test 27 was repeated as Test 27A (Figure C.53 in Appendix C).

Test 27A generated a little less NO than Test 27, but more importantly, the pH dropped only about as much as in Tests 26 and 26½. The difference appears to be related to the amounts of NaOH added during Batch #1 of the various tests (see Table 3.5).

The amount of NaOH added during Test 27 was slightly less, and the pH at the end of Test 27, Batch #1 was only slightly lower than during the other tests. However, by the end of Test 27, Batches #2 and #3, the slight deficiency in NaOH resulted in significantly lower pH values. Therefore, it appears that adding $NaNO_2$ at the beginning of Batches #2 and #3 increased the amount of NO that was generated by modest amounts (compared to not adding $NaNO_2$ as was done in Test 26), but it did not have a significant effect on the final pH values as was first indicated.

One final run, Test 29, was requested by WVNS in which the starting $NaNO_2$ concentration was increased slightly to 0.056 M and no $NaNO_2$ was added at the beginnings of Batches #2 and #3. Table 3.5 and Figure C.54 (Appendix C) show that the amounts of NO that were generated were about the same as in Test 26, which was expected since the only difference was an increase in the starting $NaNO_2$ concentration from 0.049 M to 0.056 M.

Comparing the data from these supplementary tests with that from the tests described in Section 2.0 is not straightforward because the test parameters were different. One useful comparison is the fraction of NO_2^- converted to NO gas. For example, the 3 mL of NO produced during Batch #2 of Test 27A represents 0.05% of the NO_2^- present at the start of that batch. This is only about half the fraction converted during Tests 7A/7B and 14A to 14D (see Item #4 in Section 2.3). There are two reasons for the smaller conversion to NO in Test 27A. One reason is that a somewhat smaller amount of THOREX was added during Batch #2 of Test 27A compared to the other tests. The second reason is the addition of NaOH during Batch #1 of Test 27A such that the pH remained higher than in Tests 7A/7B and 14A to 14D.

4.0 Corrosion Tests

Three separate corrosion investigations were performed in the course of this work. The first tests, called "preliminary corrosion tests," were conducted as adjuncts to the first THOREX/PUREX mixing tests to determine if any severe corrosion problems existed that would show up in short time periods. The second tests were conducted to determine the pH that might be expected in water equilibrated with NO_X evolved during THOREX/PUREX mixing. The third tests were actual corrosion tests conducted using test environments of water equilibrated with a low partial pressure of NO_2. The three tests are discussed below.

4.1 Experimental

Completely different experimental approaches were used in each of the corrosion tests. The different approaches are described in this section.

4.1.1 Preliminary Corrosion Tests

In the preliminary corrosion tests, corrosion coupons made of A516 grade 55 carbon steel (a steel similar to WVNS Tank 8D-2 material) were exposed to the environment resulting after simulated THOREX waste was added to simulated PUREX waste under laboratory test conditions. The specific tests containing the corrosion test coupons were Tests 1 and 3 (see Table 2.6). The coupons were 3/4-in. wide x 1-1/2-in. high x 1/8-in thick, and were cleaned, measured, and weighed before each test. Duplicate coupons were located at each of the three positions shown schematically in Figure C.55 in Appendix C (vapor space, liquid/vapor interface, and submerged). The tests had a duration of approximately 6 h. Corrosion rates in mpy[(a)] were based on weight loss and were calculated by assuming uniform weight loss over the entire surface of each coupon. This assumption is acceptable for these tests since no severe localized corrosion, such as pitting or liquid/vapor interfacial corrosion, was observed.

4.1.2 Determination of pH as a Function of NO_2 Partial Pressure

A series of investigations was undertaken to determine the potential seriousness of the attack of NO_X on the walls of Tank 8D-2. Before the investigations could progress to the experimental stage, it was necessary to develop a logical, conservative scenario for acid generation that would be amenable to laboratory simulation and investigation. The scenario that was developed was based on the following assumptions:

1. The amount of gas generated would be based on the experimental THOREX/PUREX mixing runs;

(a) mil/year, where 1 mil = 0.001 in.

2. The NO generated would react with air to form NO_2 at a certain partial pressure estimated from the generation rate and tank vapor-space volume;

3. The NO_2 would equilibrate with the film of water condensate assumed to be present on the steel in the tank's vapor space to form a film of continually replenished dilute acid.

The foregoing assumptions, considered strongly conservative, were reflected in the experimental approach, in which gas of a given NO or NO_2 partial pressure was allowed to equilibrate for times up to 45 h with a relatively large volume of water to determine the resulting pH as a function of the partial pressure of NO_2.

An order-of-magnitude estimate of the approximate NO_X partial pressure expected in the plenum of Tank 8D-2 during THOREX neutralization was made by using the procedure described below. It is based on the amount of NO produced in Test 2 (Table 2.6 in Section 2.2.1), which was the maximum amount of NO produced in the first three THOREX/PUREX mixing tests.

If it is assumed 1) that the amount of NO_2 generated is equal to the amount of NO that was produced in the Test 2 mixing run (equivalent to 13 mL/L of PUREX solution, or 27,000 L for the 2.1×10^6 L of PUREX solution in Tank 8D-2); 2) that the total amount of NO_2 generated is independent of the THOREX addition rate; 3) that the total volume of THOREX from Tank 8D-4 is added to Tank 8D-2 over a period of 10 days; 4) that the plenum space in the tank is 1,600,000 L; and (5) that the tank is vented at 100 ft^3/min (2,800 L/min); then

$$\text{Total air vol.} = 1.6 \times 10^6 + (2800 \text{ L/min})(1440 \text{ min/day})(10 \text{ days}) = 4.2 \times 10^7 \text{ L}$$

and

$$NO_2 \text{ concentration} = 2.7 \times 10^4 / 4.2 \times 10^7 = 6.4 \times 10^{-4} \text{ atm, or } 0.064 \text{ mole \% } NO_2.$$

This was considered to be a conservative upper limit on the NO_2 concentration expected in a stirred system.[a] Later it was determined that the total NO amounts were likely to be much less than the maximum found and referred to in the first three mixing tests. Therefore, the partial pressure of NO_2 in the third pH run in this test series was reduced by a factor of ~ 13 to <0.005 mole %, which corresponds approximately to the amounts of NO found in Tests 17A to 17C (Table 2.9 in Section 2.2.1), for example.

An experimental apparatus was set up wherein cylinders containing nitrogen oxide (either NO or NO_2), O_2, and N_2 were connected to a common manifold. The gases, blended to form the desired NO_2/simulated air mixture, were conducted through a length ($\sim 10'$) of Tygon tubing, a gas sample bulb, and a gas dispenser into a sealed resin kettle containing 2.7 L of stirred distilled water. The pH in the distilled water was monitored continuously by a temperature-compensated pH meter. Tests were conducted at temperatures ranging from 20° to 40°C.

(a) Tests 11 and 12 (Table 2.8 in Section 2.2.1) show that the amount of NO can be much higher in an unstirred system.

4.1.3 Determination of Corrosiveness of NO_2-Equilibrated Solutions

The pH values attained in the tests described above were low enough to justify performance of actual steel corrosion tests. The tests were conducted in wet and humid environments at temperatures of 40°C and 50°C. The steel coupons were ASTM A516 grade 55 carbon steel, similar in composition and microstructure to the material of construction for Tank 8D-2. The NO_2 gas was continually supplied to the system from a gas bottle and diluted by a carrier gas of ~80% N_2 and ~20% O_2. The target concentration for the NO_2 was ~100 ppm, and the total gas flow through the system was ~20 L/h. Figure C.55 (Appendix C) is a schematic representation of the test system.

Four vessels were used for the tests (Figure C.55 in Appendix C). Before coupons were added to the vessels, the gas was purged through the system to equilibrate the water with the NO_2 resulting in a pH of 4.0 in vessels 1 and 2; the pH in vessels 3 and 4 was 4.3 and 5.0, respectively. In two vessels (one at 40°C and one at 50°C) the gas was bubbled into the water through a gas sparging tube. Six coupons were suspended in each of these vessels: two in the vapor space, two at the air/water interface, and two totally submerged in the water. In the other two vessels (one at 40°C and one at 50°C) the gas flow passed into and out of the plenum region of the vessels and was not bubbled into the water. In these vessels, one coupon was suspended in each vessel so that water just covered the coupon surface.

4.2 Results

All of the corrosion test results are presented in this section of the report.

4.2.1 Preliminary Corrosion Tests

The results of the preliminary corrosion tests are presented in Table 4.1. Tests 1 and 3 in that table are the same as Tests 1 and 3 in Table 2.6 (Section 2.2.1). There was no appreciable difference in corrosion rates between submerged, interface, and vapor-space coupons. The 6 h test time was apparently not long enough to initiate and grow pits, which have always occurred on vapor space coupons (and some submerged specimens) in sludge-wash tests.

The major conclusion that was drawn from these brief corrosion tests is that no severe steel degradation was observed, such as pitting or knife-line interfacial attack. Some localized etching of some coupons was observed where they touched the supports. This observation suggests that pitting and crevice corrosion might eventually occur in these locations.

4.2.2 Determination of pH as a Function of NO_2 Partial Pressure

Figure C.56 (Appendix C) shows results from a total of three runs that were made. In Run No. 1, the nitrogen oxide gas was NO. In this run, the total gas flow rate was approximately 12 L/h. The gas analysis from the sample bulb showed the gas mixture to consist of 0.03% NO_X, 86% N_2, and

Table 4.1. Summary of Corrosion Results

Test No.	Coupon Position	Corrosion Rate (mpy)
1	Vapor	12.7
	Vapor	6.5
	Interface	5.0
	Interface	5.6
	Submerged	7.1
	Submerged	7.1
3	Vapor	4.0
	Vapor	8.5
	Interface	7.9
	Interface	9.7
	Submerged	10.1
	Submerged	7.3

14% O_2.[a] (The mass spectrometer cannot differentiate between NO and NO_2. However, because NO is known to oxidize to NO_2 in the presence of O_2, the "NO_2" in the analysis was assumed to be NO_2.) The temperature was maintained at 21 $\pm$1°C for the duration of the run, until a reasonably stable (very slowly decreasing) pH of 3.3 was observed at ~23 h. The temperature of the system was then increased to 39°C, and a reasonably stable (very slowly decreasing) pH of 3.1 resulted. The pH values reported are temperature-corrected.

The second run, Run No. 2, was performed in essentially the same way as the first, except that nitrogen dioxide (NO_2) was substituted for the NO of the previous run, and the flow rate of the diluent gas, N_2, was increased. The total flow rate in the second run was approximately 40 L/h. The gas in the second run consisted of 0.06% NO_2, 76.4% N_2, and 23.4% O_2. After 25 h, the pH of the water was a reasonably stable (very slowly decreasing) value of 3.0. The temperature of the system was then increased to 39°C, and a (very slowly decreasing) pH of 2.9 was observed after ~3 h.

The third run, Run No. 3, was an attempt to obtain an NO_2 concentration in the gas stream of ~0.009%. The gas analysis mass spectrometer was not successful in sensing the NO_2 concentration in this run. The limit of detection of the mass spectrometer for NO_2 is estimated to be ~0.005 mole % under the circumstances of the analysis; this value is probably as valid an estimate for the NO_2 concentration as can be achieved for this test. When the solution temperature was increased to 40°C at 48 h total test time, the pH decreased from 3.96 to 3.89. The test was then terminated.

(a) All gas compositions are given in mole %.

The pH values attained over periods of 20 to 40 h were low enough (<4) to be considered potentially important in assessing the corrosive effects of such gas-water-equilibrated solutions on carbon steel (Whitman, Russell and Altieri 1924). A corrosion test was therefore conducted to obtain actual corrosion data.

4.2.3 Determination of Corrosiveness of NO_2-Equilibrated Solution

The corrosion tests were conducted for 20 days. Only a limited supply of NO_2 gas was available at the beginning of the test, and a second bottle was ordered on an emergency basis before testing began. When it had not been received about halfway through the test, the NO_2 flow was reduced to about half the initial flow, thus reducing its concentration in the test vessels to ~50 ppm. The bottle was still not delivered by the end of the test; before the planned test end, the NO_2 was exhausted. During the last four days only N_2 and O_2 passed through the system. The pH of the water in the vessels was monitored during the test, and remained fairly constant between about 3.5 and 4.5 with the NO_2 flowing (even at the lower concentration). The pH did start to increase once the NO_2 ran out and increased to 5.5 in vessel 1 and about 8.0 in the other three vessels at the conclusion of the test.

After 20 days exposure, the coupons were removed and cleaned in an inhibited acid solution to remove corrosion products. The coupons were then weighed and examined. The uniform corrosion rates calculated from weight loss measurements are shown in Table 4.2. Pits were observed on all specimens. Pit depths were measured with an optical micrometer. The depths of the deepest pits observed on each specimen are shown in Table 4.2. Pitting was markedly more severe on wetted coupons. Those coupons suspended in the vapor spaces of the first two vessels described above were nearly free of pits.

The test temperature, over the narrow range employed, appeared to have some effect on corrosion, with the highest corrosion rates observed at the lower temperature. The statistical significance of this observation is not clear, given the limited number of specimens and the limited test duration.

Neither the uniform corrosion of the test specimens nor the nonuniform (pitting) corrosion would appear to present any potential hazard to Tank 8D-2 if the laboratory simulation described herein represents a reasonably close approximation to the conditions existing within the tank during the actual THOREX neutralization process.

4.3 Discussion

Passage of simulated air containing low concentrations of NO_2 into a fixed volume of H_2O has been shown to be capable of reducing the pH of the gas-equilibrated H_2O to values <4, even at concentrations of NO_2 as low as 0.005 mole %. The potential for high corrosion rates therefore exists, if NO_2-equilibrated H_2O were to contact carbon steel for protracted periods of time, and if the NO_2 were continually replenished to maintain such a low pH level at the steel surface. Actual steel corrosion tests performed in the presence of low partial pressures of NO_2 and either liquid water or water vapor showed that for "short" time periods, e.g., time periods of <100 days, there would be no significant degradation of a tank wall if it were contacted by NO_2^- equilibrated H_2O at NO_2 concentrations of 0.01 to 0.005 mole % in air.

Table 4.2. Corrosion Rates and Pit Depths for NO_2 Corrosion Tests

Vessel ID/ Temperature	Coupon Position	Uniform Corrosion Rate (mils/year)	Deepest Pits (mils)	Coupon ID#
Vessel #1 40°C	Vapor	1.05	5	421
		1.02	6	422
	Interface	14.87	10	423
		15.31	14	424
	Submerged	21.12	7	425
		22.75	8	426
Vessel #2 50°C	Vapor	0.58	5	427
		0.43	4	428
	Interface	15.21	11	429
		13.76	10	430
	Submerged	12.82	11	431
		12.96	11	432
Vessel #3 / 40°C	Wetted	5.51	6	433
Vessel #4 / 50°C	Wetted	4.78	5	434

5.0 References

Bray, L.A., and B.M. Wise. 1986. *Chemistry Required for Tank 8D-4 Thoria Waste Removal*, WVST 86/59 JRC. Pacific Northwest Laboratory, Richland, Washington.

Whitman, W., R. Russell, and V. Altieri. 1924. *Industrial Engineering Chemistry*, Vol. 16, p. 665.

Yost, D.U., and H.R. Russell, Jr. 1944. *Systematic Chemistry of the 5th and 6th Group* Nonmetallic Elements, Prentice Hall.

Appendix A

Rheological and Flow Properties of NT-1 and NT-5 Samples

Appendix A

Rheological and Flow Properties of NT-1 and NT-5 Samples

The rheological properties of two THOREX was samples were measured using the Bohlin CS viscometer modified for glovebox operations. The measuring geometry used for these samples consisted of concentric cylinders with a 25 mm diameter inner cylinder and a 2.5 mm gap between the cylinders (Bohlin C25 measuring sensor). These properties were obtained by measuring the shear rate required to obtain a specified shear stress. The specified shear stresses were ramped to provide a shear rate range from 0 to approximately 500 s^{-1}. Duplicate runs were performed on each sample at two temperatures (25 and 65°C). Plots of the shear stress and viscosity as a function of shear rate are attached.

Both samples exhibited some dilatant behavior over the measuring range (0 to 500 s^{-1}), but this effect is minimal. Dilatancy generally occurs in concentrated suspensions which tend to gel upon mixing. The viscosity of dilatant liquids increases with increasing shear rate. For the NT-1 samples the viscosity of this sample at 25°C ranges from 6 to 3 cP (mPa•s) over most of the shear rate range. At 65°C the viscosity is somewhat lower than at 25°C. The viscosity of this sample at 65°C ranges between 4 and 2 cP.

The NT-5 sample has a significant yield stress, and the data was fit to a power law equation (see Equation A.1). The yield stress and power law curve fit parameters for the duplicate runs at 25 and 65°C are reported in Table A.1. The data was fit to a power law fit to obtain the necessary parameters to model the flow properties of these samples. The flow properties of these samples were determined using the method of Hanks to calculate Hedstrom Numbers, values of friction factor as a function of Reynolds number, and pressure drop as a function of velocity for turbulent, non-Newtonian fluid flow. The data obtained from this analysis are given in Table A.2 and on the attached computer printouts.

$$T = T_S + K\gamma^n \qquad (A.1)$$

where T is the shear stress of the sample,
T_S is the yield stress of the sample,
K is the consistency parameter,
γ is the shear rate, and
n is the flow behavior index.

Table A.1. Power Law Curve Fit Parameters for Sample NT-5

Temperature (°C)	Run	Yield Stress (Pa)	Consistency Parameter (Pa•s)	Flow Behavior Index
25	1	0.71	2.37×10^{-2}	0.86
	2	0.73	8.87×10^{-3}	1.00
65	3	0.53	3.83×10^{-3}	1.09
	4	0.63	3.63×10^{-4}	1.43

Table A.2. Flow Behavior Properties for NT-5 Sample

				Values for Critical		
Pipe Diameter (in.)	Temp. (°C)	Run	Hedstrom Number	Reynolds Number	Velocity (ft/s)	Flow Rate (GPM)
2	25	1	13,900	3,800	2.3	24
		2	32,700	4,700	2.0	21
	65	3	56,500	5,800	1.6	16
		4	205,000	14,300	1.3	13
3	25	1	30,600	4,600	2.0	47
		2	72,100	6,100	1.8	41
	65	3	124,000	7,900	1.4	31
		4	422,000	22,600	1.1	25

BOHLIN CS RHEOMETER
Stress viscometry test
1993-08-19 09: 26: 13 # 1

- Viscosity
o-o Shear stress

C 25

CDt 10 s It 60 s
No of M 1
MI 5 s

T 24.9 - 25.1 C

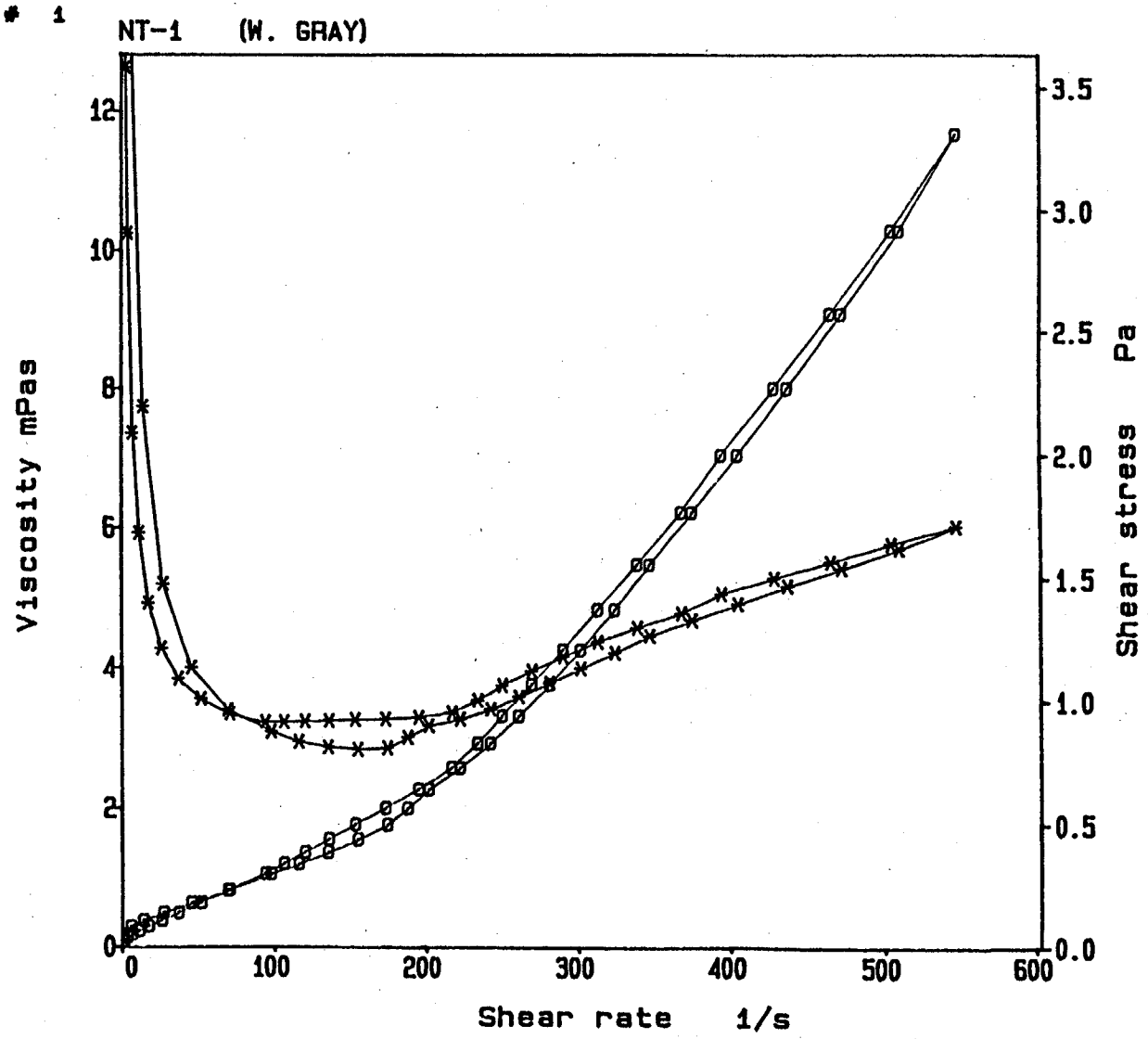

BOHLIN CS RHEOMETER
Stress viscometry test
1993-08-19 10:44:19 # 1

- Viscosity
⊖-⊖ Shear stress

C 25

CDt 10 s It 60 s
No of M 1
MI 5 s

T 24.9 - 25.1 C

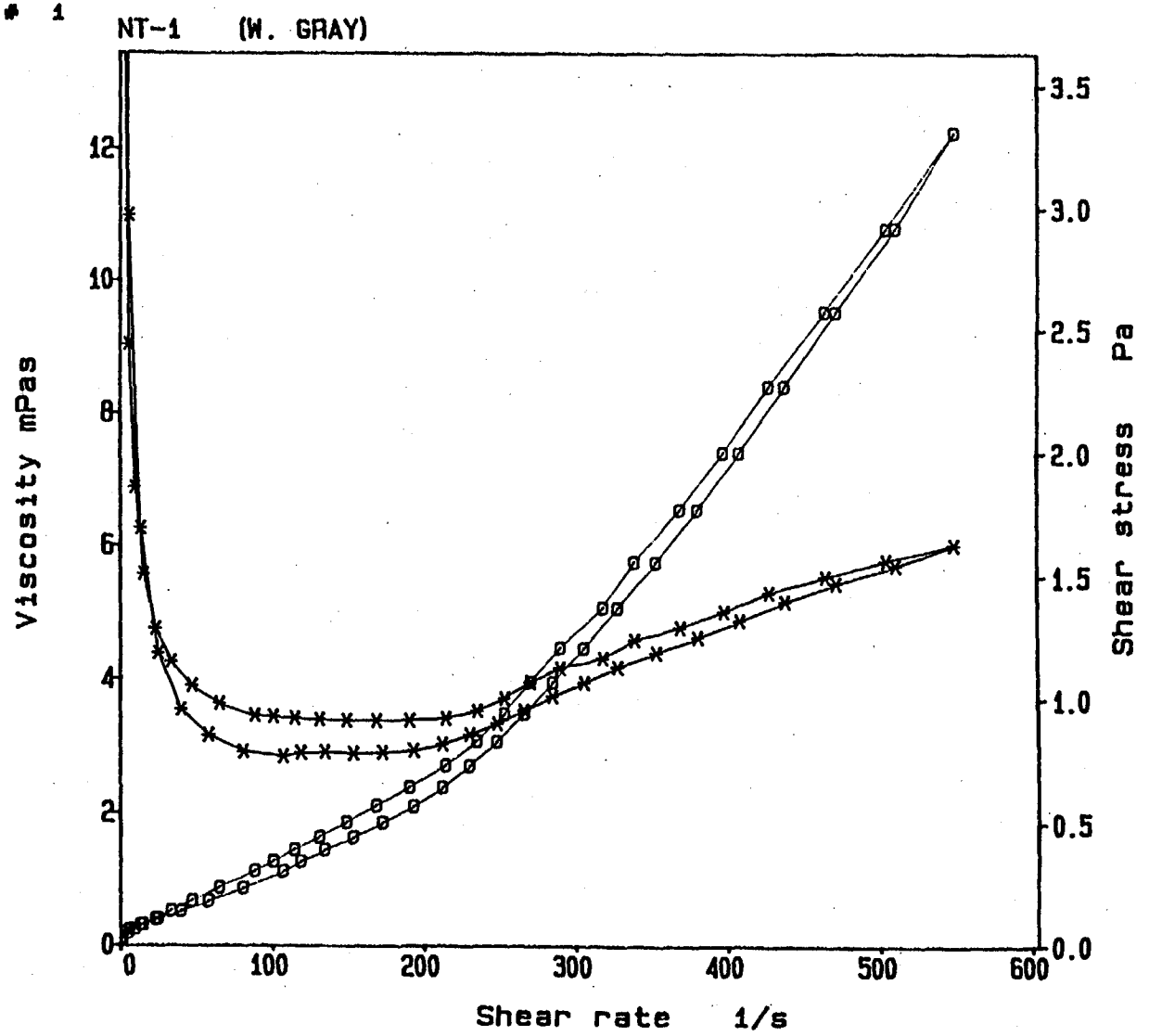

BOHLIN CS RHEOMETER
Stress viscometry test
1993-08-20 11:09:29 # 1

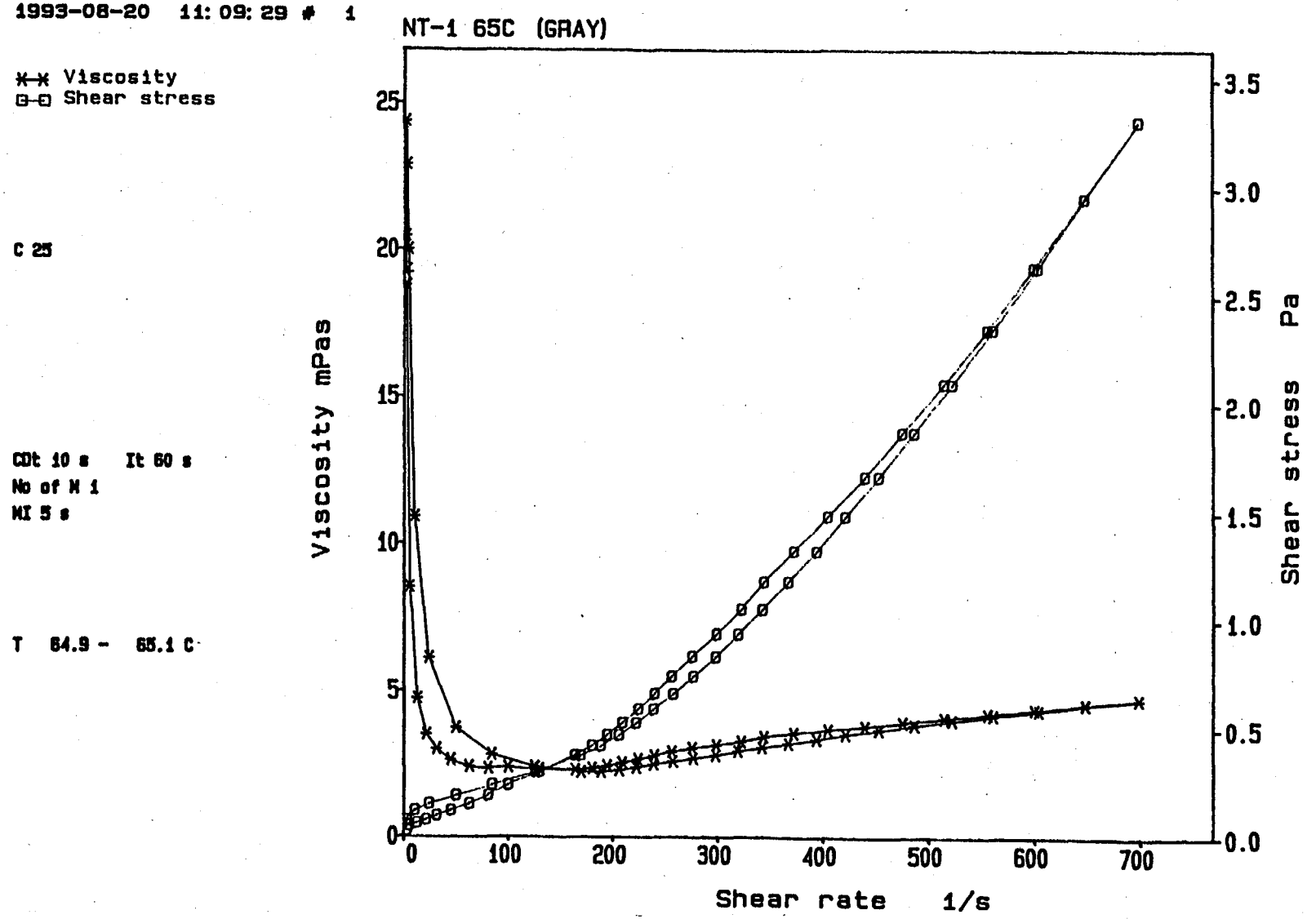

BOHLIN CS RHEOMETER
Stress viscometry test
1993-08-20 10:16:39 # 1

*
- Viscosity
o-o Shear stress

C 25

COt 10 s It 60 s
No of M 1
MI 5 s

T 64.9 - 65.1 C

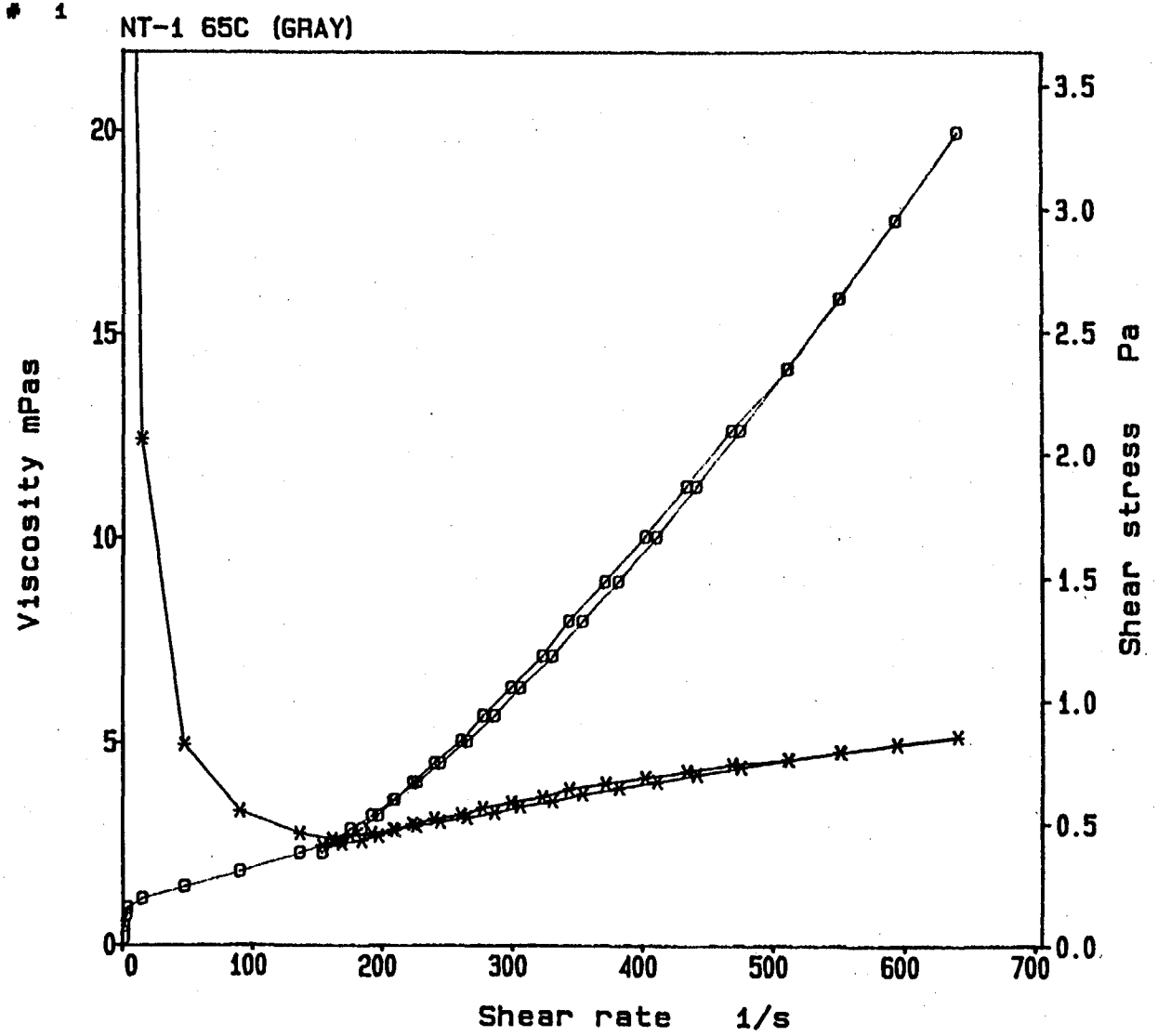

BOHLIN CS RHEOMETER
Stress viscometry test
1993-08-19 13:30:58 # 1

X–X Viscosity
⊡–⊡ Shear stress

C 25

CDt 10 s It 60 s
No of M 1
MI 5 s

T 24.9 - 25.1 C

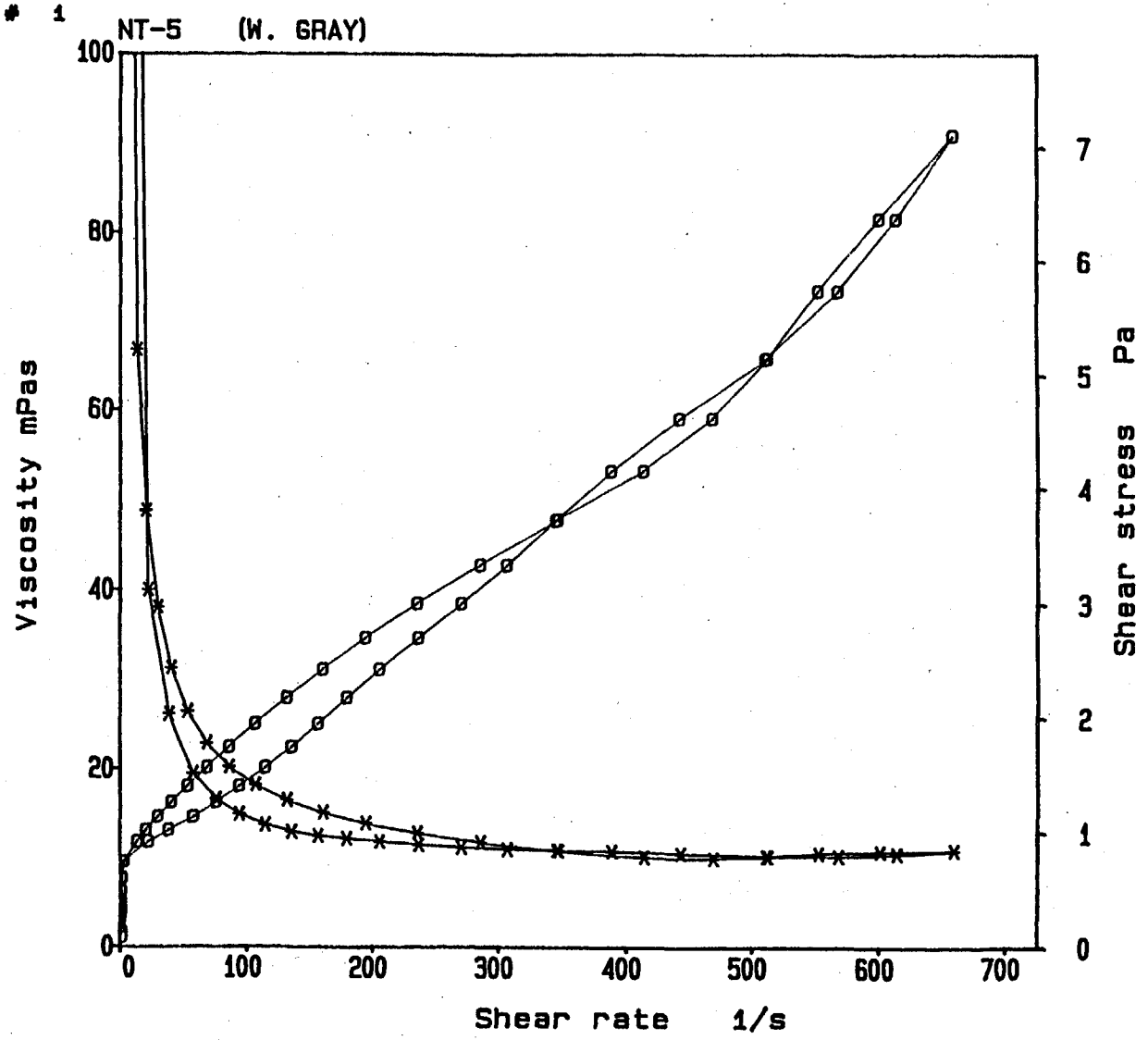

BOHLIN CS RHEOMETER
Stress viscometry test
1993-08-19 12:20:02 # 1

X–X Viscosity
⊡–⊡ Shear stress

C 25

COt 10 s It 60 s
No of M 1
MI 5 s

T 24.9 - 25.1 C

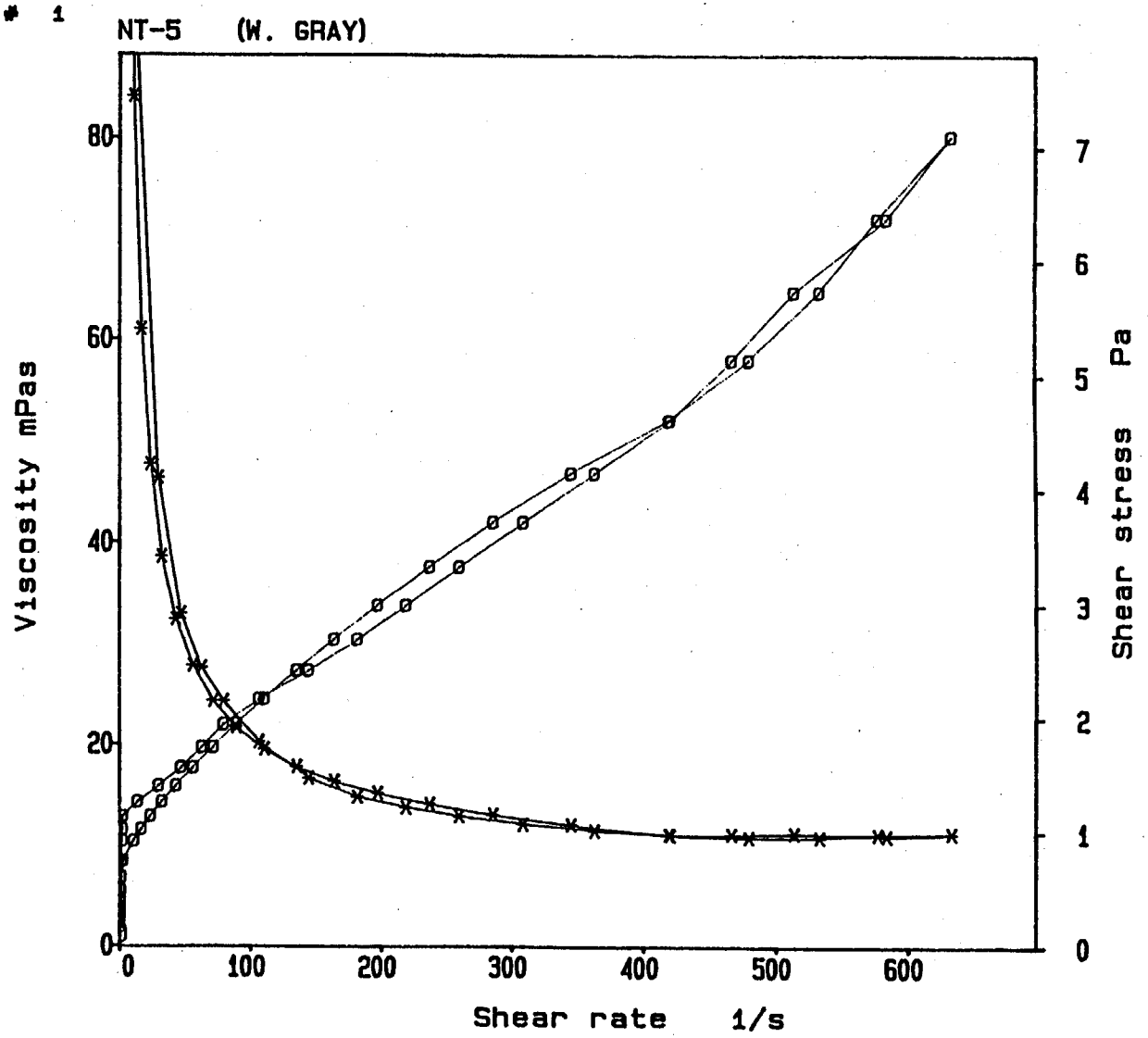

BOHLIN CS RHEOMETER
Stress viscometry test
1999-08-20 12:37:53 # 1

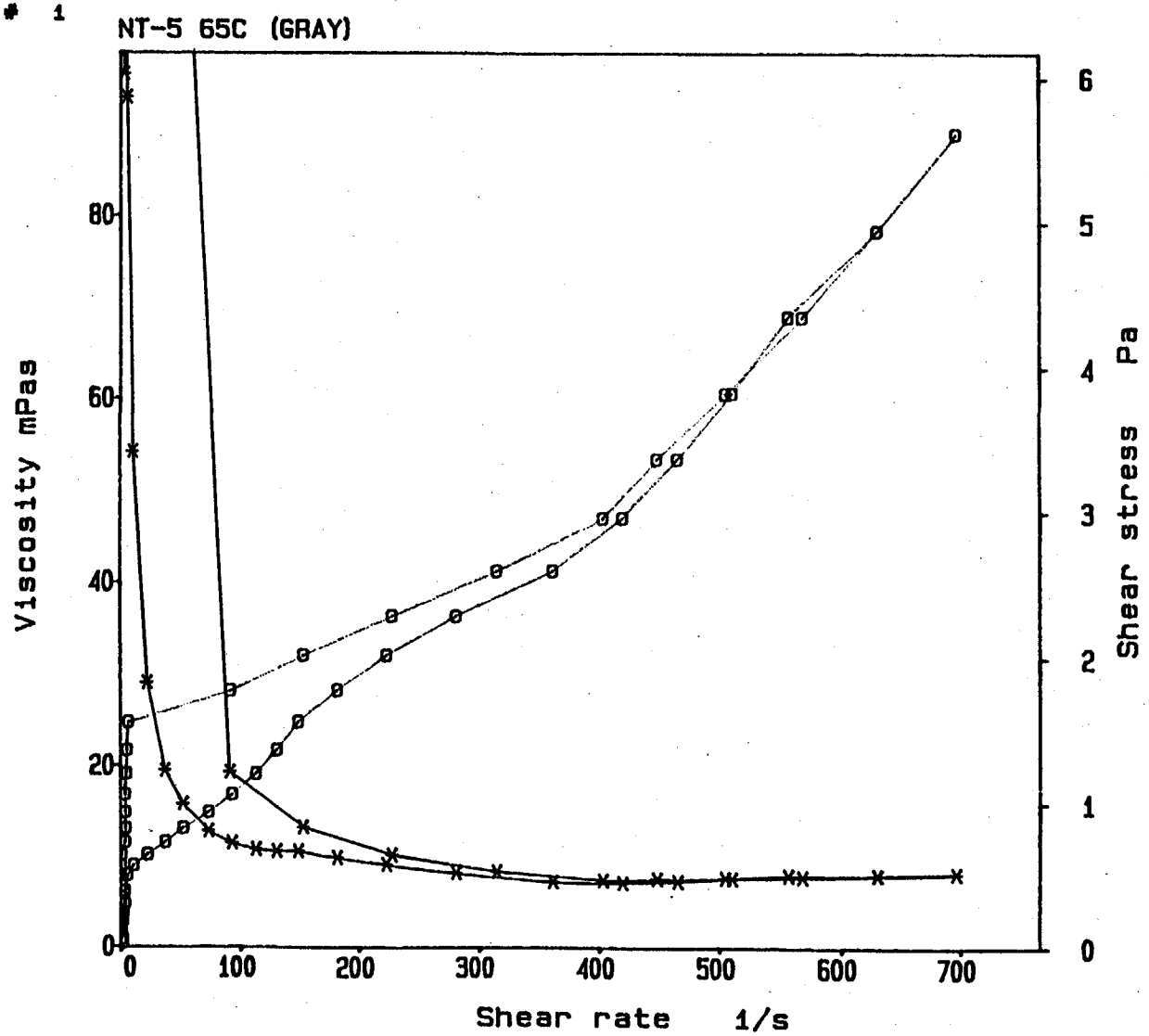

C 25

CDt 10 s It 60 s
No of M 1
MI 5 s

T 64.9 - 65.2 C

C:\DATA\NT565C1

BOHLIN CS RHEOMETER
Stress viscometry test
1993-08-20 13:39:44 # 1

- Viscosity
o-o Shear stress

C 25

CDt 10 s It 60 s
No of M 1
MI 5 s

T 64.9 - 65.1 C

C:\DATA\NT565C2

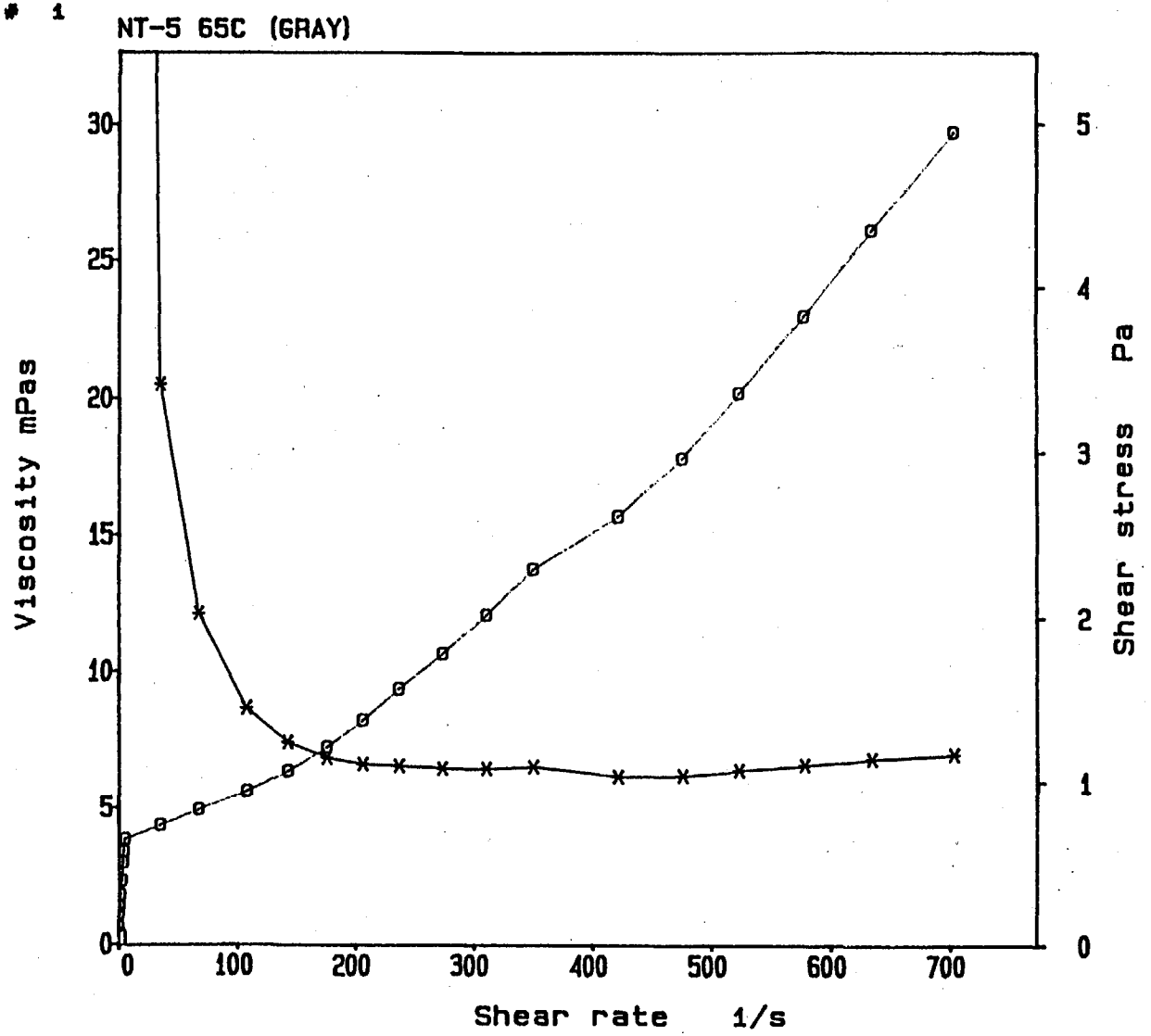

YIELD POWER LAW MODEL

NT-5 Run # 1 25°C

DIAMETER = 2.07 in.
YIELD STRESS (To) = 0.71 Pa
CONSISTENCY (K) = 0.237E-01 Pa*s^m
DENSITY = 1.28 g/cm^3
FLOW BEHAVIOR INDEX (M) = 0.857

HEDSTROM NUMBER = 13869.6
RECRIT = 3791.7
VCRIT = 2.33 ft/S
FLOW CRIT = 24.33 GPM
B = 45.301128

POINT	VELOCITY Vel(fps)	REYNOLDS Re	FRICTION FACTOR f	PRESSURE GRADIENT dP/L (Psi/100 ft)
0	0.50	654.2	0.08419	0.420
1	1.00	1444.8	0.02634	0.526
2	1.50	2296.6	0.01382	0.621
3	2.00	3190.7	0.00889	0.710
4	2.50	4117.7	0.00644	0.804
5	3.00	5071.8	0.00596	1.072
6	3.50	6049.0	0.00572	1.398
7	4.00	7046.4	0.00549	1.752
8	4.50	8061.8	0.00529	2.138
9	5.00	9093.6	0.00512	2.556
10	5.50	10140.2	0.00498	3.006
11	6.00	11200.5	0.00485	3.487
12	6.50	12273.6	0.00474	3.999
13	7.00	13358.5	0.00464	4.541
14	7.50	14454.6	0.00455	5.113
15	8.00	15561.2	0.00447	5.714

YIELD POWER LAW MODEL

NT-5 Run #2 25°C

DIAMETER = 2.07 in.
YIELD STRESS (To) = 0.73 Pa
CONSISTENCY (K) = 0.887E-02 Pa*s^m
DENSITY = 1.28 g/cm^3
FLOW BEHAVIOR INDEX (M) = 1.000

HEDSTROM NUMBER = 32736.6
RECRIT = 4694.2
VCRIT = 2.03 ft/S
FLOW CRIT = 21.26 GPM
B = 30.278660

POINT	VELOCITY Vel(fps)	REYNOLDS Re	FRICTION FACTOR f	PRESSURE GRADIENT dP/L (Psi/100 ft)
0	0.50	1154.6	0.07468	0.373
1	1.00	2309.3	0.02265	0.452
2	1.50	3463.9	0.01171	0.526
3	2.00	4618.5	0.00749	0.598
4	2.50	5773.2	0.00657	0.819
5	3.00	6927.8	0.00646	1.160
6	3.50	8082.5	0.00629	1.538
7	4.00	9237.1	0.00613	1.959
8	4.50	10391.7	0.00600	2.425
9	5.00	11546.4	0.00588	2.936
10	5.50	12701.0	0.00578	3.490
11	6.00	13855.6	0.00569	4.087
12	6.50	15010.3	0.00560	4.726
13	7.00	16164.9	0.00552	5.406
14	7.50	17319.6	0.00545	6.126
15	8.00	18474.2	0.00539	6.886

NT-5 Run #3 65°C

YIELD POWER LAW MODEL

DIAMETER = 2.07 in.
YIELD STRESS (To) = 0.53 Pa
CONSISTENCY (K) = 0.383E-02 Pa*s^m
DENSITY = 1.28 g/cm^3
FLOW BEHAVIOR INDEX (M) = 1.090

HEDSTROM NUMBER = 56476.0
RECRIT = 5801.4
VCRIT = 1.56 ft/S
FLOW CRIT = 16.31 GPM
B = 24.805401

POINT	VELOCITY Vel(fps)	REYNOLDS Re	FRICTION FACTOR f	PRESSURE GRADIENT dP/L (Psi/100 ft)
0	0.50	2061.2	0.05178	0.259
1	1.00	3873.0	0.01557	0.311
2	1.50	5601.4	0.00803	0.361
3	2.00	7277.6	0.00667	0.533
4	2.50	8916.1	0.00653	0.815
5	3.00	10525.2	0.00638	1.146
6	3.50	12110.2	0.00625	1.529
7	4.00	13674.9	0.00615	1.964
8	4.50	15222.1	0.00606	2.449
9	5.00	16753.8	0.00598	2.983
10	5.50	18271.8	0.00590	3.565
11	6.00	19777.3	0.00584	4.195
12	6.50	21271.7	0.00577	4.870
13	7.00	22755.7	0.00571	5.591
14	7.50	24230.2	0.00566	6.357
15	8.00	25695.8	0.00561	7.167

YIELD POWER LAW MODEL

NT-5 Run #4 65°C

DIAMETER = 2.07 in.
YIELD STRESS (To) = 0.63 Pa
CONSISTENCY (K) = 0.363E-03 Pa*s^m
DENSITY = 1.28 g/cm^3
FLOW BEHAVIOR INDEX (M) = 1.420

HEDSTROM NUMBER = 204550.6
RECRIT = 14382.9
VCRIT = 1.26 ft/S
FLOW CRIT = 13.23 GPM
B = 16.522469

POINT	VELOCITY Vel(fps)	REYNOLDS Re	FRICTION FACTOR f	PRESSURE GRADIENT dP/L (Psi/100 ft)
0	0.50	8397.7	0.05141	0.257
1	1.00	12553.3	0.01436	0.287
2	1.50	15881.4	0.00709	0.318
3	2.00	18765.2	0.00538	0.430
4	2.50	21358.1	0.00520	0.648
5	3.00	23740.3	0.00522	0.938
6	3.50	25960.7	0.00528	1.292
7	4.00	28051.2	0.00535	1.710
8	4.50	30034.5	0.00542	2.191
9	5.00	31927.1	0.00548	2.734
10	5.50	33741.7	0.00553	3.338
11	6.00	35488.2	0.00557	4.003
12	6.50	37174.6	0.00560	4.728
13	7.00	38807.3	0.00564	5.514
14	7.50	40391.7	0.00566	6.358
15	8.00	41932.3	0.00568	7.262

Appendix B

Particle-Size Distribution Results

Appendix B

Particle-Size Distribution Results

This appendix shows the results of particle-size distribution measurements made by a Brinkman particle-size analyzer on two slurries produced by mixing dilute THOREX with 1 M NaOH (designated NT-1) and with 5 M NaOH (designated NT-5). Results are also shown for a glass sphere reference standard, Duke 147, with a nominal mean particle diameter of 20 μm.

Results for the standard are shown on a volume density graph using a logarithmic scale. Results for the two slurries are shown in three ways: (1) a number density graph with a logarithmic scale; (2) a volume density graph with a logarithmic scale; and (3) a volume density graph using a linear scale.

The number density graphs list the mean particle diameter based on the total number of particles, which was calculated by Equation (B.1).

$$\text{Mean(nl)} = \Sigma d/n \qquad \text{(B.1)}$$

where Σd = summation over the measured individual particle diameters
n = total number of particles.

The volume density graphs list mean particle diameters based on the total volume of particles in two ways, Equations (B.2) and (B.3).

$$\text{Mean(nv)} = \Sigma V/n \qquad \text{(B.2)}$$

where ΣV = summation over the measured individual particle volumes
n = total number of particles

$$\text{Mean(vm)} = \Sigma Vd/\Sigma V \qquad \text{(B.3)}$$

where ΣVd = summation over the measured individual particle volumes multiplied by their measured diameters
ΣV = total volume of particles

The last equation gives the mean particle diameter that is probably most useful. See Section 3.1.3 for additional discussion of the different ways of representing the particle-size results.

G A L A I — C I S — 1

Computerized Inspection System

SAMPLE NAME : DUKE 147
FILE NAME : DUKE147.072

MCBurt

DATE	: 12/08/1993	ACQ. RANGE	: 0.5-150	COUNTS	: 36964
TIME	: 09:23	ACQ. MODE	: SAMPLE	S.N.F.	: 0.74
CONFIG.	: 1 (0.7 S1)	ACQ. TIME	: 189 SEC	S.D.U.	: 2895
CELL TYPE	: MAGNETIC (2)	SAMPLE SIZE	: 2	CONCENTR.	: 3.2E+05 #/ml
SAMPLE TYPE	: REGULAR	REQ. CONF.	: 95.00 %(V)	SOLIDS	: 9.5E-03 %

M+TE WC02018
Proc. ALO-530

PROBABILITY VOLUME DENSITY GRAPH

Name: DUKE 147
9.5E-05 cc/ml(100.0%)
Mode at 21.39 µm
<< SCALE RANGE (µm): ADJUSTED >>

Mean(nv): 8.29µm
S.D.(nv): 6.44µm

Median : 20.32µm
Mean(vm): 19.57µm
S.D.(vm): 4.99µm
Conf(vm): 99.28 %

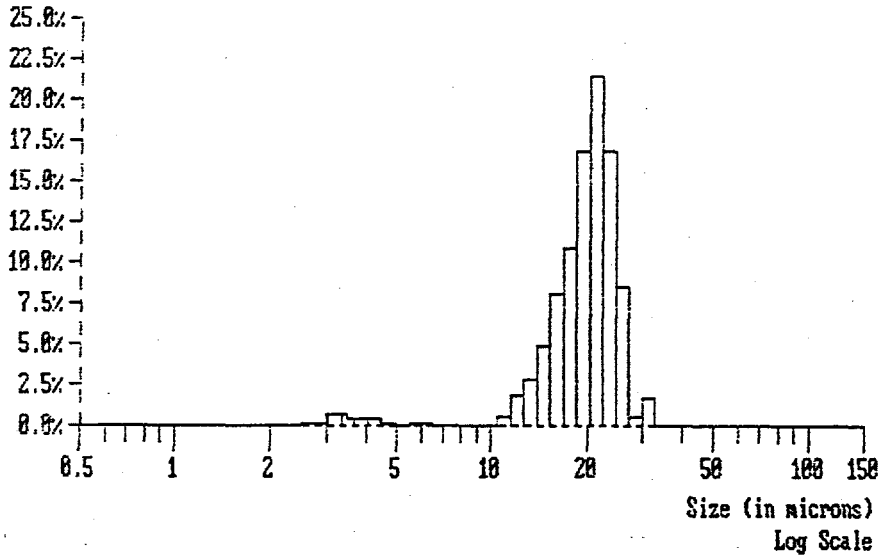

SAMPLE NAME : 93-10459/NT-1
FILE NAME : 9310459.001

DATE	: 12/08/1993	ACQ. RANGE	: 0.5-150	COUNTS	: 29561
TIME	: 09:39	ACQ. MODE	: SAMPLE	S.N.F.	: 0.59
CONFIG.	: 1 (0.7 S1)	ACQ. TIME	: 202 SEC	S.D.U.	: 2268
CELL TYPE	: MAGNETIC (2)	SAMPLE SIZE	: 3 (ABORTED)	CONCENTR.	: 6.8E+05 #/ml
SAMPLE TYPE	: SPECIAL	REQ. CONF.	: 95.00 %(V)	SOLIDS	: 5.7E-02 %

PROBABILITY NUMBER DENSITY GRAPH

Name: 93-10459/NT-1
6.8E+05 #/ml(100.0%)
Mode at 1.25 µm
<< SCALE RANGE (µm): ADJUSTED >>

Median : 1.25µm
Mean(nl): 2.27µm
S.D.(nl): 5.00µm
Conf(nl): 93.48 %

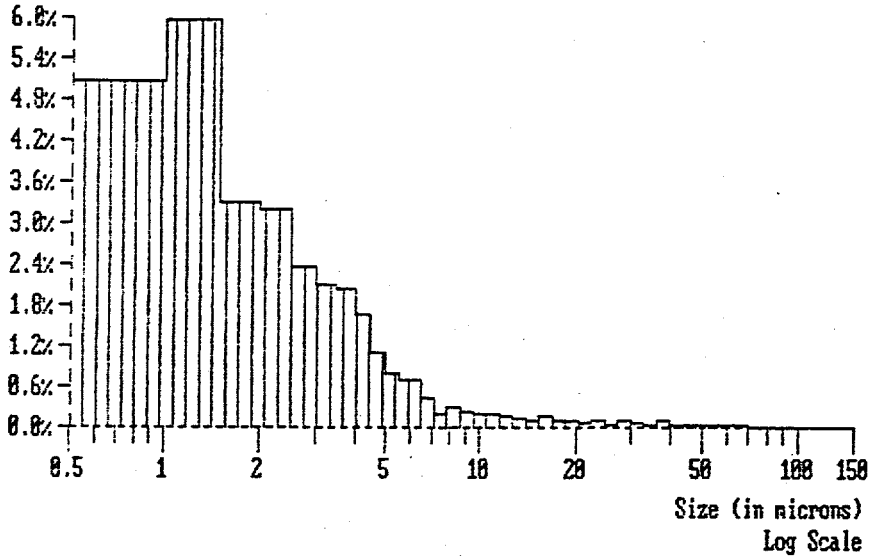

G A L A I — C I S — 1

Computerized Inspection System

SAMPLE NAME : 93-10459/NT-1
FILE NAME : 9310459.001

MCBurt

DATE	: 12/08/1993	ACQ. RANGE	: 0.5-150	COUNTS	: 29561
TIME	: 09:39	ACQ. MODE	: SAMPLE	S.N.F.	: 0.59
CONFIG.	: 1 (0.7 S1)	ACQ. TIME	: 202 SEC	S.D.U.	: 2268
CELL TYPE	: MAGNETIC (2)	SAMPLE SIZE	: 3 (ABORTED)	CONCENTR.	: 6.8E+05 #/ml
SAMPLE TYPE	: SPECIAL	REQ. CONF.	: 95.00 %(V)	SOLIDS	: 5.7E-02 %

M&TE WC02018
Proc. ALO-530

PROBABILITY VOLUME DENSITY GRAPH

Name: 93-10459/NT-1
5.7E-04 cc/ml(100.0%)
Mode at 107.67 µm
<< SCALE RANGE (µm): ADJUSTED >>

Mean(nv): 11.65µm
S.D.(nv): 10.63µm

Median : 75.16µm
Mean(vm): 76.77µm
S.D.(vm): 31.36µm
Conf(vm): 97.60 %

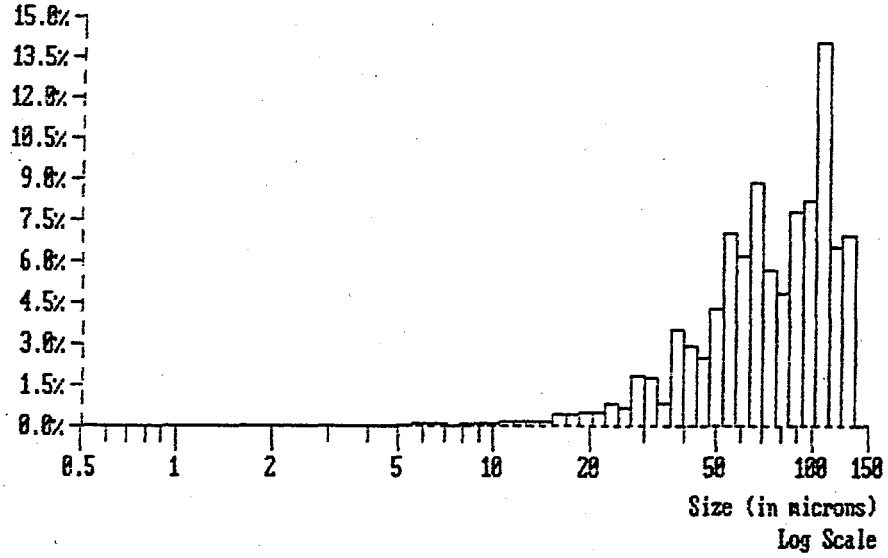

SAMPLE NAME : 93-10459/NT-1
FILE NAME : 9310459.001

DATE	: 12/08/1993	ACQ. RANGE	: 0.5-150	COUNTS	: 29561
TIME	: 09:39	ACQ. MODE	: SAMPLE	S.N.F.	: 0.59
CONFIG.	: 1 (0.7 S1)	ACQ. TIME	: 202 SEC	S.D.U.	: 2268
CELL TYPE	: MAGNETIC (2)	SAMPLE SIZE	: 3 (ABORTED)	CONCENTR.	: 6.8E+05 #/ml
SAMPLE TYPE	: SPECIAL	REQ. CONF.	: 95.00 %(V)	SOLIDS	: 5.7E-02 %

PROBABILITY VOLUME DENSITY GRAPH

Name: 93-10459/NT-1
5.7E-04 cc/ml(100.0%)
Mode at 68.75 µm
<< SCALE RANGE (µm): ADJUSTED >>

Mean(nv): 11.65µm
S.D.(nv): 10.63µm

Median : 75.16µm
Mean(vm): 76.77µm
S.D.(vm): 31.36µm
Conf(vm): 97.60 %

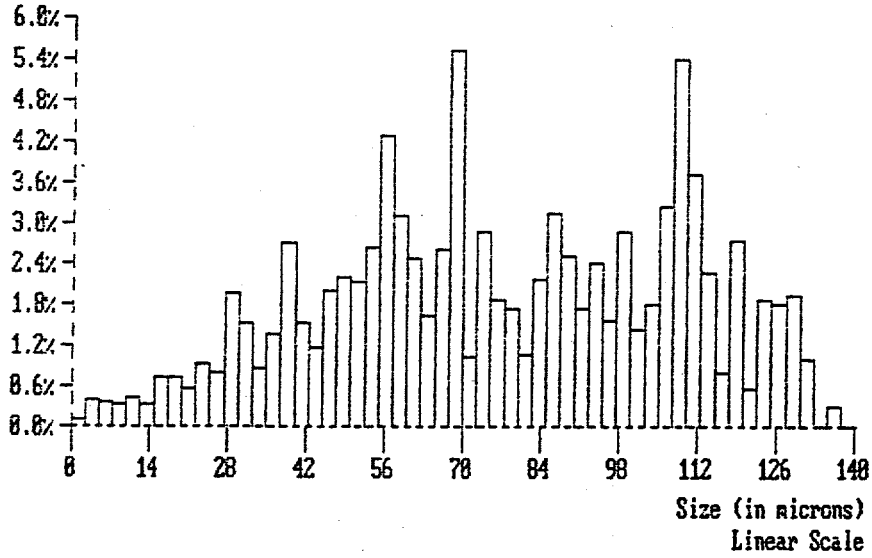

SAMPLE NAME : 93-10460/NT-5
FILE NAME : 9310460.001

DATE	: 12/08/1993	ACQ. RANGE	: 0.5-150	COUNTS	: 8667
TIME	: 10:04	ACQ. MODE	: SAMPLE	S.N.F.	: 0.39
CONFIG.	: 1 (0.7 S1)	ACQ. TIME	: 58 SEC	S.D.U.	: 2228
CELL TYPE	: MAGNETIC (2)	SAMPLE SIZE	: 2	CONCENTR.	: 1.3E+06 #/ml
SAMPLE TYPE	: SPECIAL	REQ. CONF.	: 95.00 %(V)	SOLIDS	: 1.5E-01 %

PROBABILITY NUMBER DENSITY GRAPH

Name: 93-10460/NT-5
1.3E+06 #/ml(100.0%)
Mode at 1.25 µm
<< SCALE RANGE (µm): ADJUSTED >>

Median : 1.18µm
Mean(nl): 2.02µm
S.D.(nl): 5.13µm
Conf(nl): 81.81 %

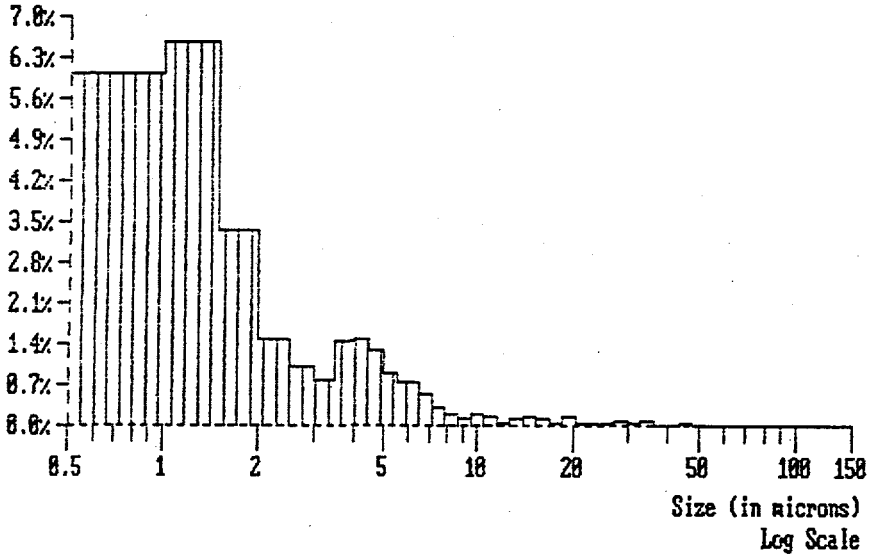

G A L A I — C I S — 1

Computerized Inspection System

SAMPLE NAME : 93-10460/NT-5
FILE NAME : 9310460.001

MCBurt

DATE	: 12/08/1993	ACQ. RANGE	: 0.5-150	COUNTS	: 8667
TIME	: 10:04	ACQ. MODE	: SAMPLE	S.N.F.	: 0.39
CONFIG.	: 1 (0.7 S1)	ACQ. TIME	: 58 SEC	S.D.U.	: 2228
CELL TYPE	: MAGNETIC (2)	SAMPLE SIZE	: 2	CONCENTR.	: 1.3E+06 #/ml
SAMPLE TYPE	: SPECIAL	REQ. CONF.	: 95.00 %(V)	SOLIDS	: 1.5E-01 %

M+TE WC02018
PROC ALO-530

PROBABILITY VOLUME DENSITY GRAPH

Name: 93-10460/NT-5
1.5E-03 cc/ml(100.0%)
Mode at 118.40 µm
<< SCALE RANGE (µm): ADJUSTED >>

Mean(nv): 12.73µm
S.D.(nv): 11.88µm

Median :108.40µm
Mean(vm): 95.47µm
S.D.(vm): 32.58µm
Conf(vm): 95.52 %

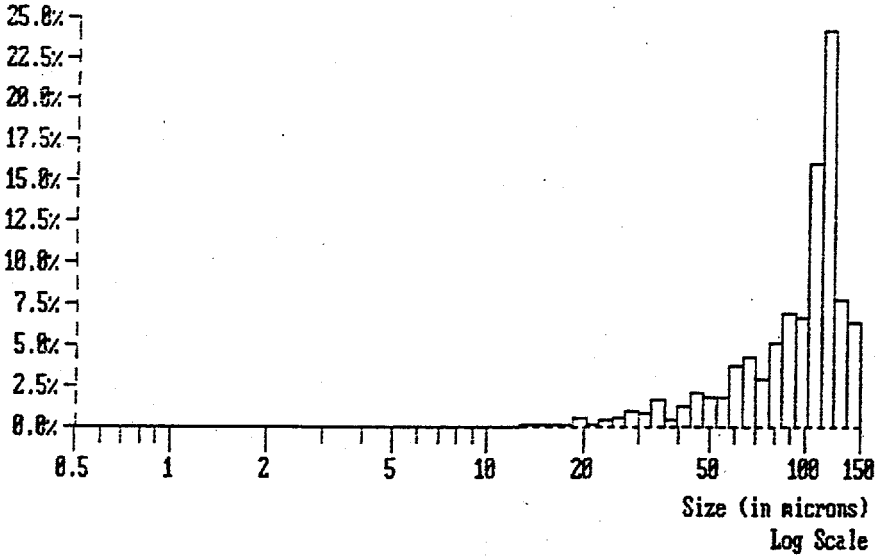

SAMPLE NAME : 93-10460/NT-5
FILE NAME : 9310460.001

DATE	: 12/08/1993	ACQ. RANGE	: 0.5-150	COUNTS	: 8667
TIME	: 10:04	ACQ. MODE	: SAMPLE	S.N.F.	: 0.39
CONFIG.	: 1 (0.7 S1)	ACQ. TIME	: 58 SEC	S.D.U.	: 2228
CELL TYPE	: MAGNETIC (2)	SAMPLE SIZE	: 2	CONCENTR.	: 1.3E+06 #/ml
SAMPLE TYPE	: SPECIAL	REQ. CONF.	: 95.00 %(V)	SOLIDS	: 1.5E-01 %

PROBABILITY VOLUME DENSITY GRAPH

Name: 93-10460/NT-5
1.5E-03 cc/ml(100.0%)
Mode at 118.75 µm
<< SCALE RANGE (µm): ADJUSTED >>

Mean(nv): 12.73µm
S.D.(nv): 11.88µm

Median :108.40µm
Mean(vm): 95.47µm
S.D.(vm): 32.58µm
Conf(vm): 95.52 %

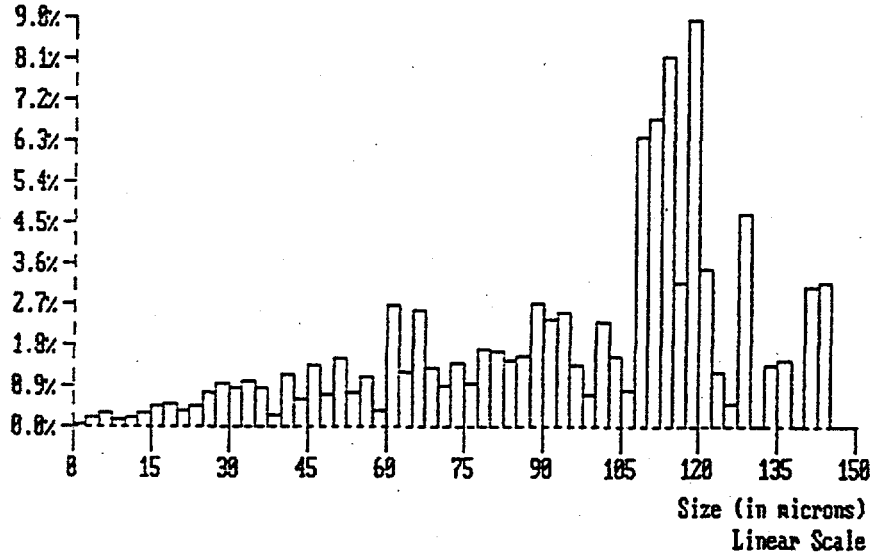

Appendix C

Figures

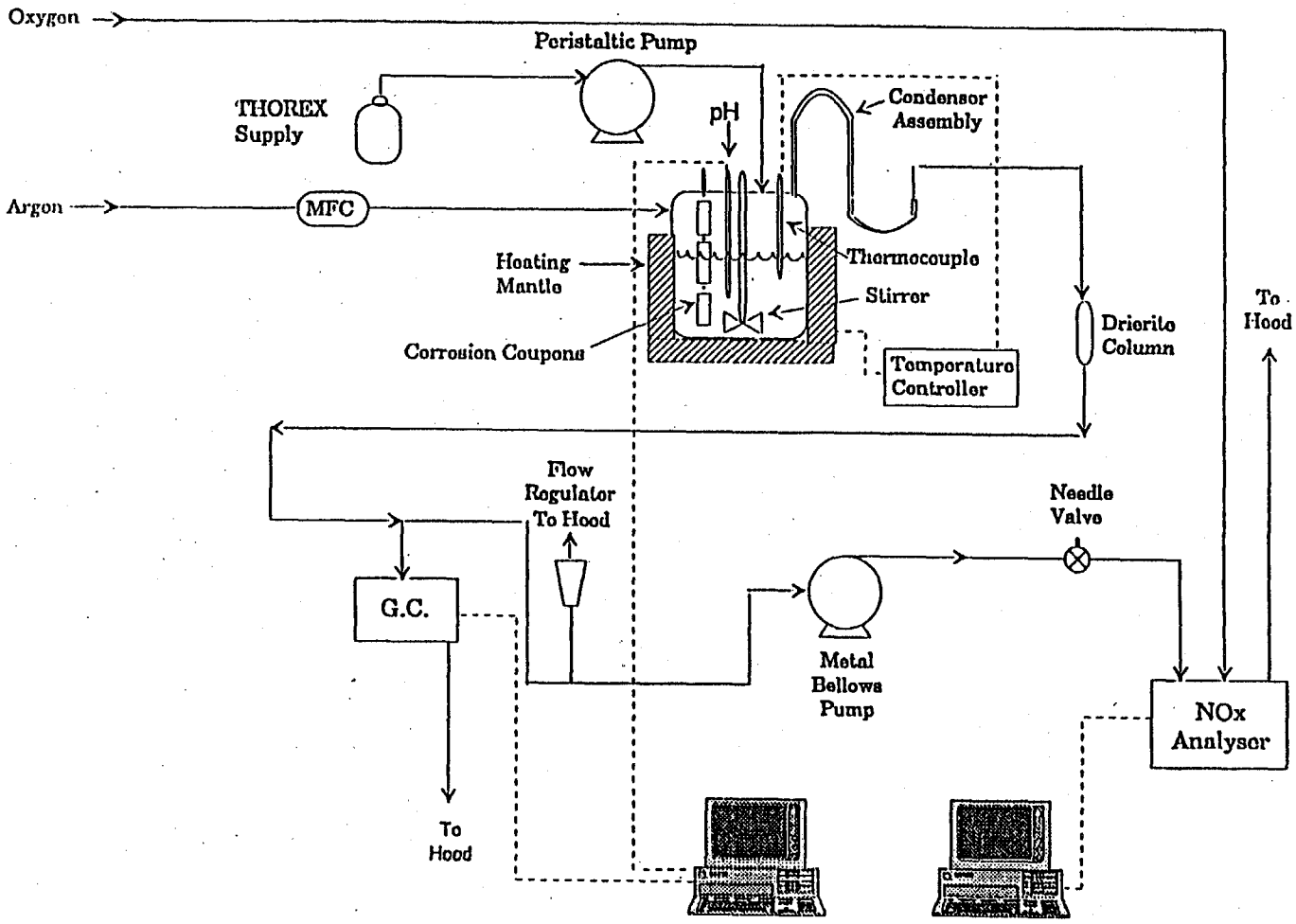

Figure C.1. Schematic Diagram of THOREX/PUREX Mixing Apparatus and Gas Analysis Equipment

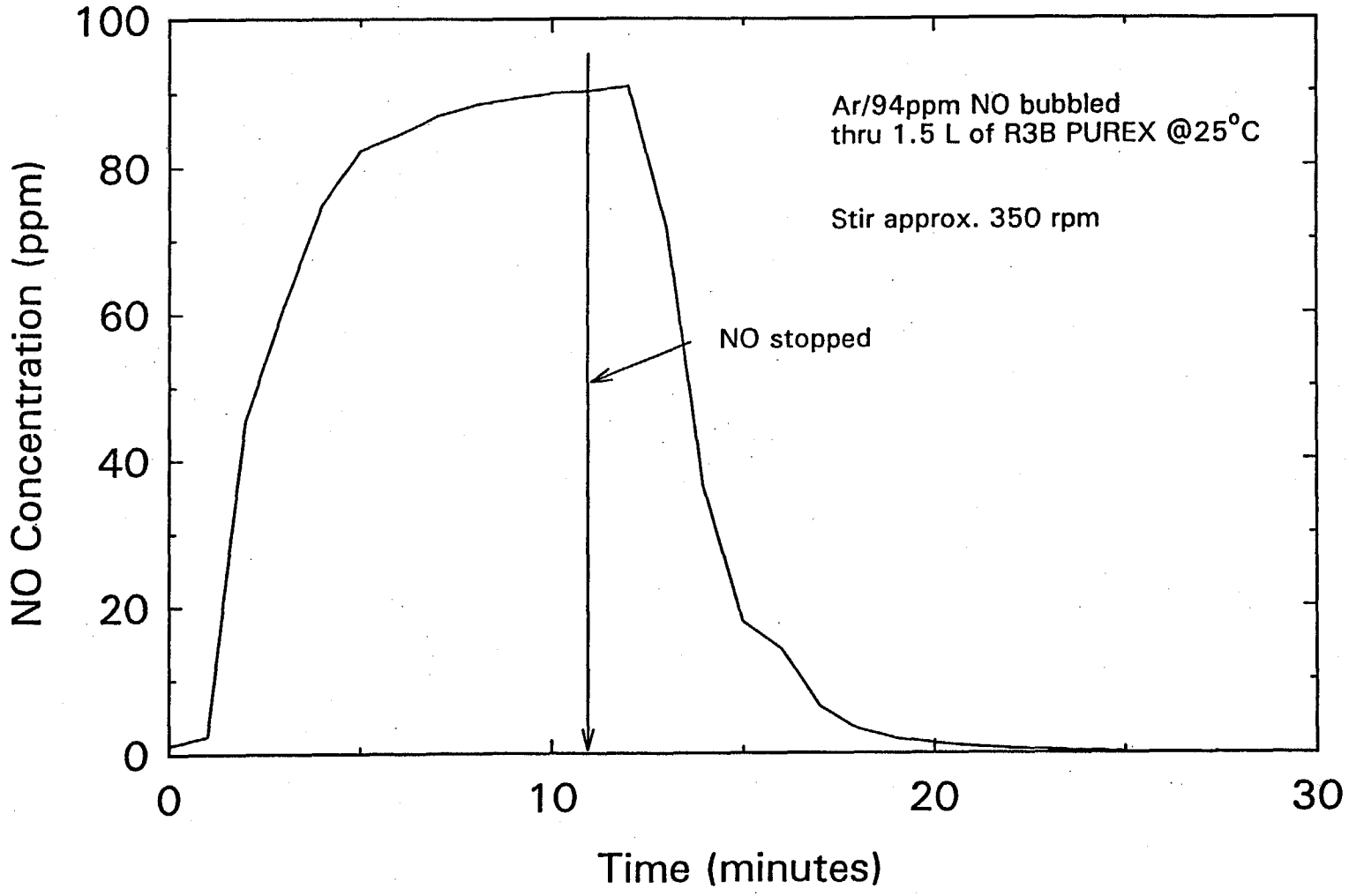

Figure C.2. Performance Check of System, 94 ppm NO in Ar bubbled through R3 PUREX at 650 mL/min. After NO was shut off, Ar still bubbled through PUREX at 566 mL/min.

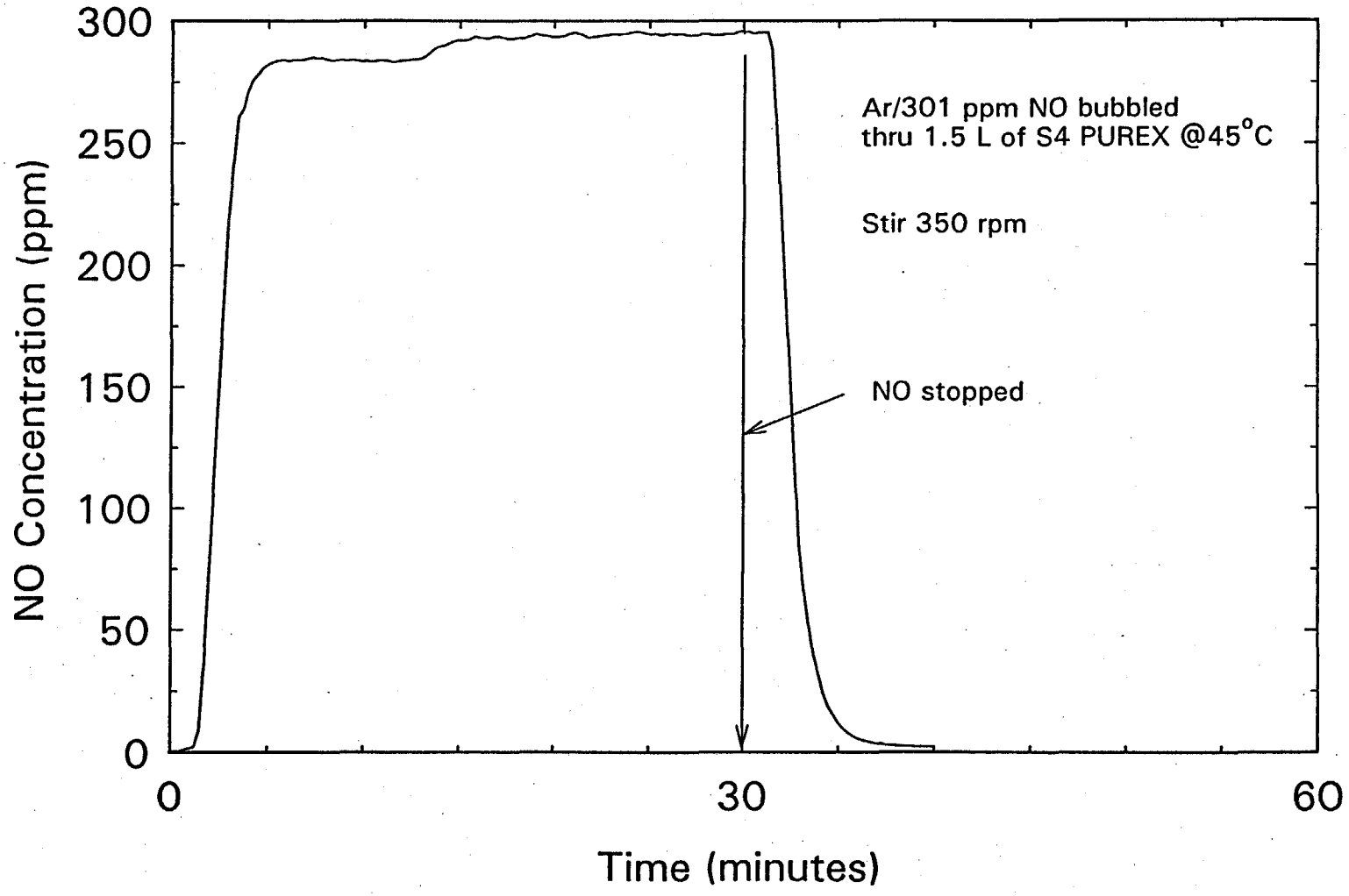

Figure C.3. Performance Check of System, 301 ppm NO in Ar bubbled through S4 PUREX at 1500 mL/min. After NO was shut off, Ar still passed through vessel at 1090 mL/min.

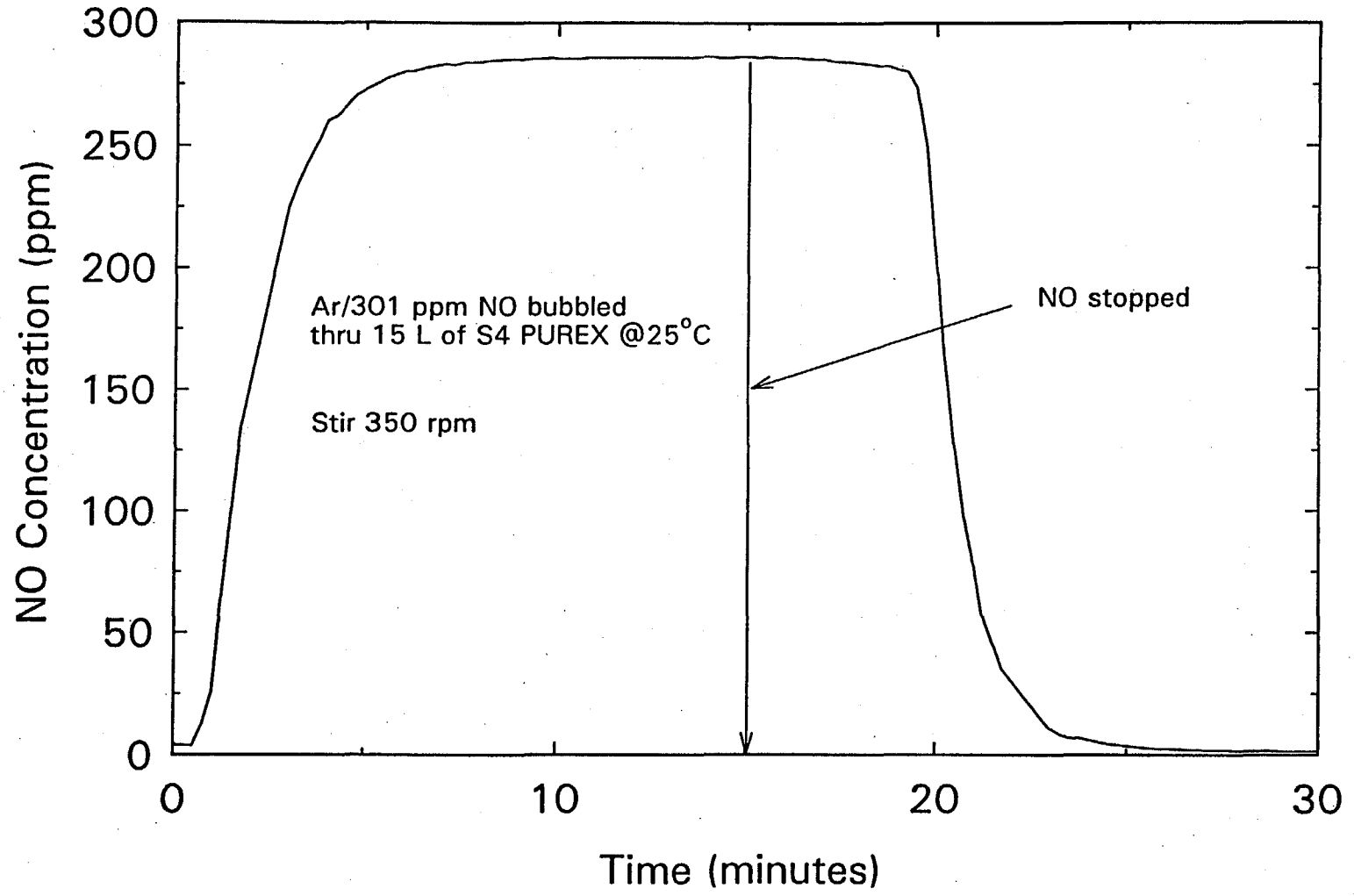

Figure C.4. Performance Check of Large-Scale System, 301 ppm NO in Ar bubbled through S4 PUREX at 1510 mL/min. After NO was shut off, Ar still bubbled through PUREX at 1090 mL/min.

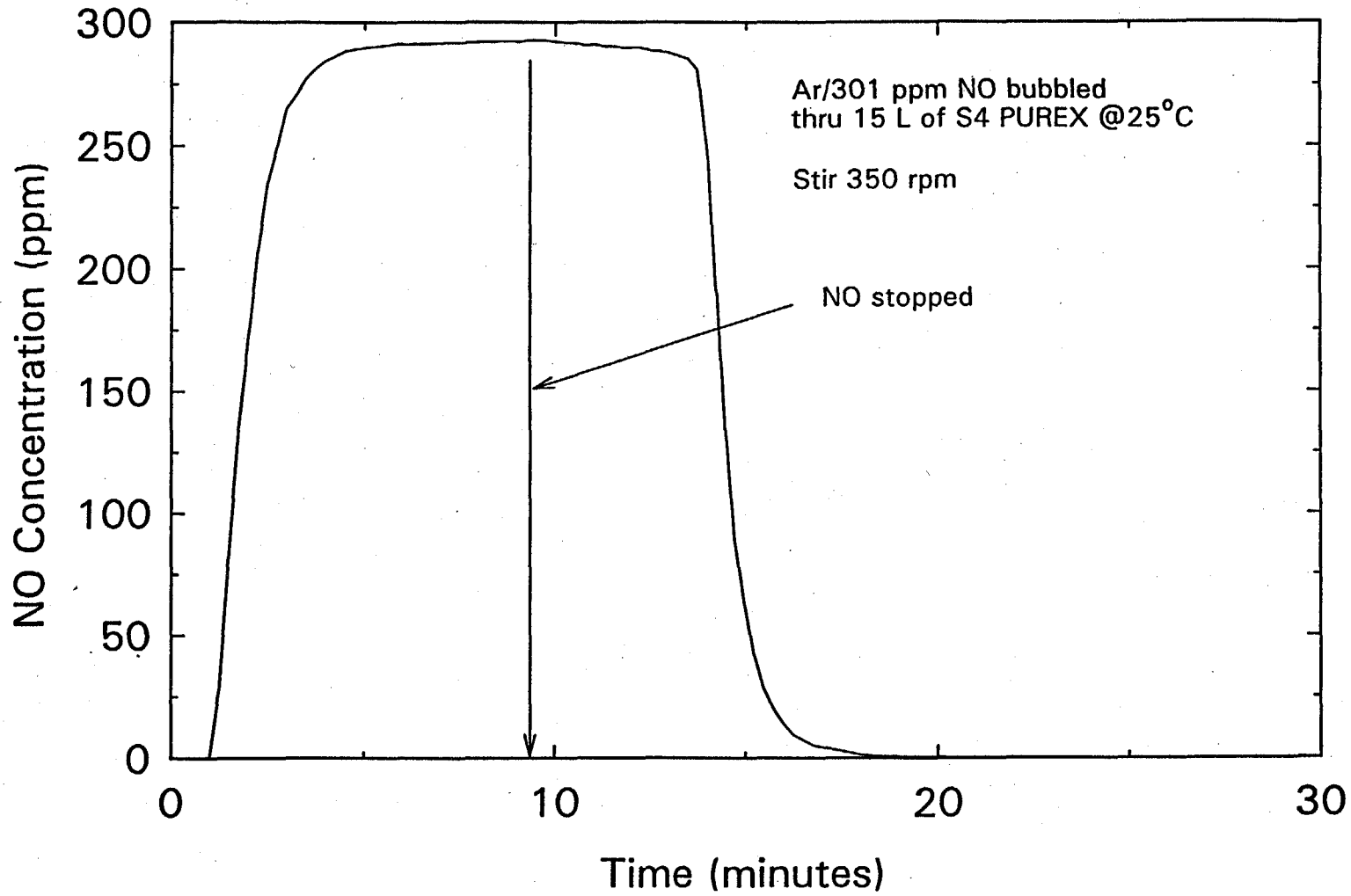

Figure C.5. Performance Check of Large-Scale System, 301 ppm NO in Ar bubbled through S4 PUREX at 1510 mL/min following Test 23B; thus, the vessel contained the solids that resulted from Test 23B. After NO was shut off, Ar still bubbled through PUREX at 1090 mL/min.

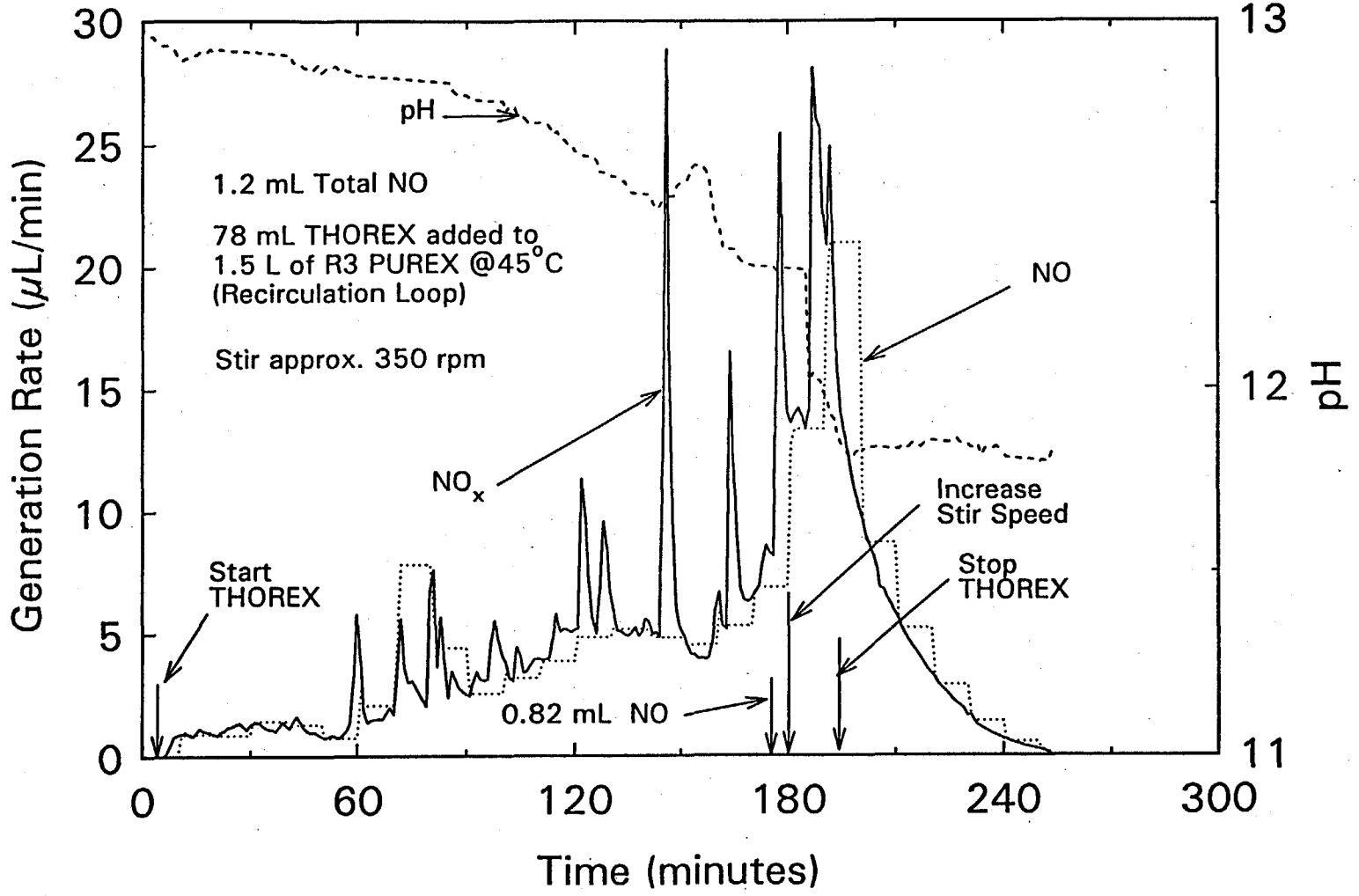

Figure C.6. Test 1. This Test, Along with Tests 2 and 3 (Figures C.7 and C.8), was Conducted to Determine Whether Pumping THOREX Into a PUREX Recirculation Loop would Generate less NO than Addition of THOREX Directly into the PUREX.

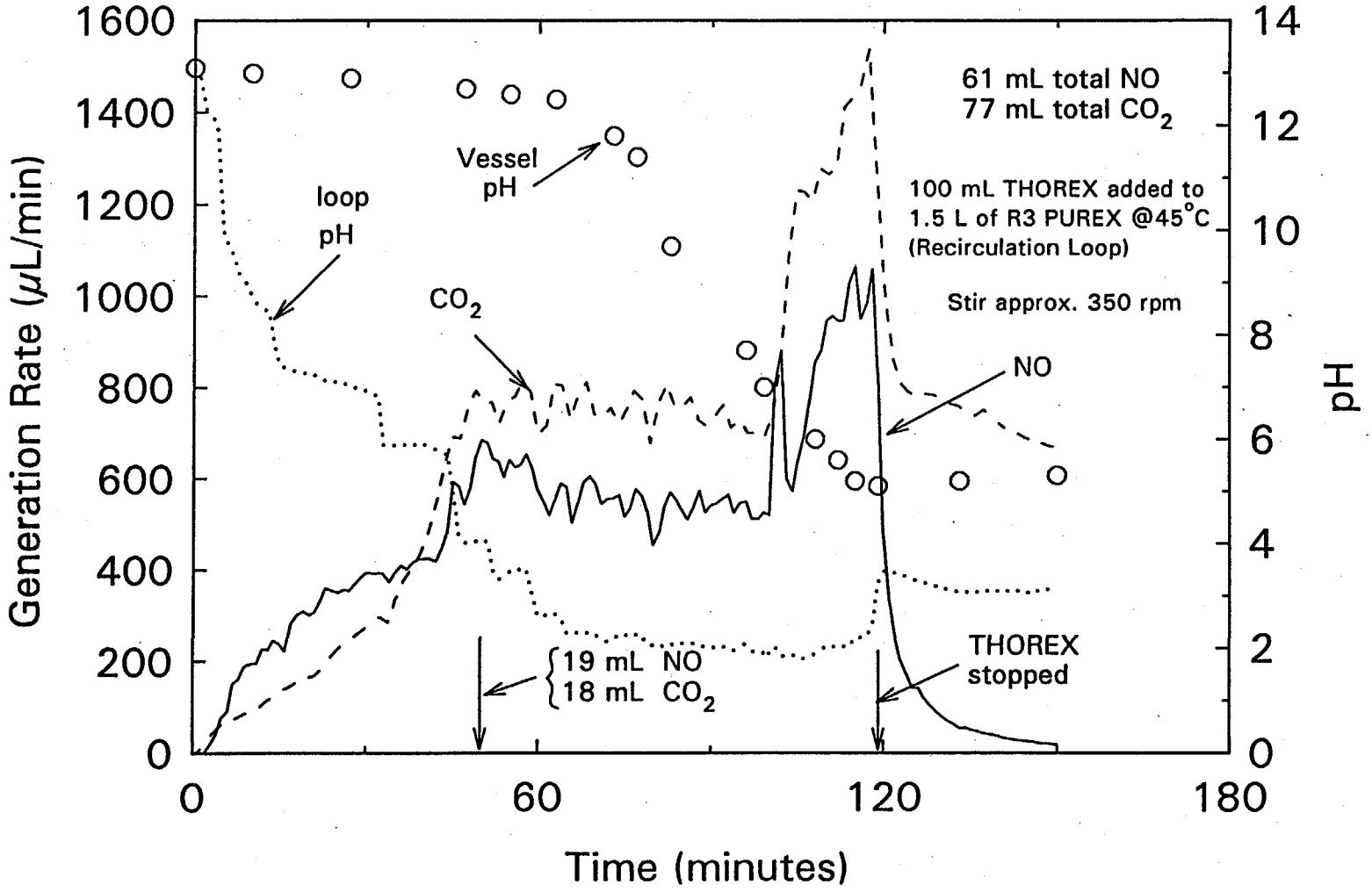

Figure C.7. Test 2. The Ratio of Loop-Flow-Rate to THOREX-Addition-Rate was much Lower than that Represented in Figure C.6

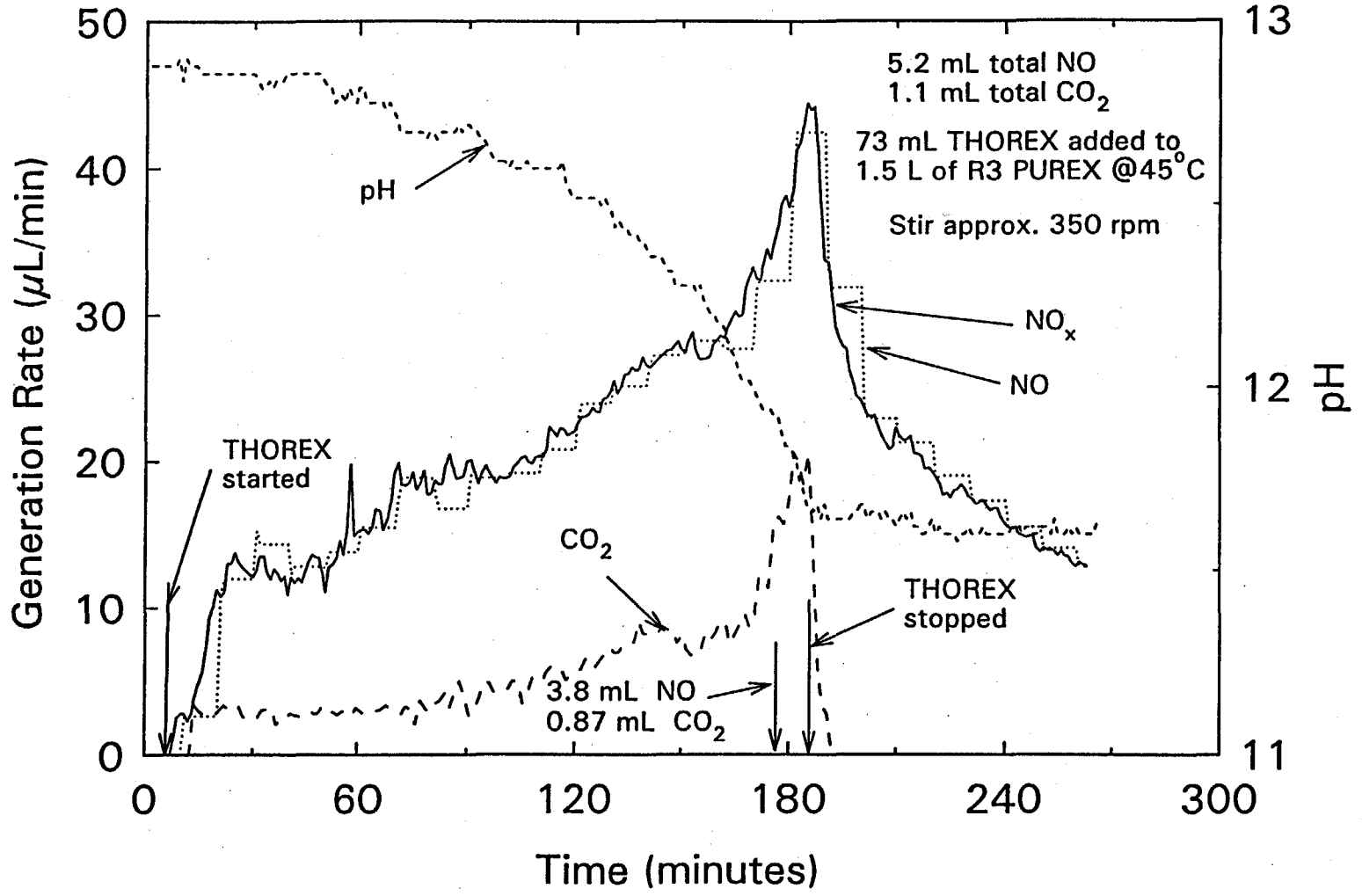

Figure C.8. Test 3. Direct Addition of THOREX into PUREX. Compare these results to the recirculation loop results in Figures C.6 and C.7.

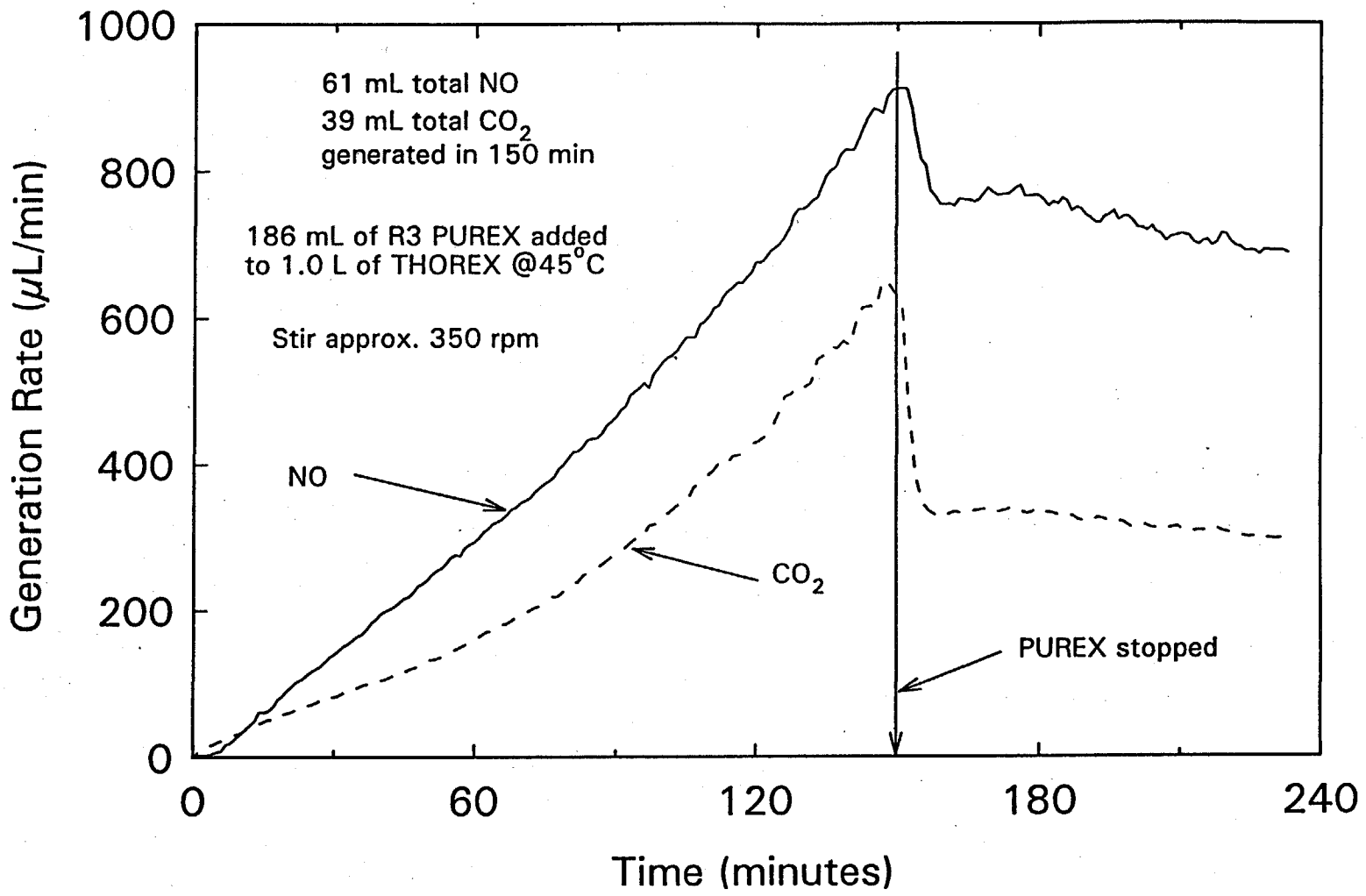

Figure C.9. Test 4. First Back-Flow Test. PUREX was pumped into reaction vessel containing THOREX. The object was to provide data on the consequence of an accidental reverse flow situation in which PUREX was injected into THOREX in Tank 8D-4.

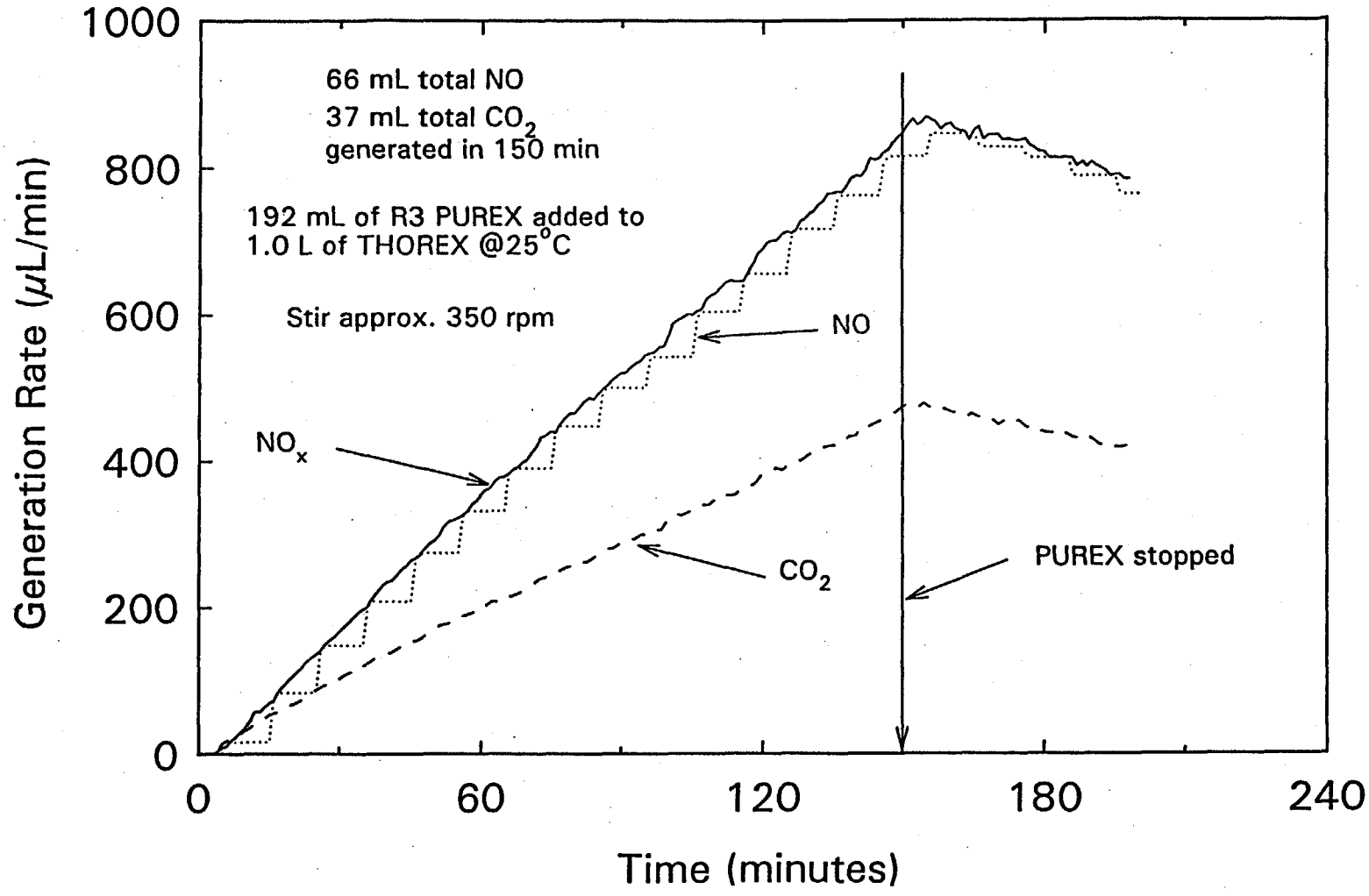

Figure C.10. Test 5. Second Back-Flow Test. Test conditions were the same as in Figure C.9 except the temperature was reduced from 45°C to 25°C.

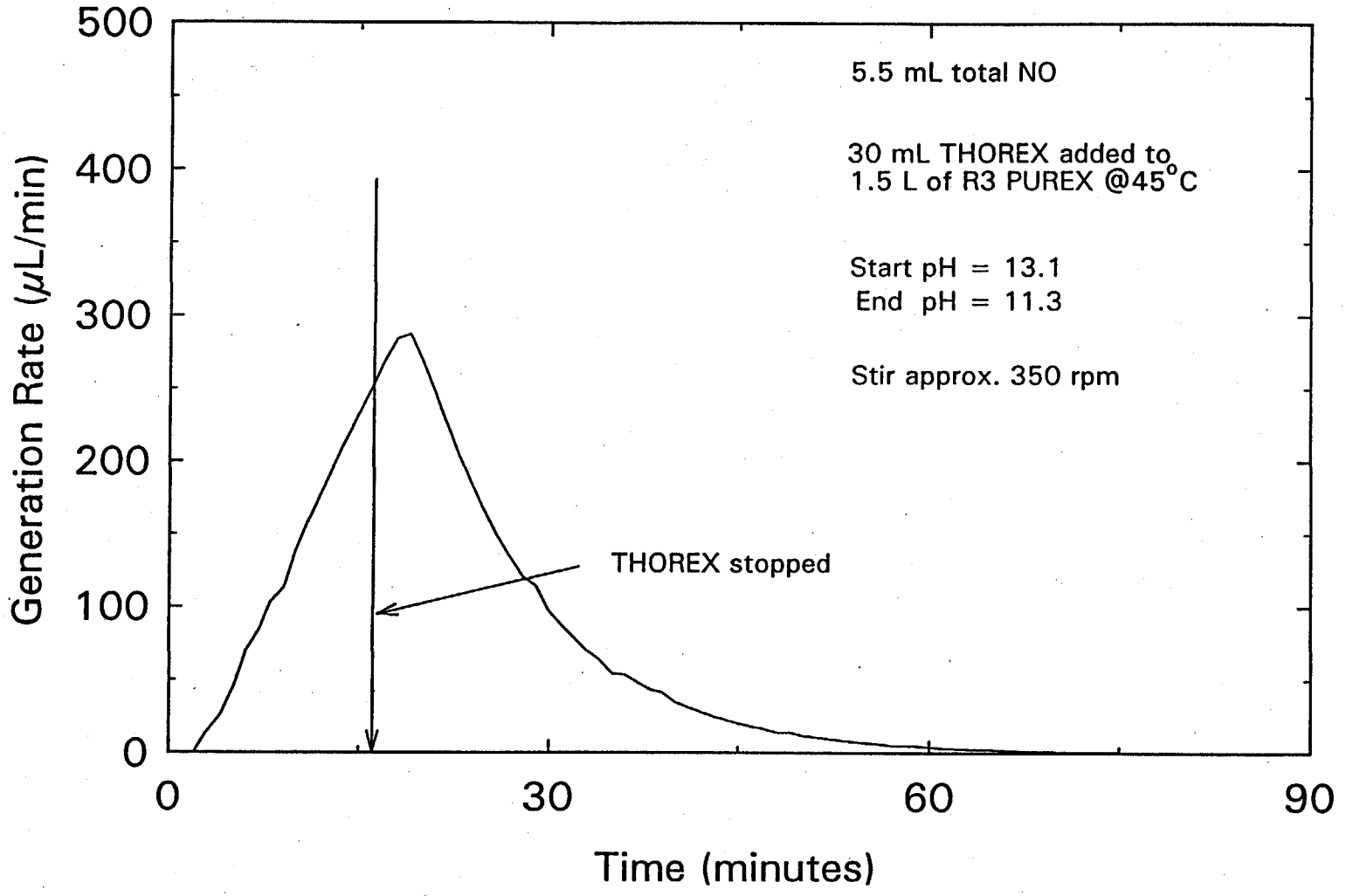

Figure C.11. Test 6. This test along with Tests 7A and 7B in Figures C.12 and C.13 provide a comparison of results obtained with Full-Compliment PUREX and simplified PUREX.

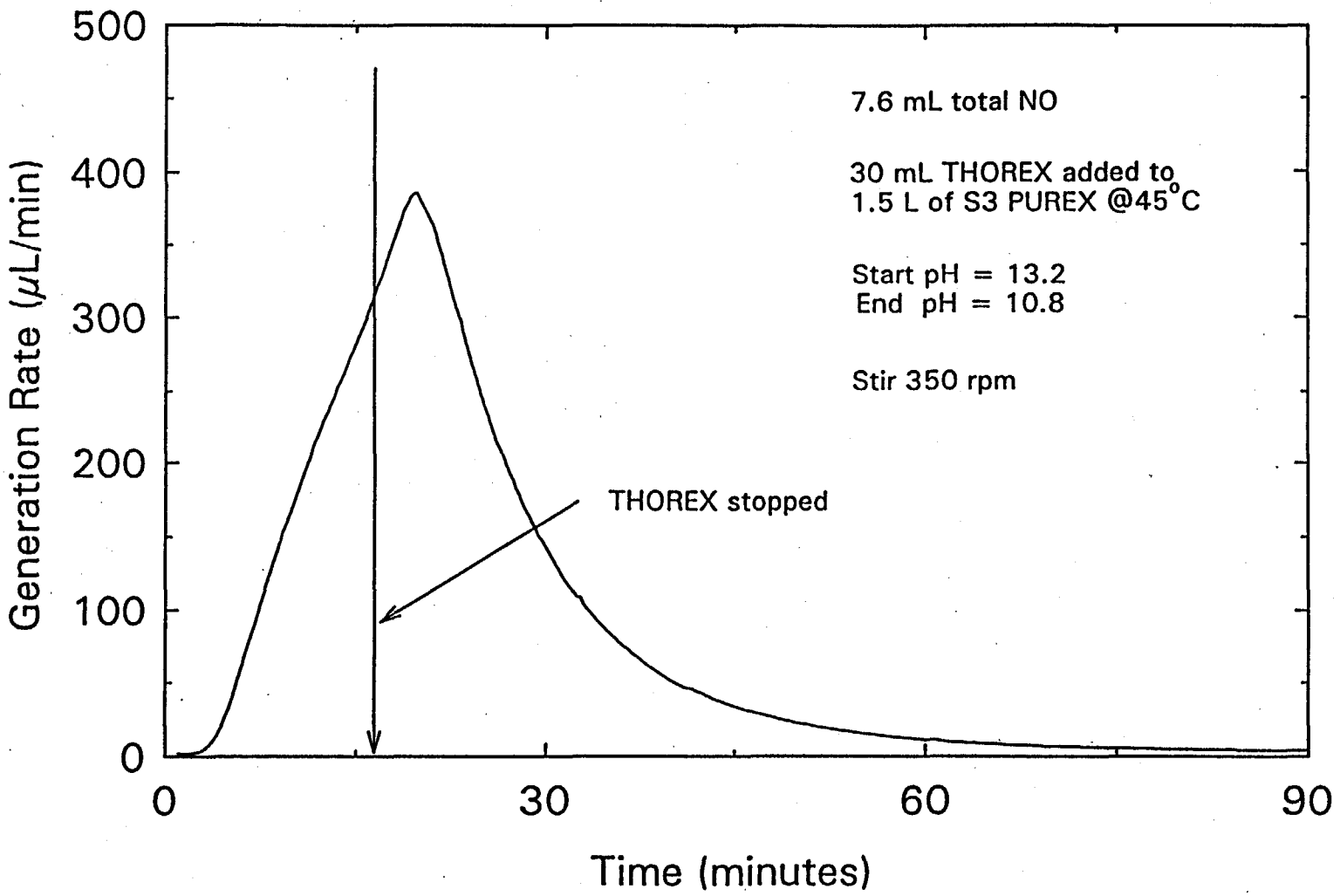

Figure C.12. Test 7A. See Figure C.13 for a Duplicate Run and Figure C.11 for a Similar Test Conducted with Full-Compliment PUREX Instead of Simplified PUREX.

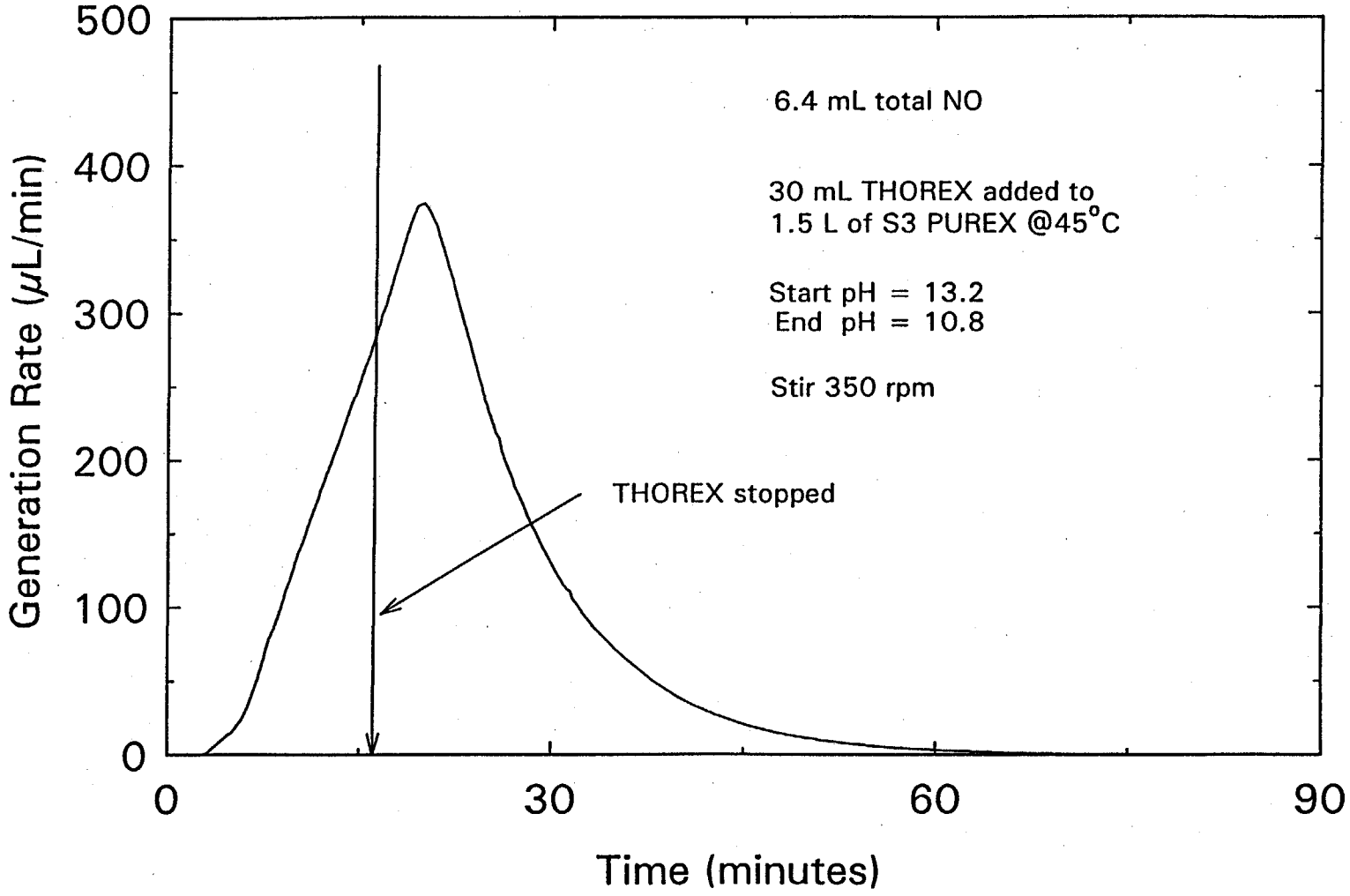

Figure C.13. Test 7B. See Figure C.12 for a Duplicate Run and Figure C.11 for a Similar Test Conducted with Full-Compliment PUREX Instead of Simplified PUREX.

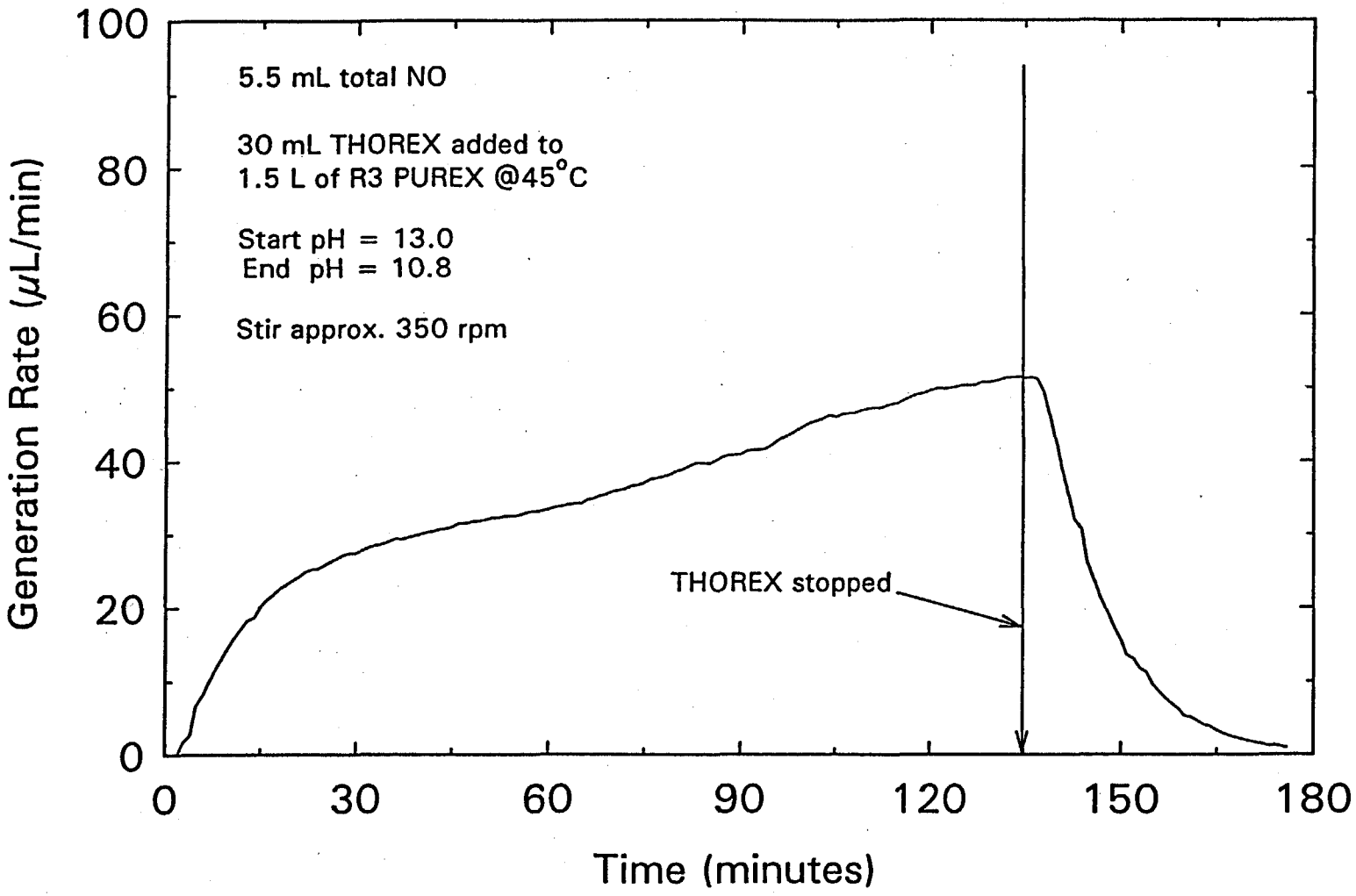

Figure C.14. Test 8 was Conducted to Determine the Effect of Slower THOREX Addition Rate

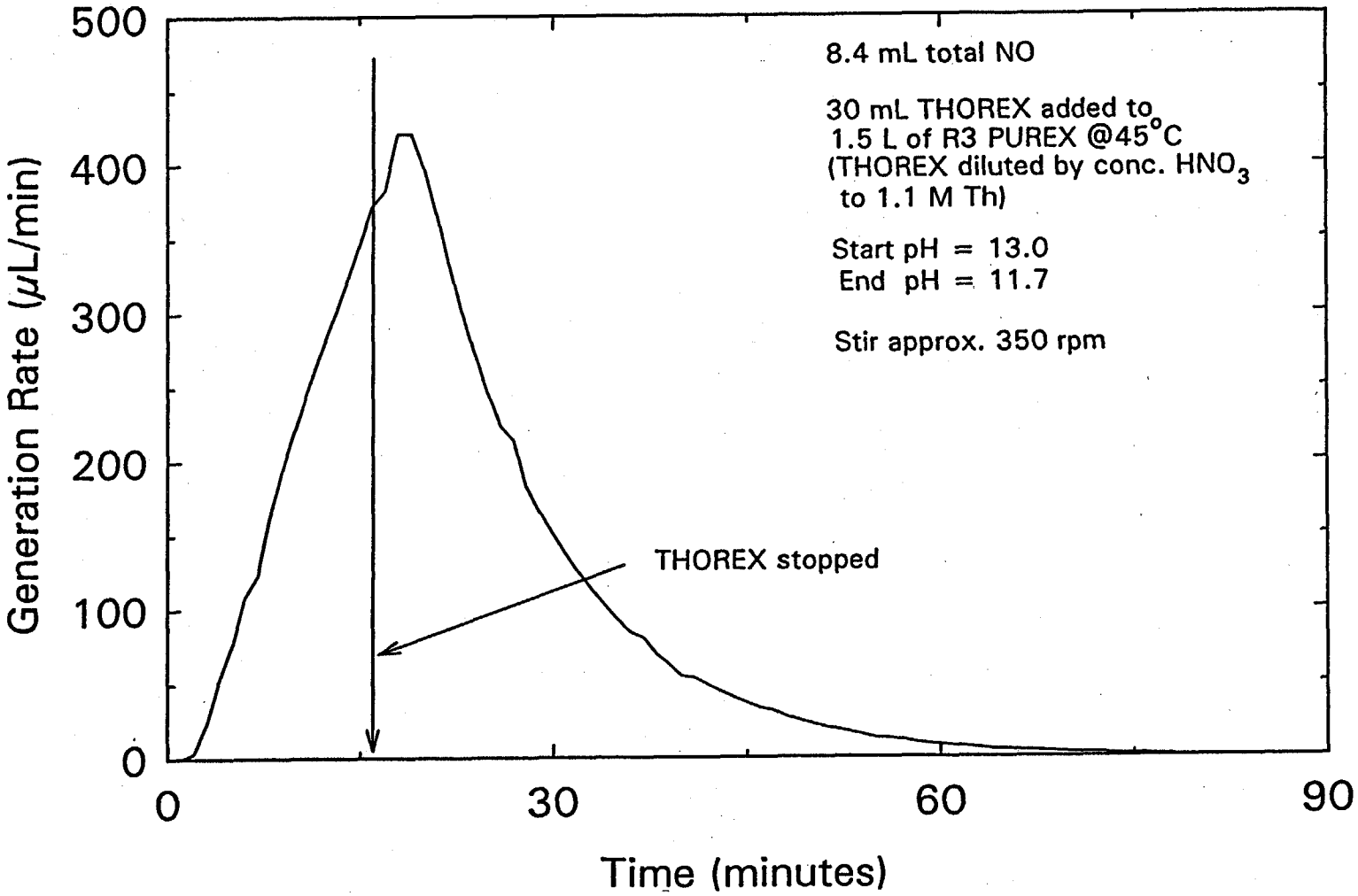

Figure C.15. Test 9 was Conducted with THOREX to Which Additional HNO_3 had been Added to Test the Effect of Higher-Than-Anticipated Acidity in Tank 8D-4.

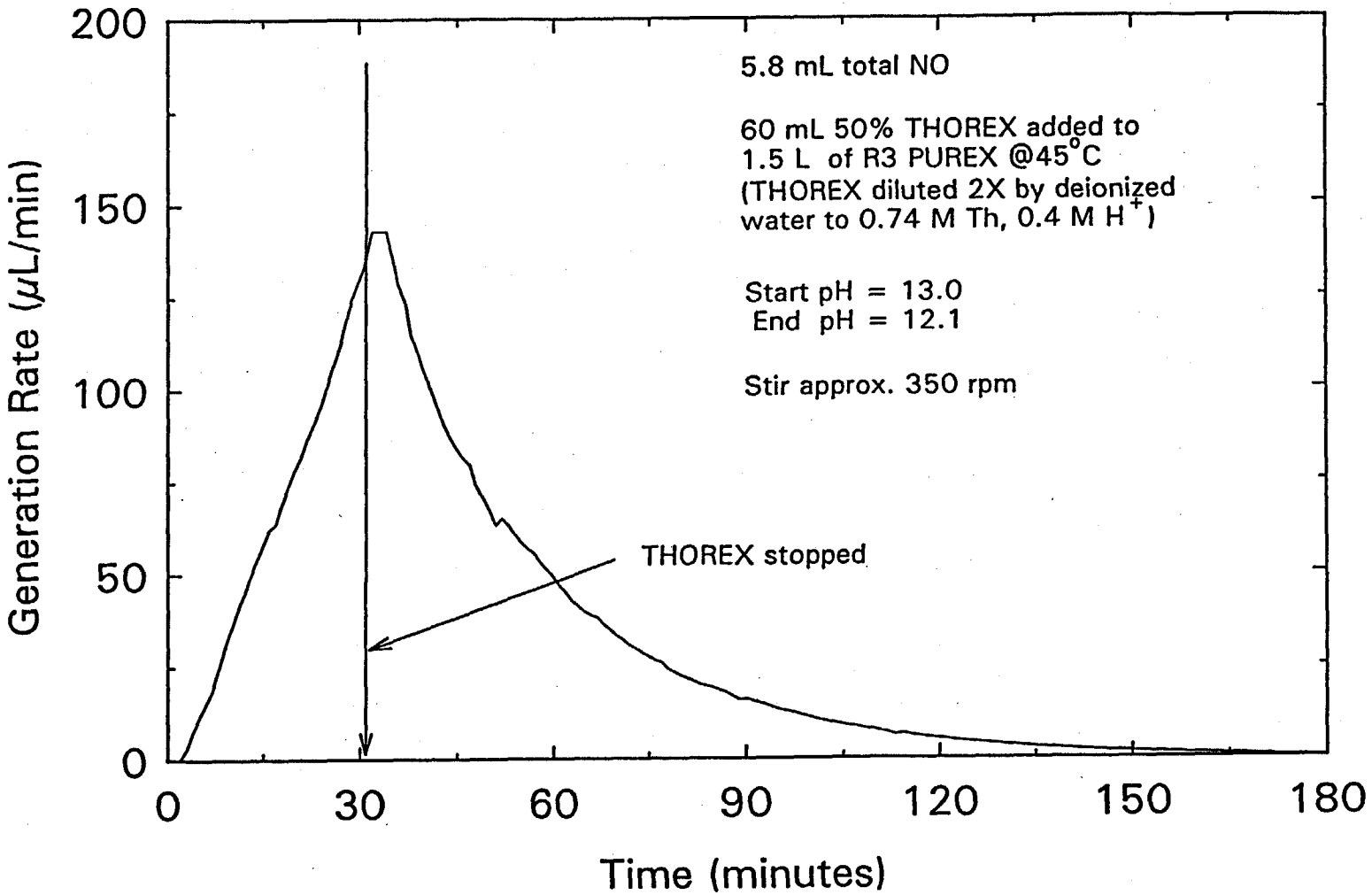

Figure C.16. Test 10 was Conducted to Determine the Effect of Simply Diluting the THOREX by a Factor of Two

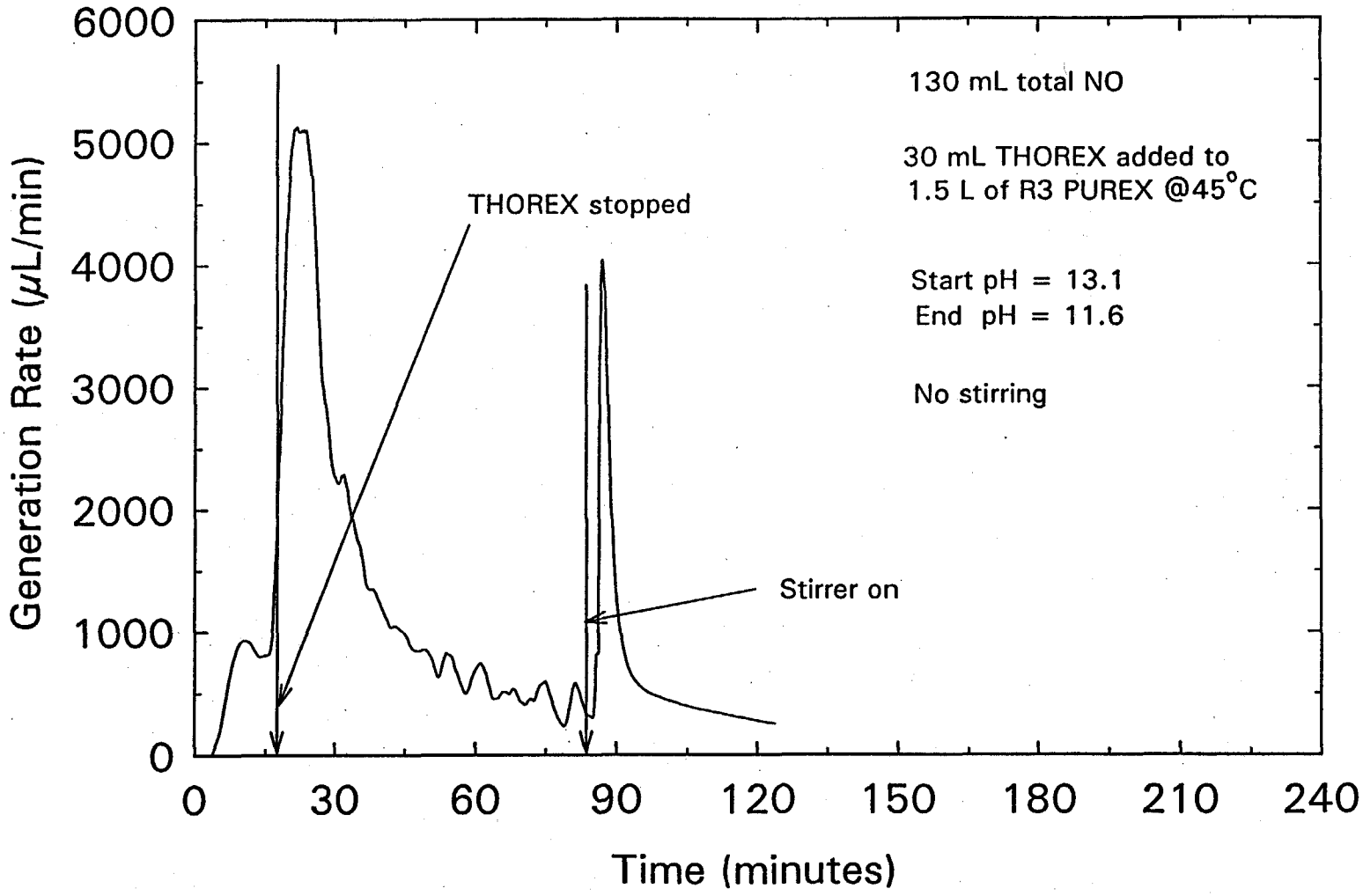

Figure C.17. Test 11, Together with Test 12 (Figure C.18), was Conducted with no Stirring. Test 11 used full-compliment PUREX and Test 12 used simplified PUREX.

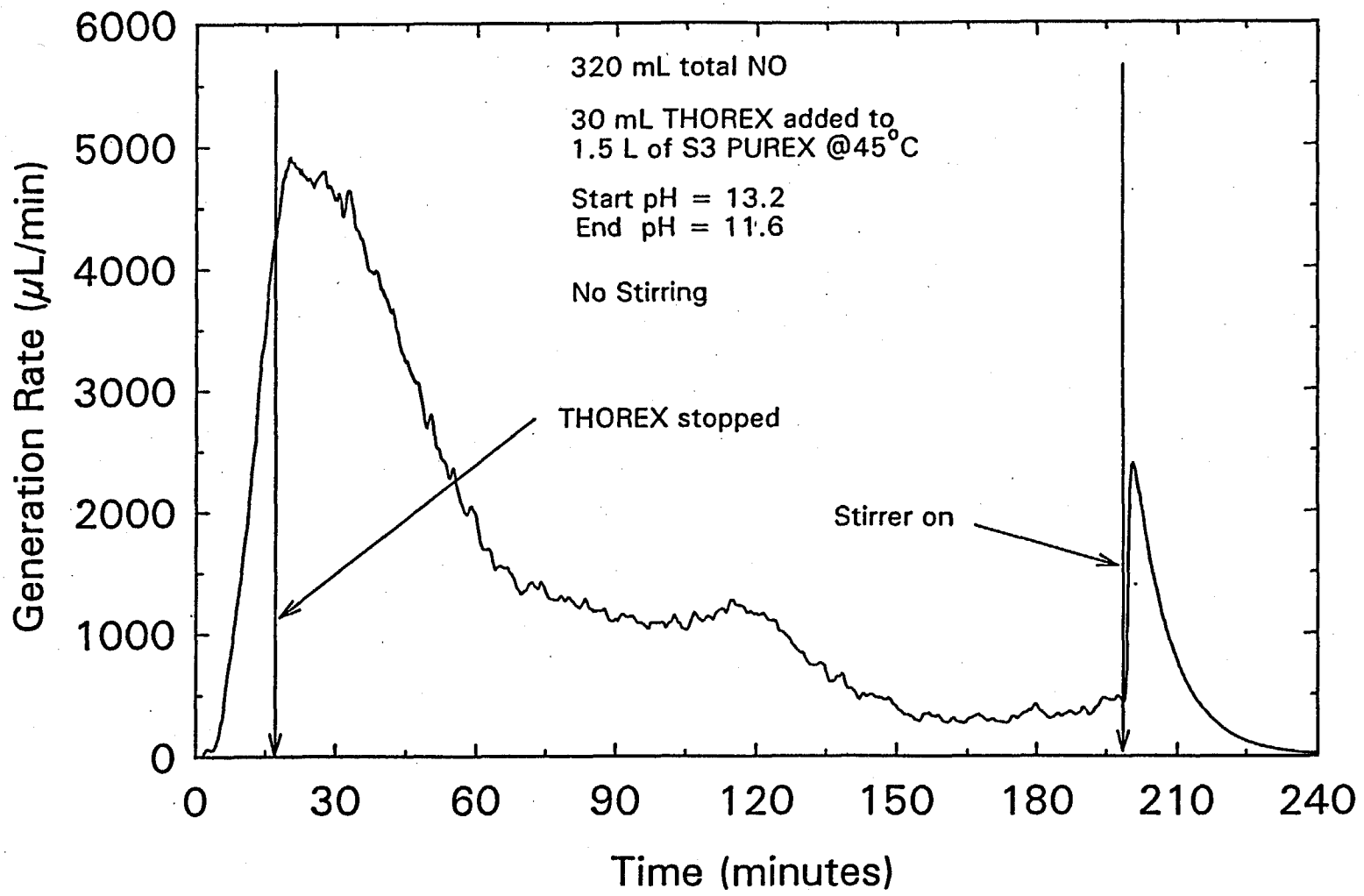

Figure C.18. Test 12, Together with Test 11 (Figure C.17), was Conducted with no Stirring. Test 11 used full-compliment PUREX and Test 12 used simplified PUREX.

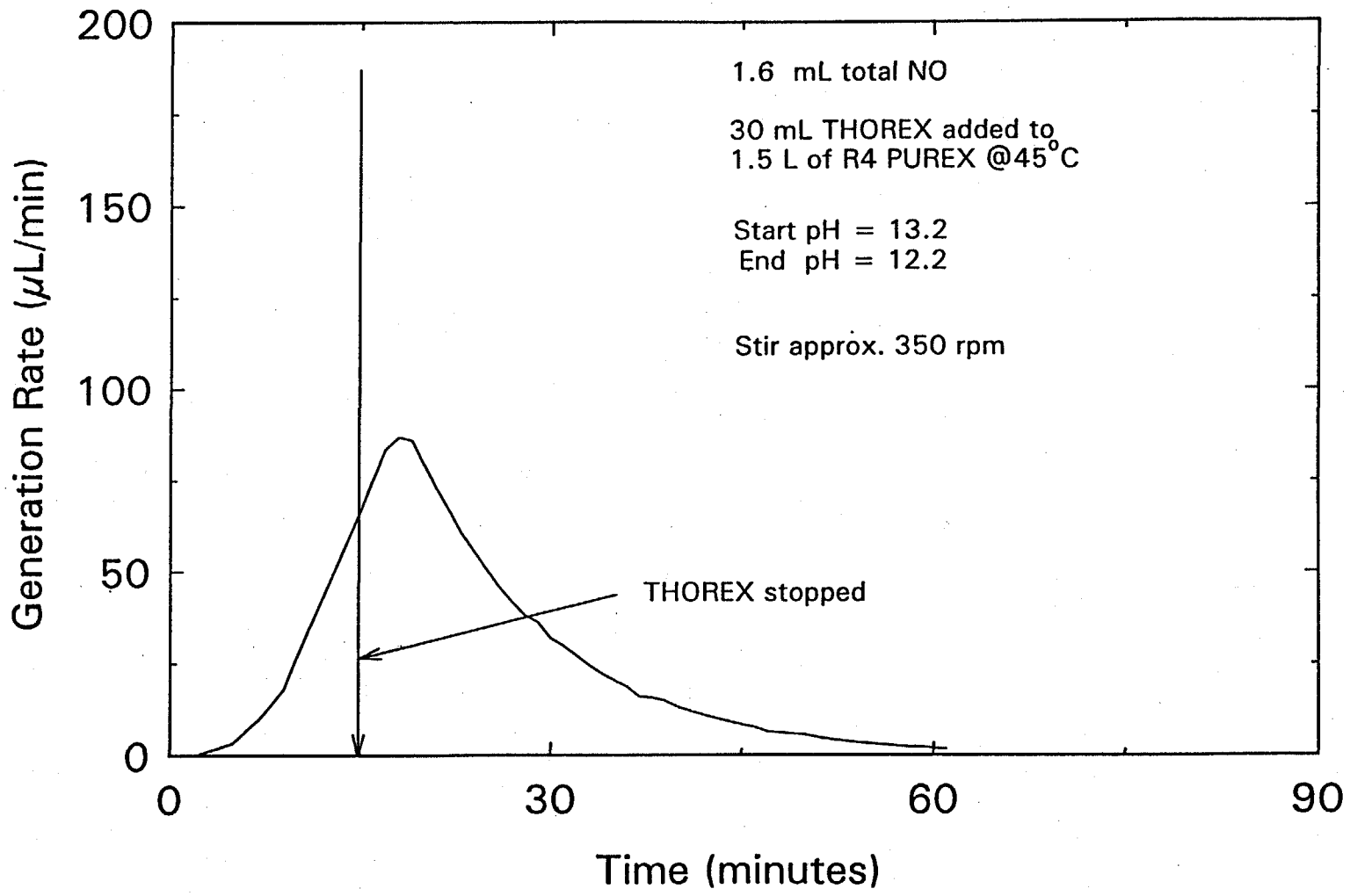

Figure C.19. Test 13 was the First Test Performed with Fourth-Wash PUREX. These results can be compared with Tests 14A to 14D (Figures C.20 to C.23), which were performed with simplified fourth-wash PUREX.

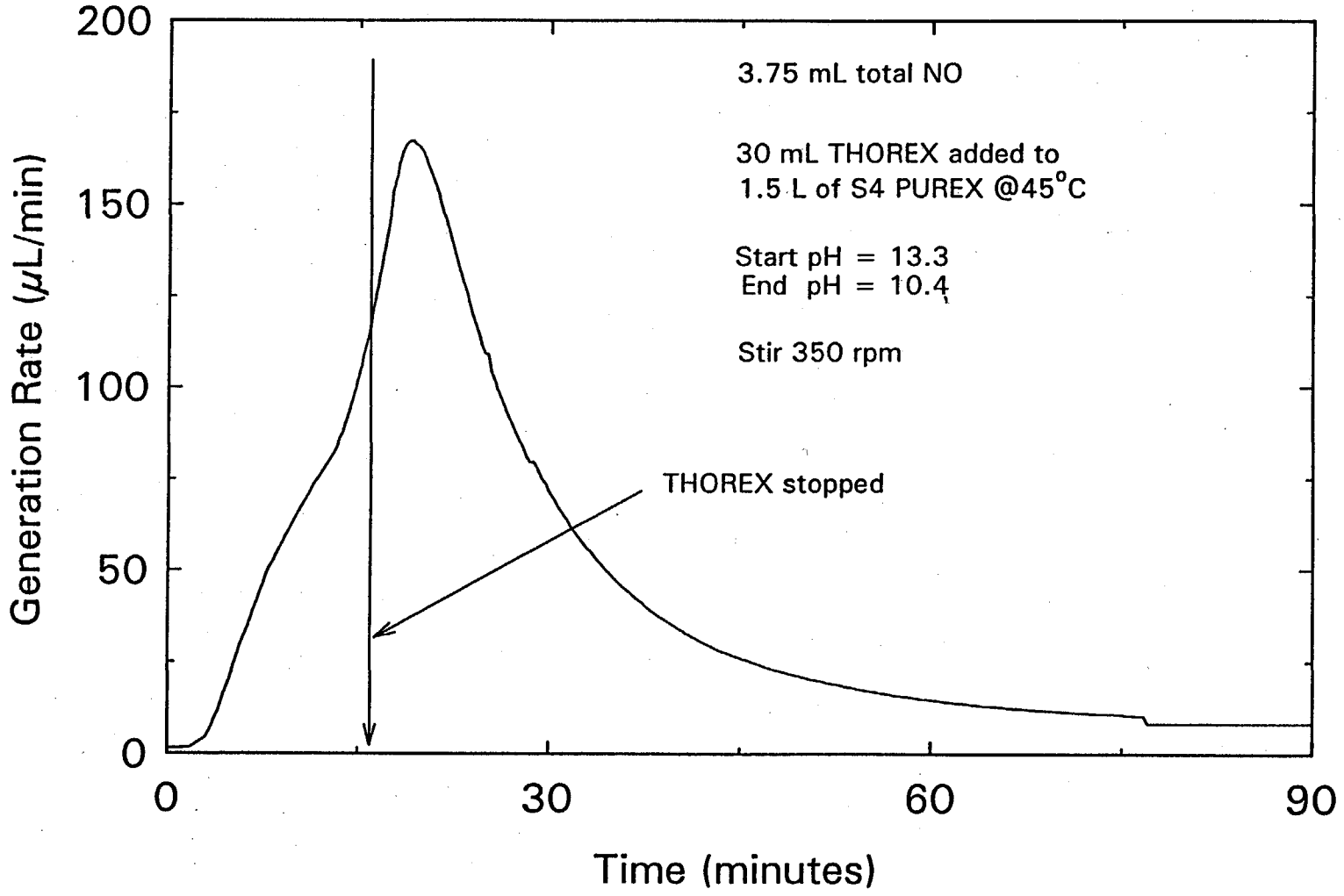

Figure C.20. Test 14A was the First of Four Tests (Figures C.20 to C.23) to be Run with Simplified Fourth-Wash PUREX

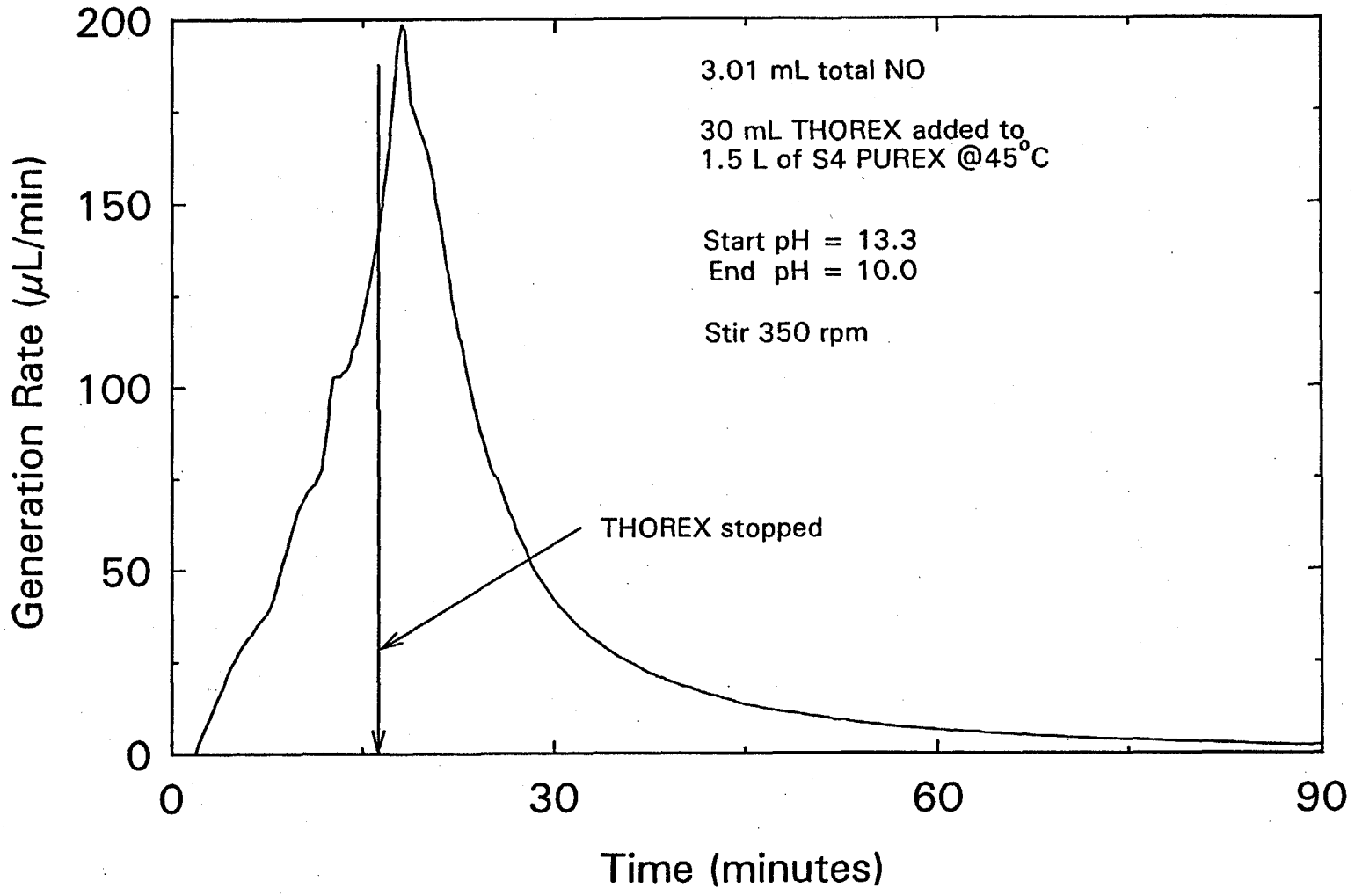

Figure C.21. Test 14B was the Second of Four Tests (Figures C.20 to C.23) to be Run with Simplified Fourth-Wash PUREX

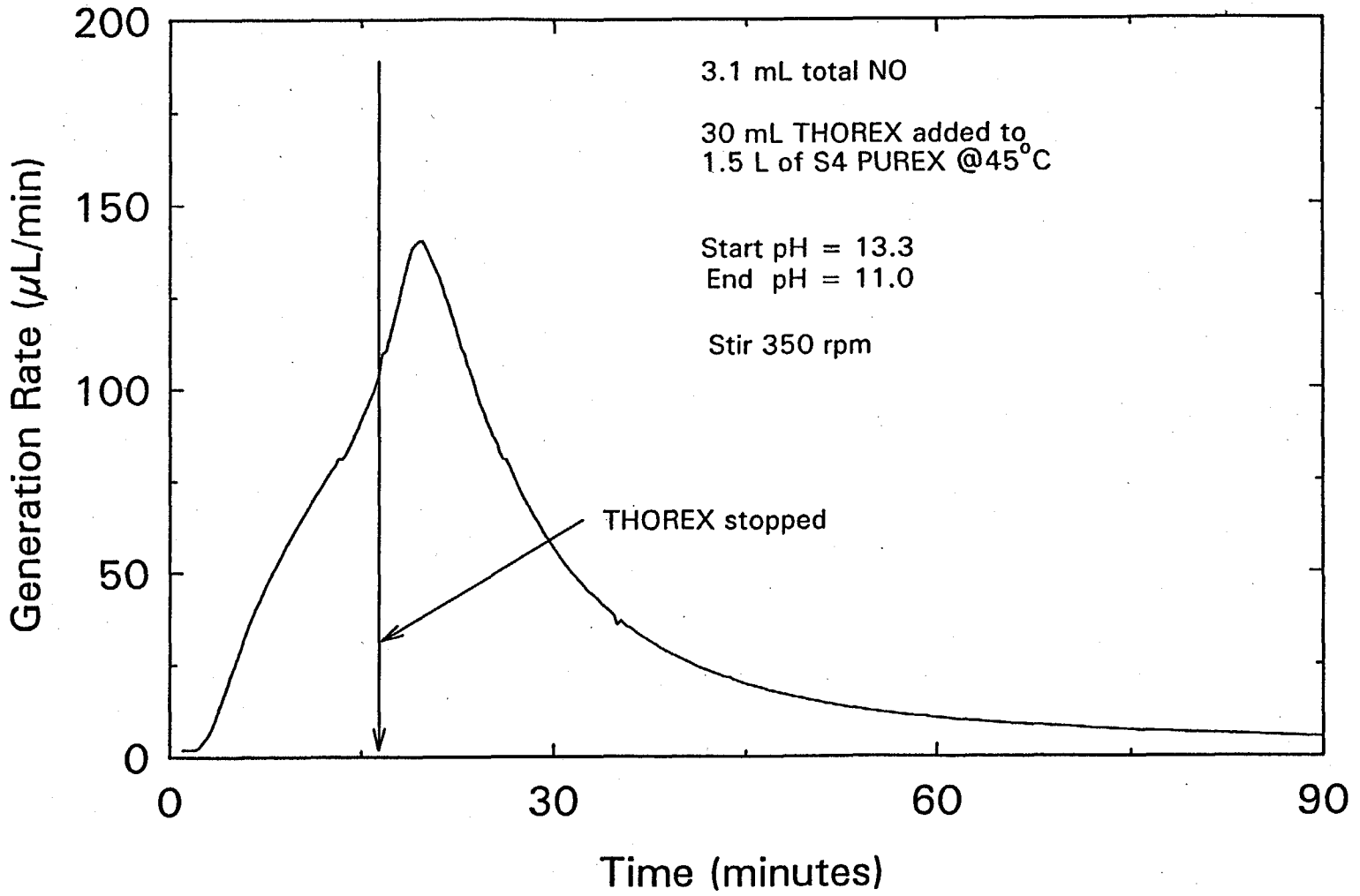

Figure C.22. Test 14C was the Third of Four Tests (Figures C.20 to C.23) to be Run with Simplified Fourth-Wash PUREX

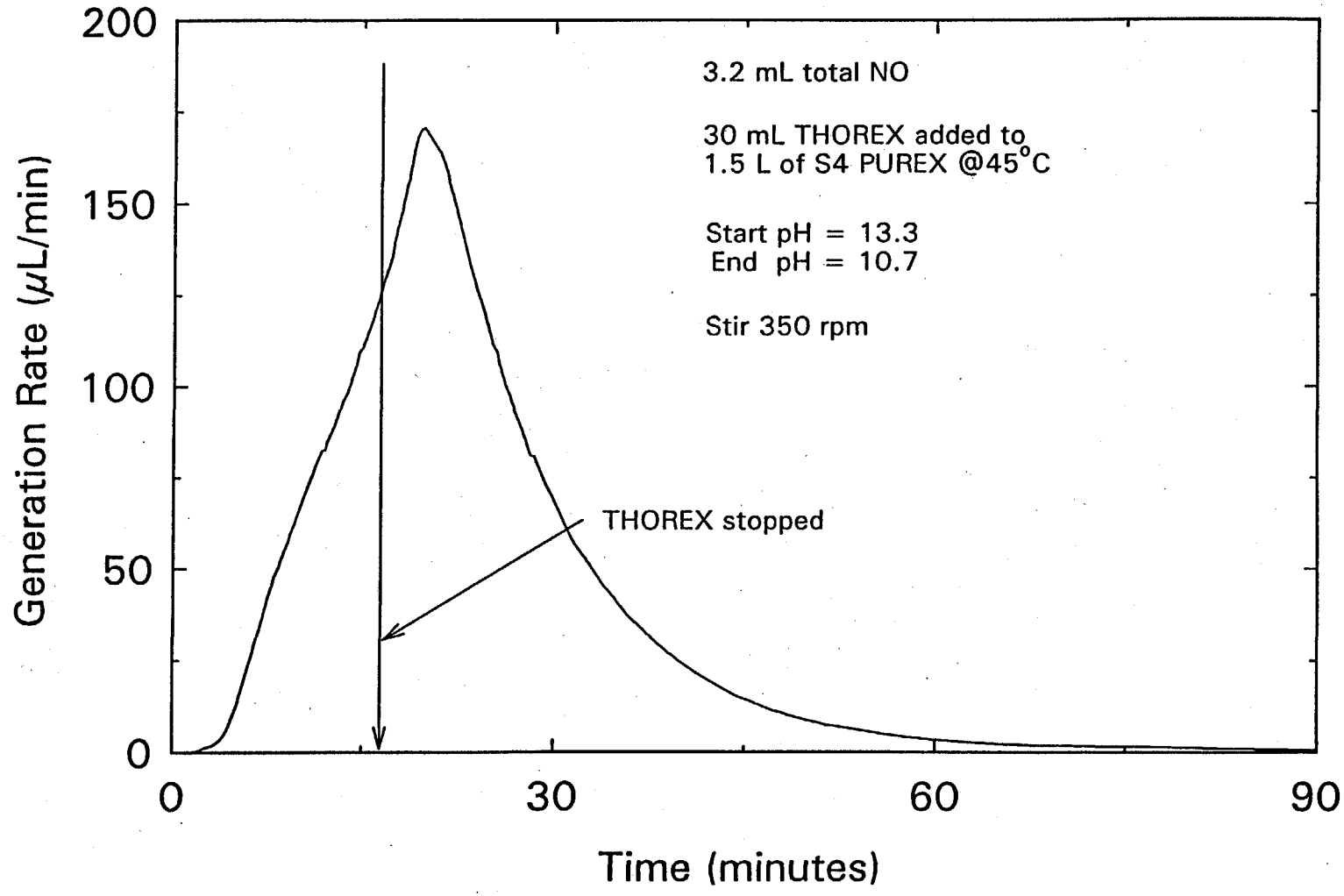

Figure C.23. Test 14D was the Fourth of Four Tests (Figures C.20 to C.23) to be Run with Simplified Fourth-Wash PUREX

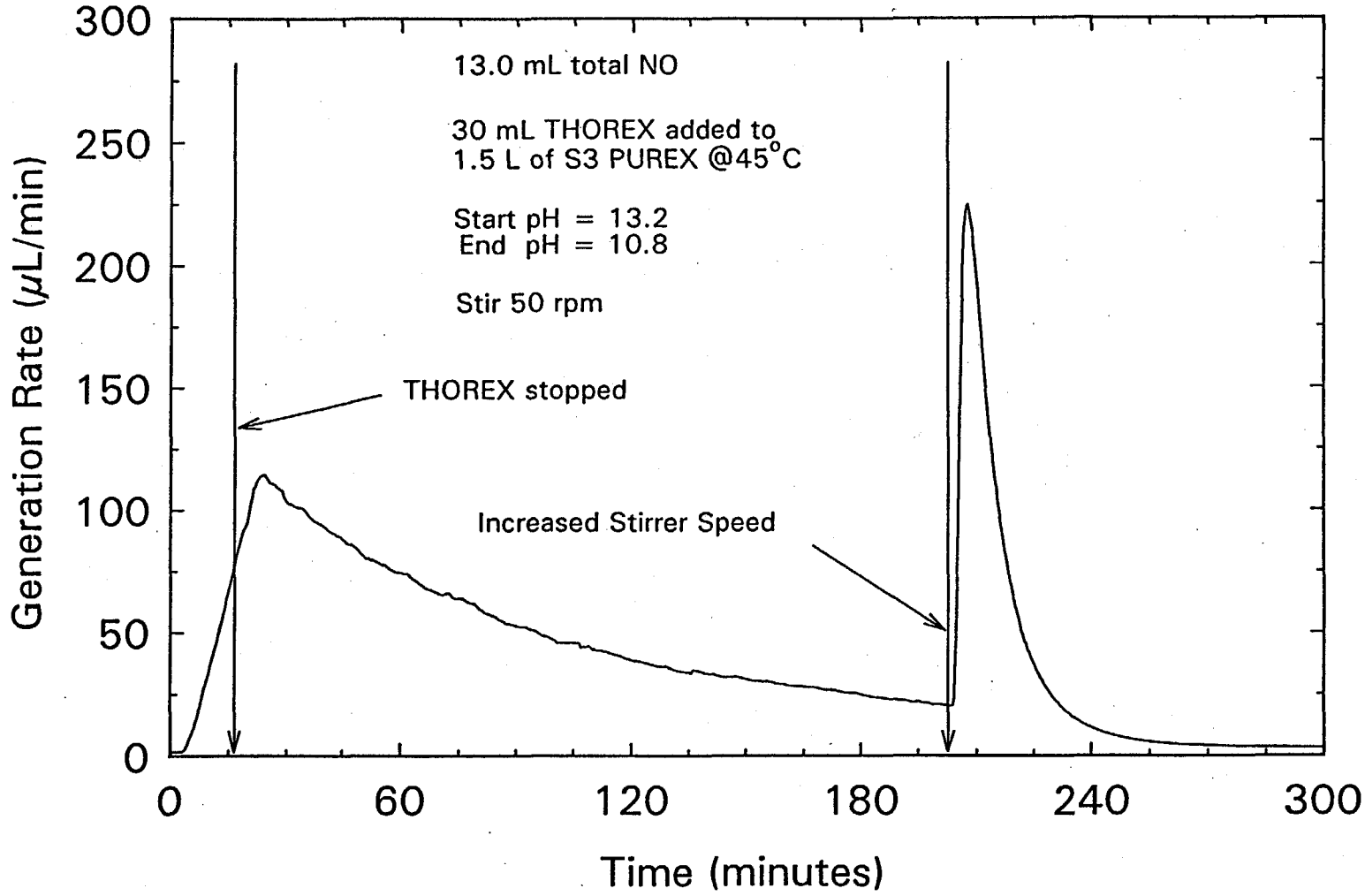

Figure C.24. Test 15 was Performed to Determine the Effect of a Slower Stirring Rate. See Figure C.25 for a test with a faster stirring rate.

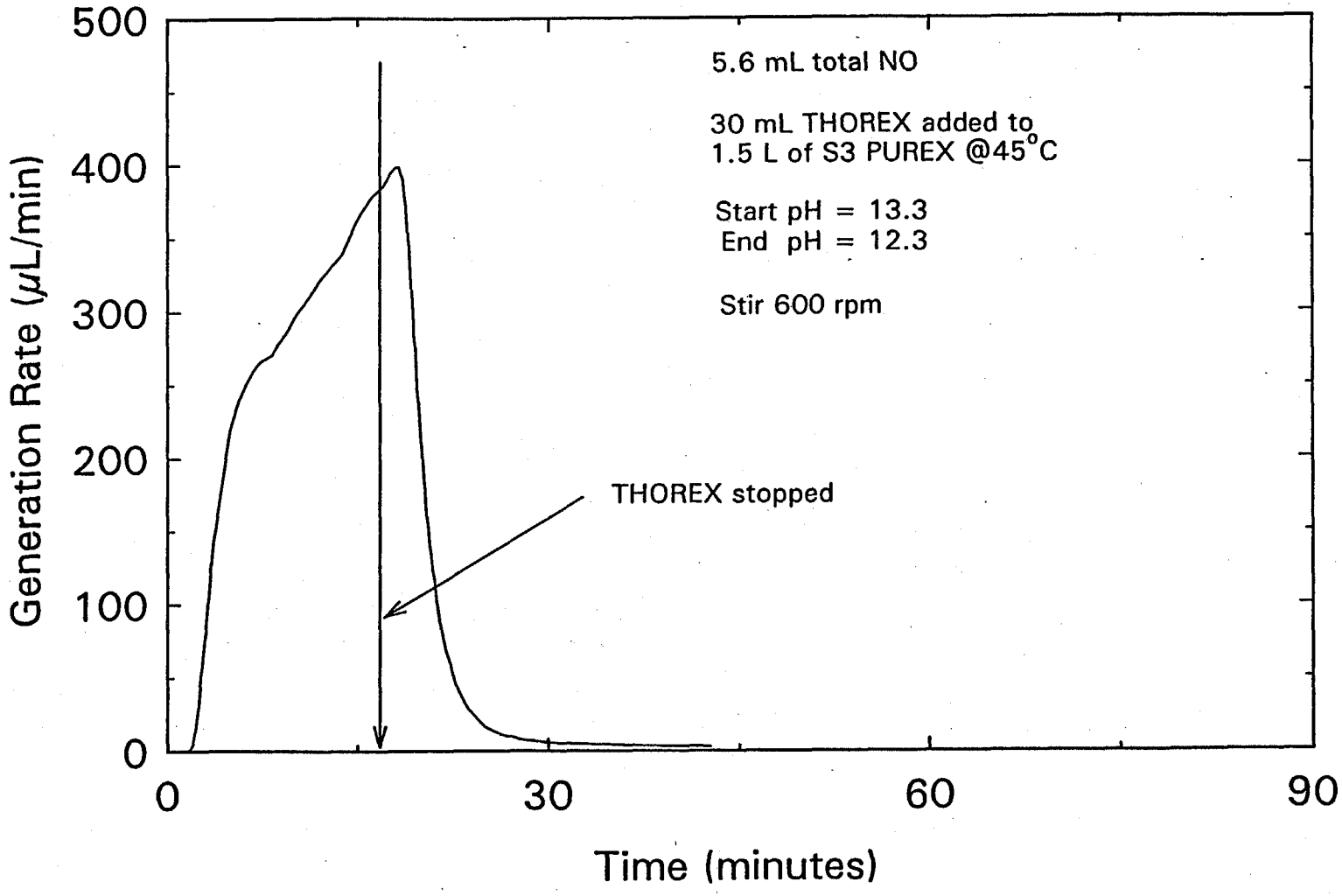

Figure C.25. Test 16 was Performed to Determine the Effect of a Faster Stirring Rate. See Figure C.24 for a test with a slower stirring rate.

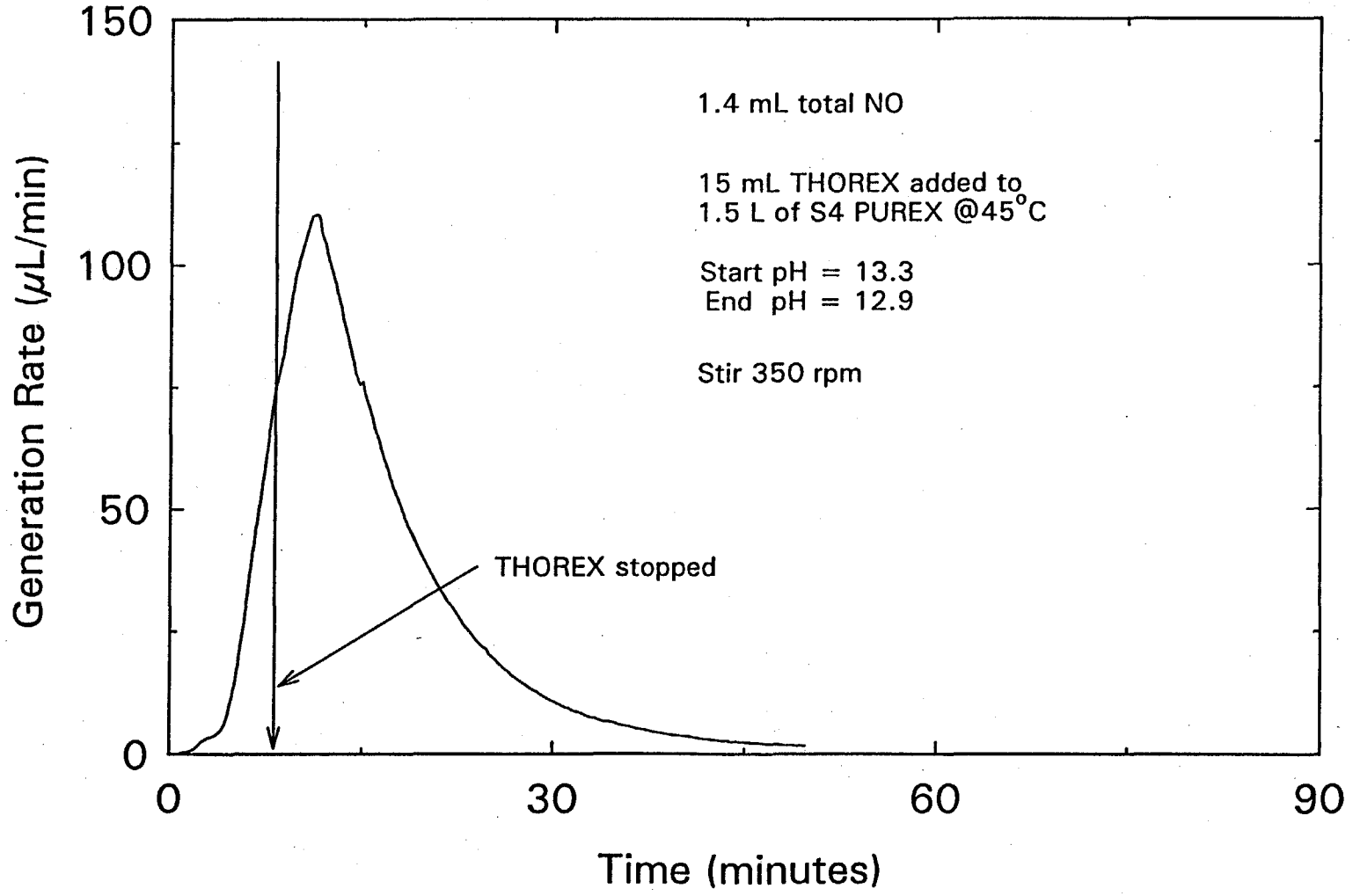

Figure C.26. Test 17A, Along with Tests 17B and 17C (Figures C.27 and C.28) was Conducted with Simplified Fourth-Wash PUREX and Added only Enough THOREX to Reduce the OH^- Concentration to 0.1 M (pH 13.0)

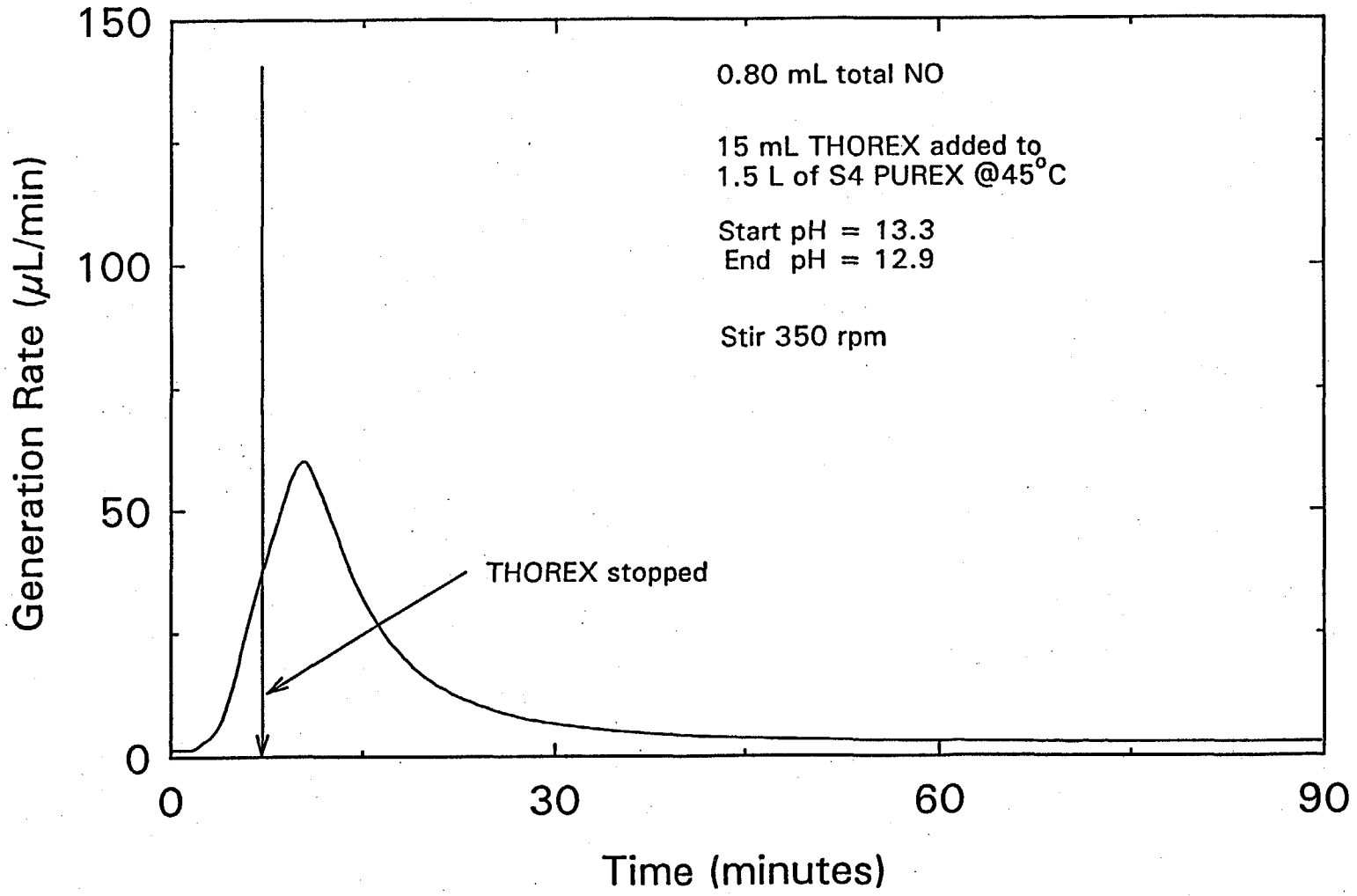

Figure C.27. Test 17B, Along with Tests 17A and 17C (Figures C.26 and C.28) was Conducted with Simplified Fourth-Wash PUREX and Added only Enough THOREX to Reduce the OH^- Concentration to 0.1 M (pH 13.0)

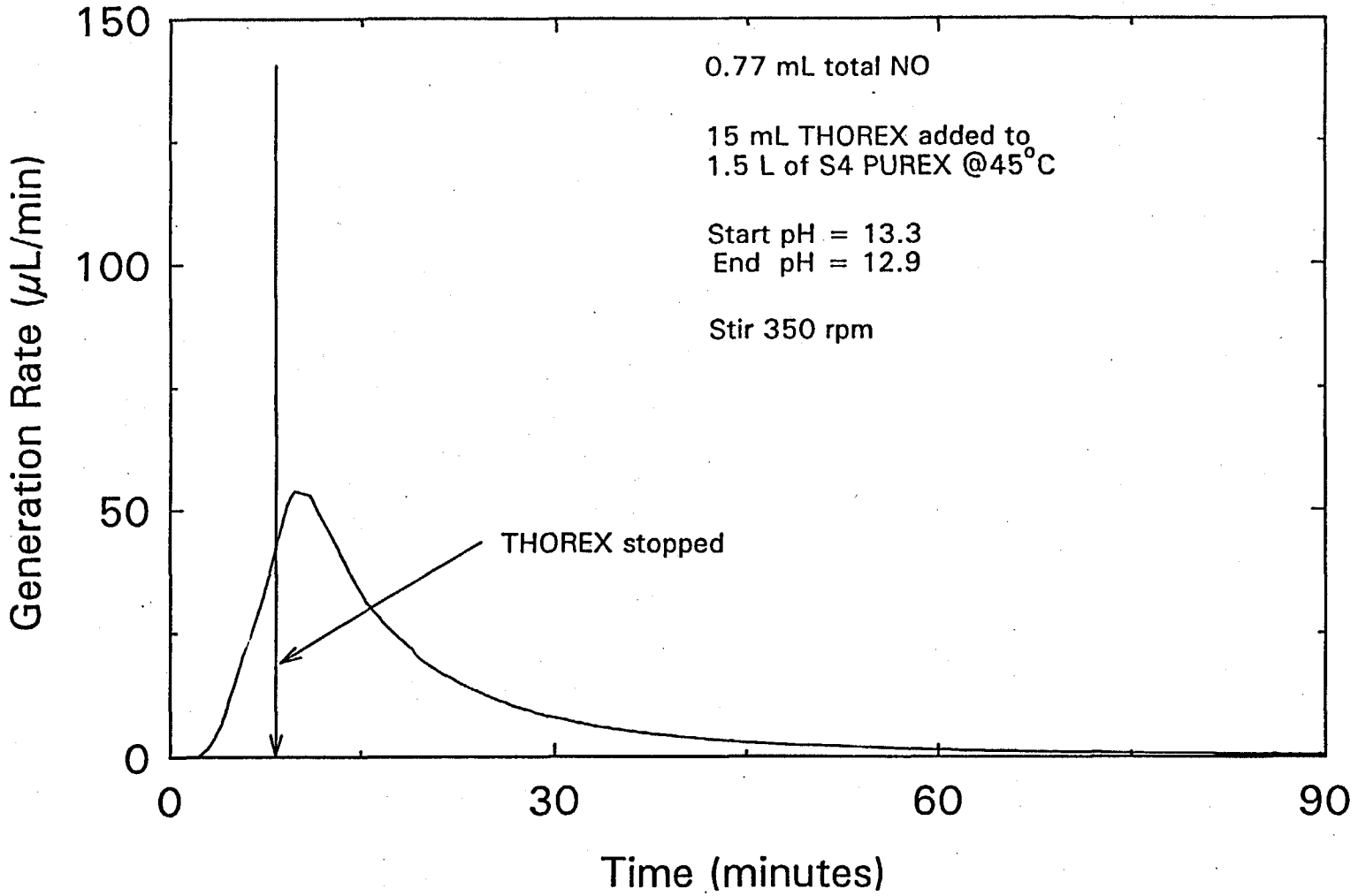

Figure C.28. Test 17C, Along with Tests 17B and 17C (Figures C.26 and C.27) was Conducted with Simplified Fourth-Wash PUREX and Added only Enough THOREX to Reduce the OH^- Concentration to 0.1 M (pH 13.0)

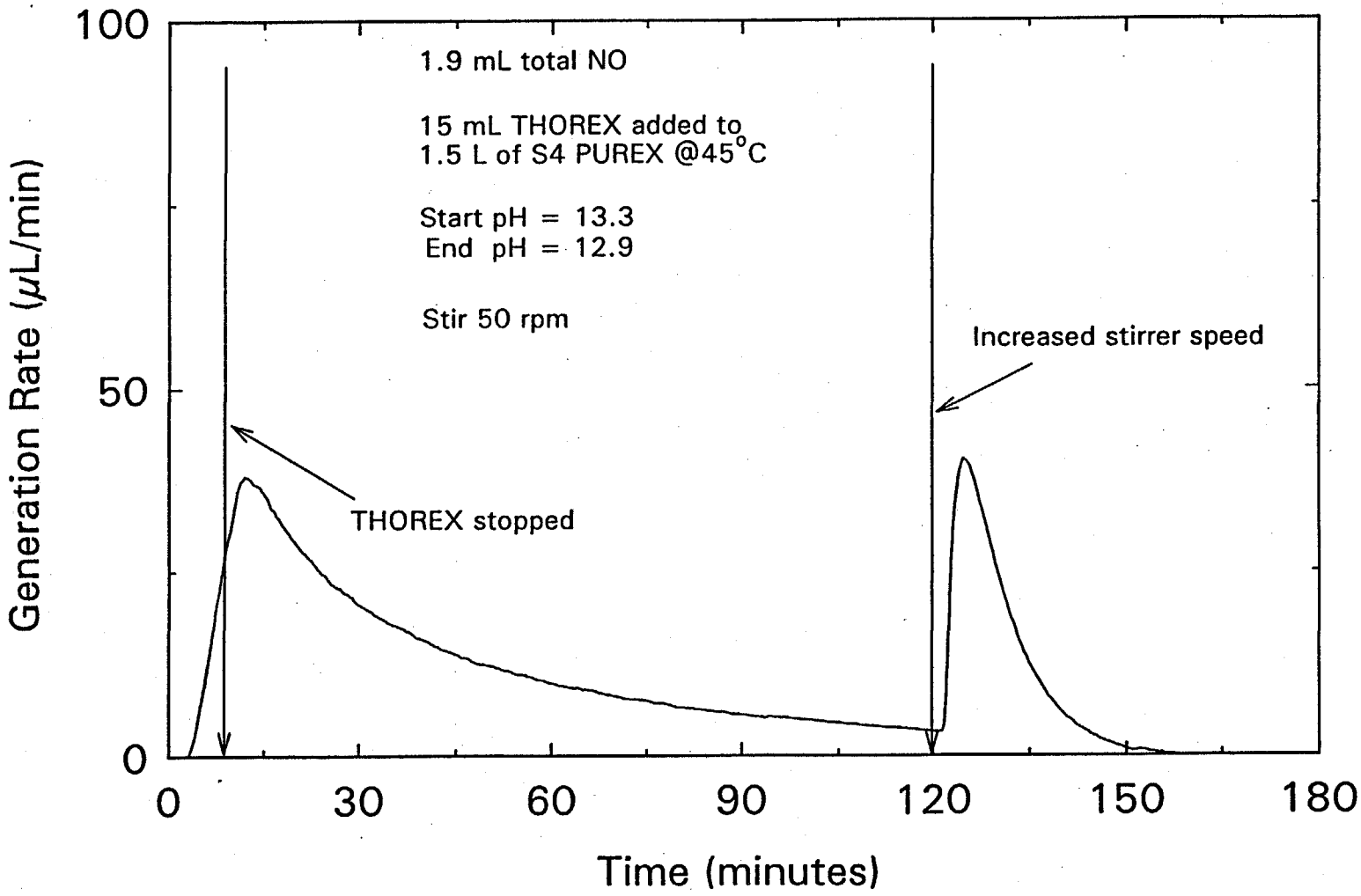

Figure C.29. Test 18 was Conducted Under the Same Conditions as Tests 17A to 17C (Figures C.26 to C.28) Except that a Slower Stirring Rate was Used

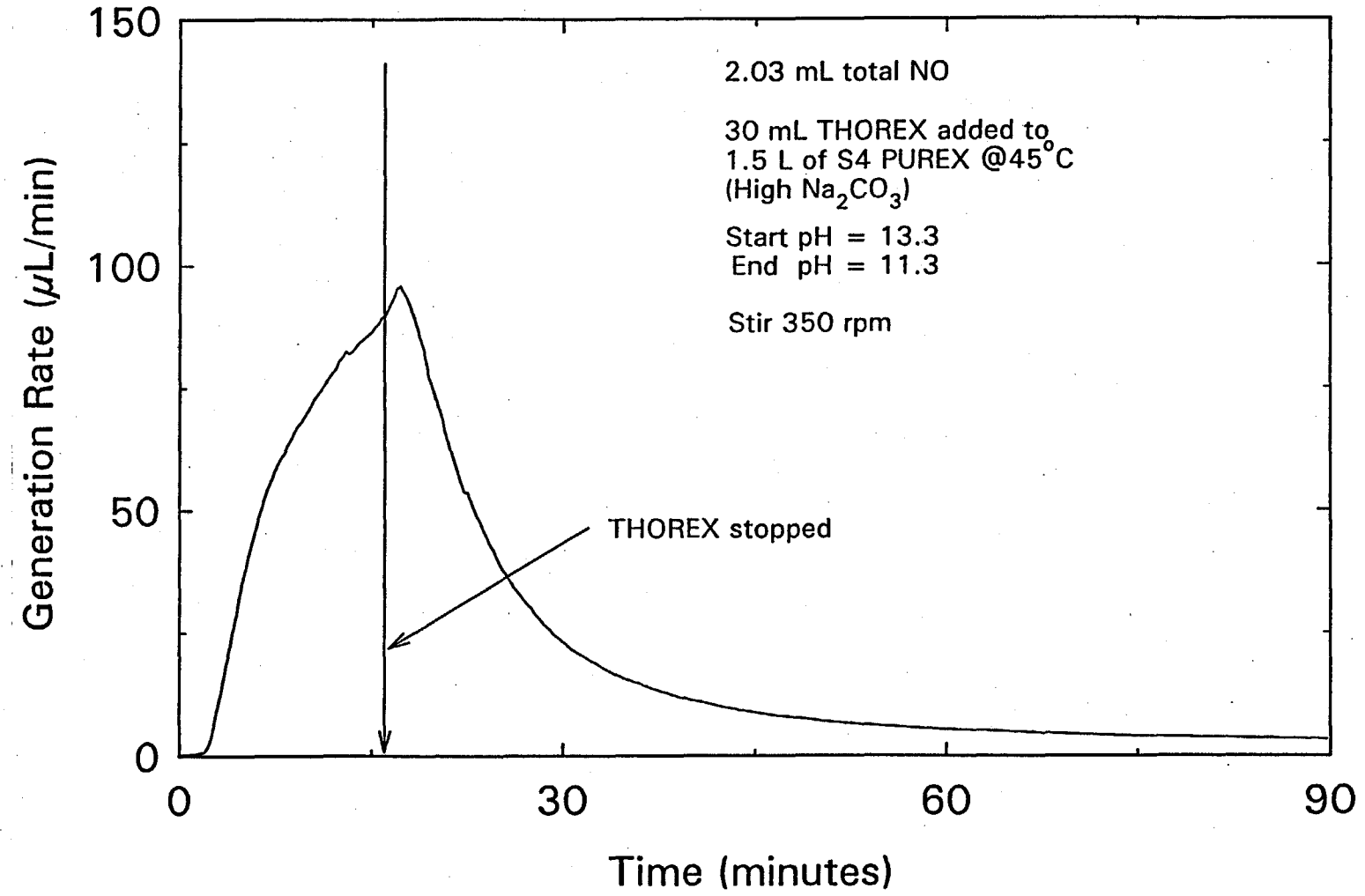

Figure C.30. Test 19 was Conducted with Conditions Similar to Those in Tests 14A to 14D (Figures C.20 to C.23) Except that the Na_2CO_3 Concentration Here was Increased Ten-Fold

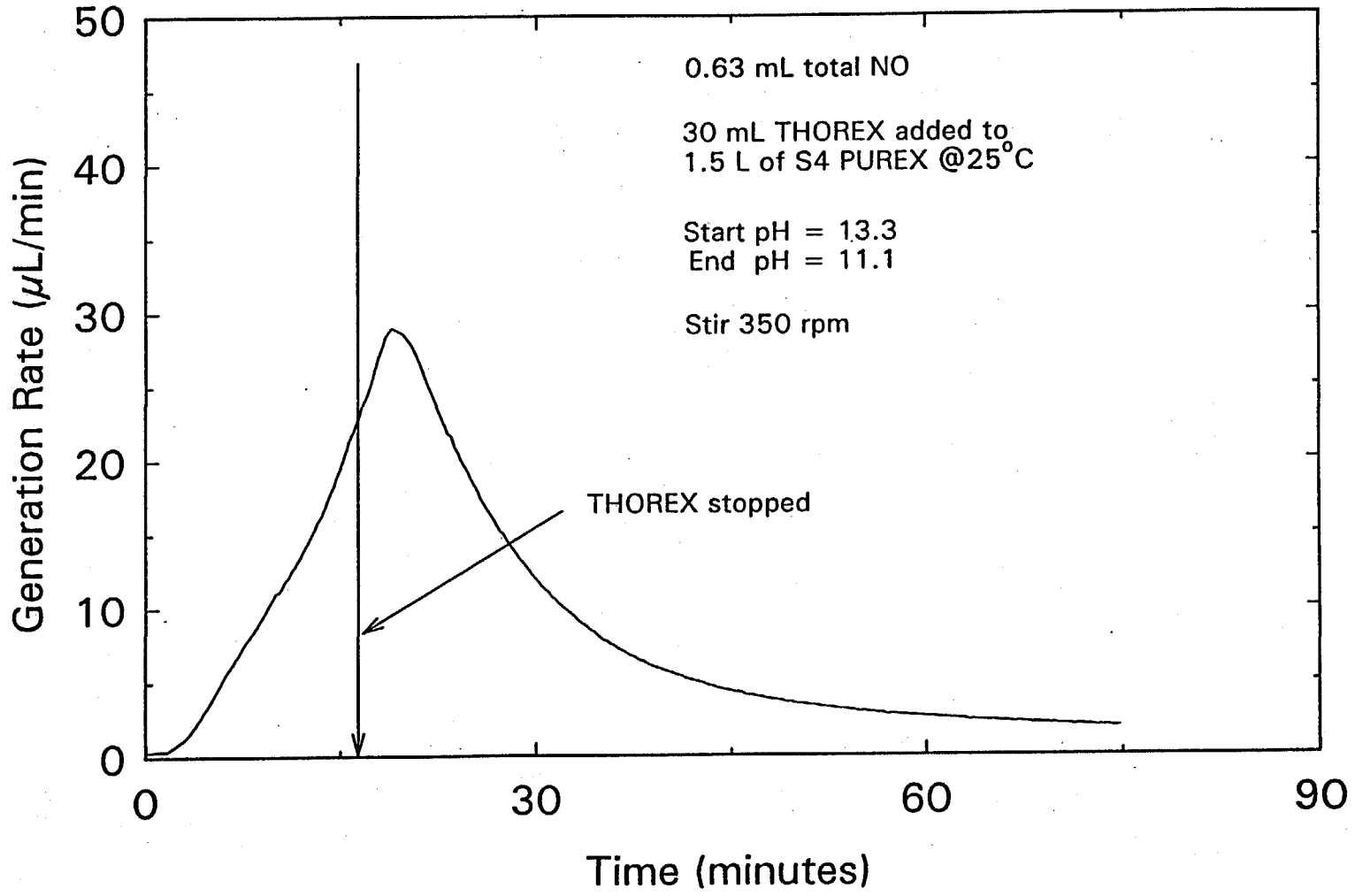

Figure C.31. Test 20A, Along with Tests 20B, 21A, and 21B (Figures C.32 to C.34) was Conducted to Explore the Effect of Temperature. Except for temperature, conditions were the same as in Tests 14A to 14D (Figures C.20 to C.23).

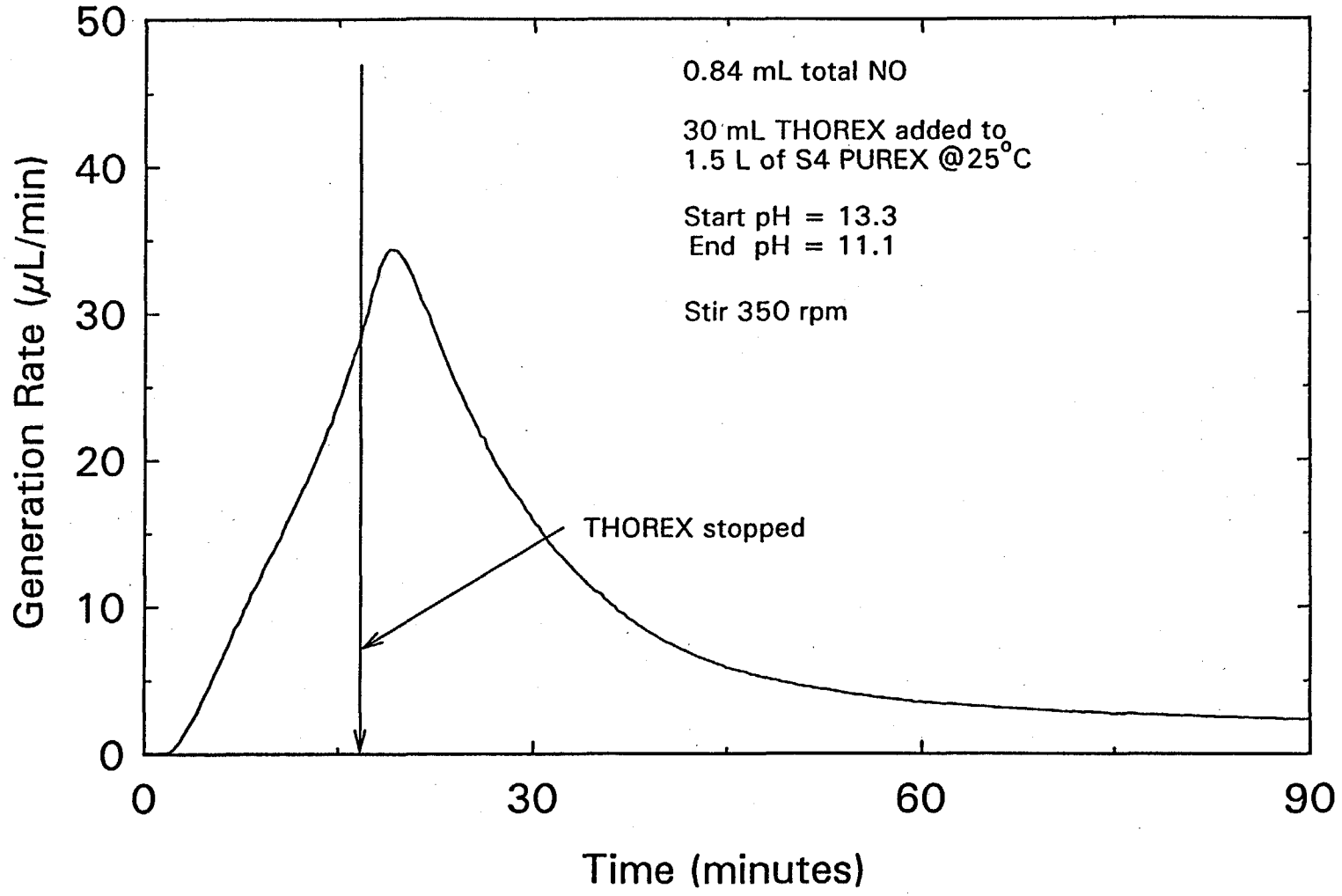

Figure C.32. Test 20B, Along with Tests 20A, 21A, and 21B (Figures C.31, C.33, and C.34) was Conducted to Explore the Effect of Temperature. Except for temperature, conditions were the same as in Tests 14A to 14D (Figures C.20 to C.23).

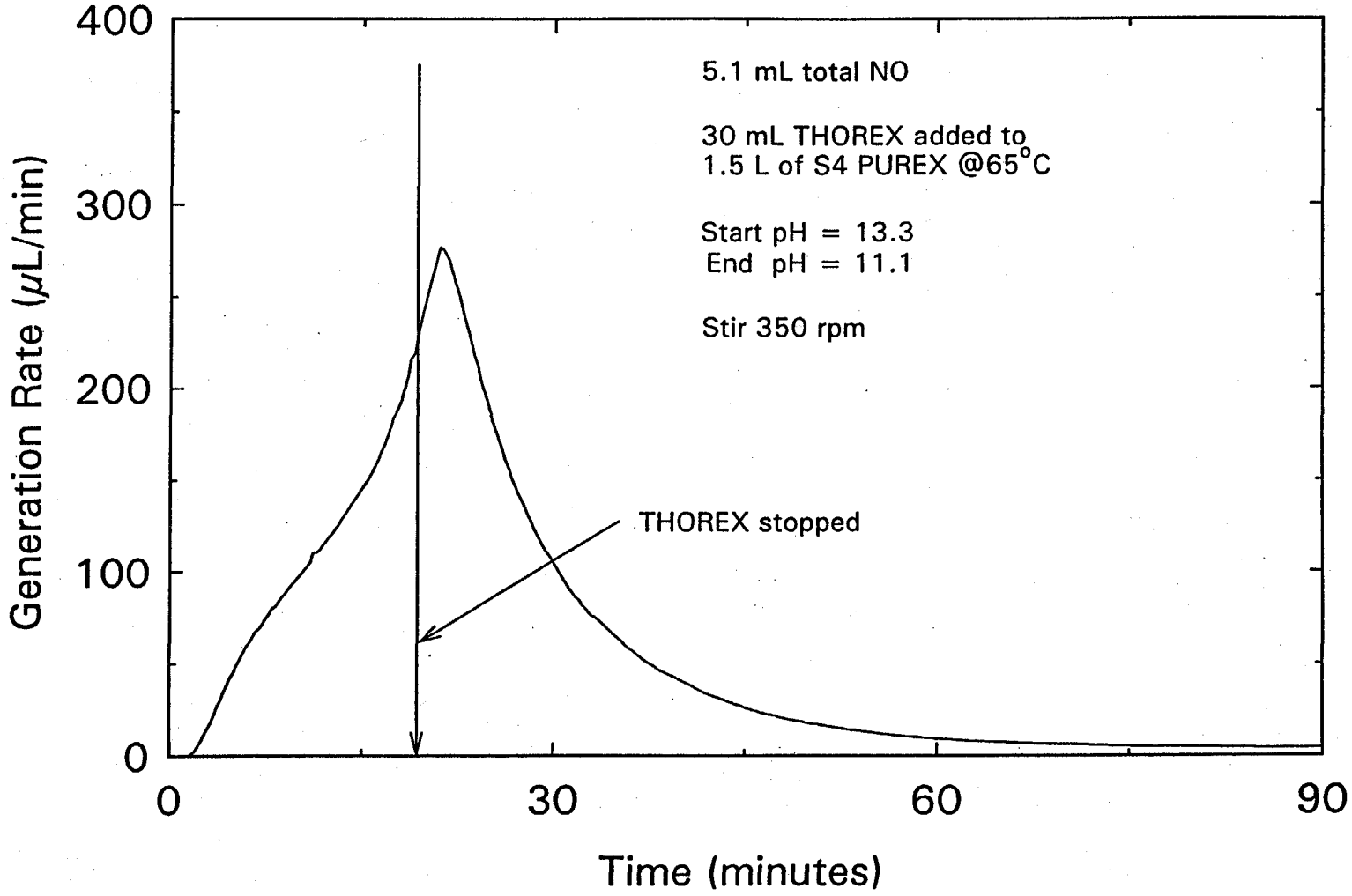

Figure C.33. Test 21A, Along with Tests 20A, 20B, and 21B (Figures C.31, C.32, and C.34) was Conducted to Explore the Effect of Temperature. Except for temperature, conditions were the same as in Tests 14A to 14D (Figures C.20 to C.23).

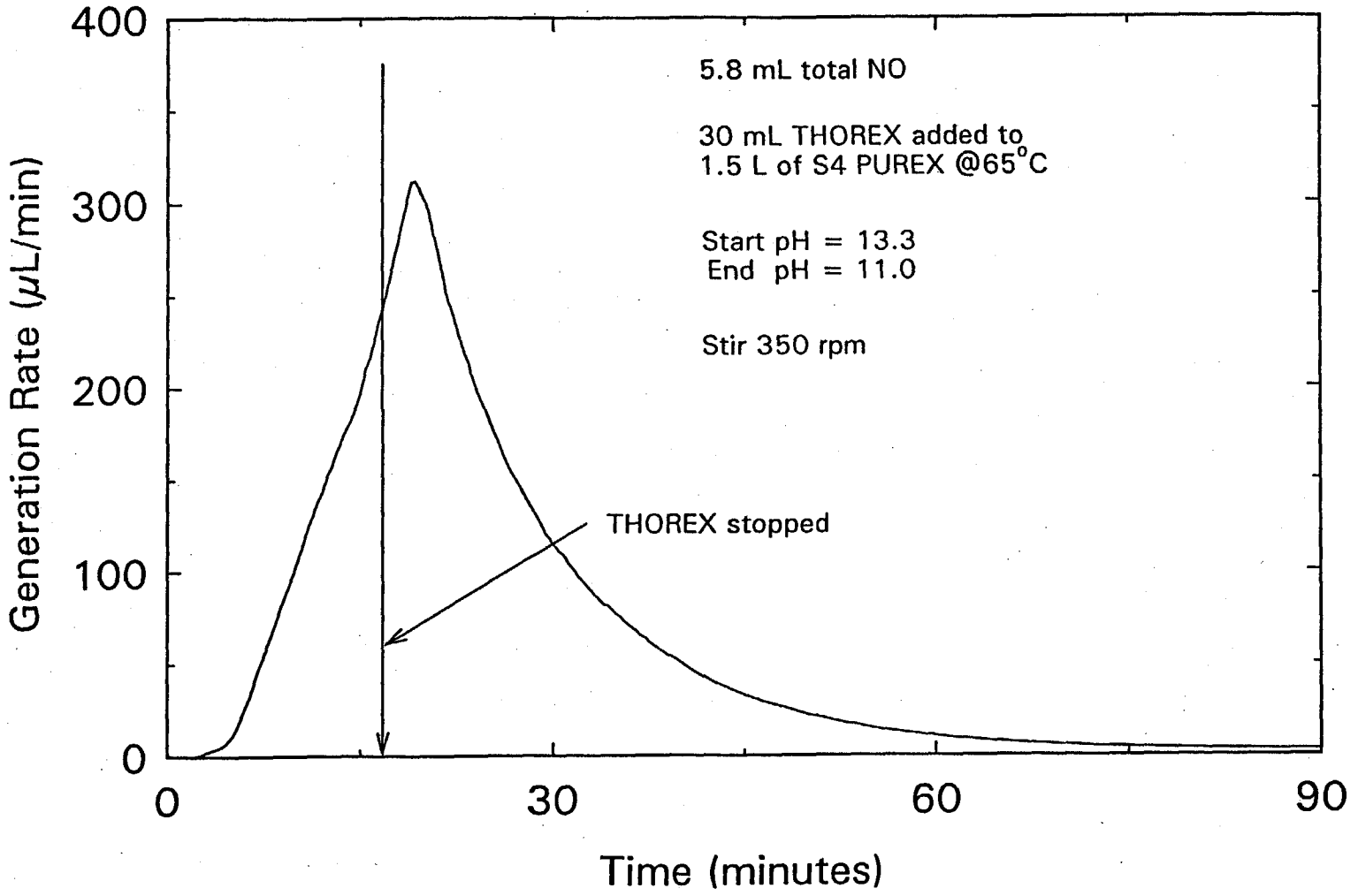

Figure C.34. Test 21B, Along with Tests 20A, 20B, and 21A (Figures C.31 to C.33) was Conducted to Explore the Effect of Temperature. Except for temperature, conditions were the same as in Tests 14A to 14D (Figures C.20 to C.23).

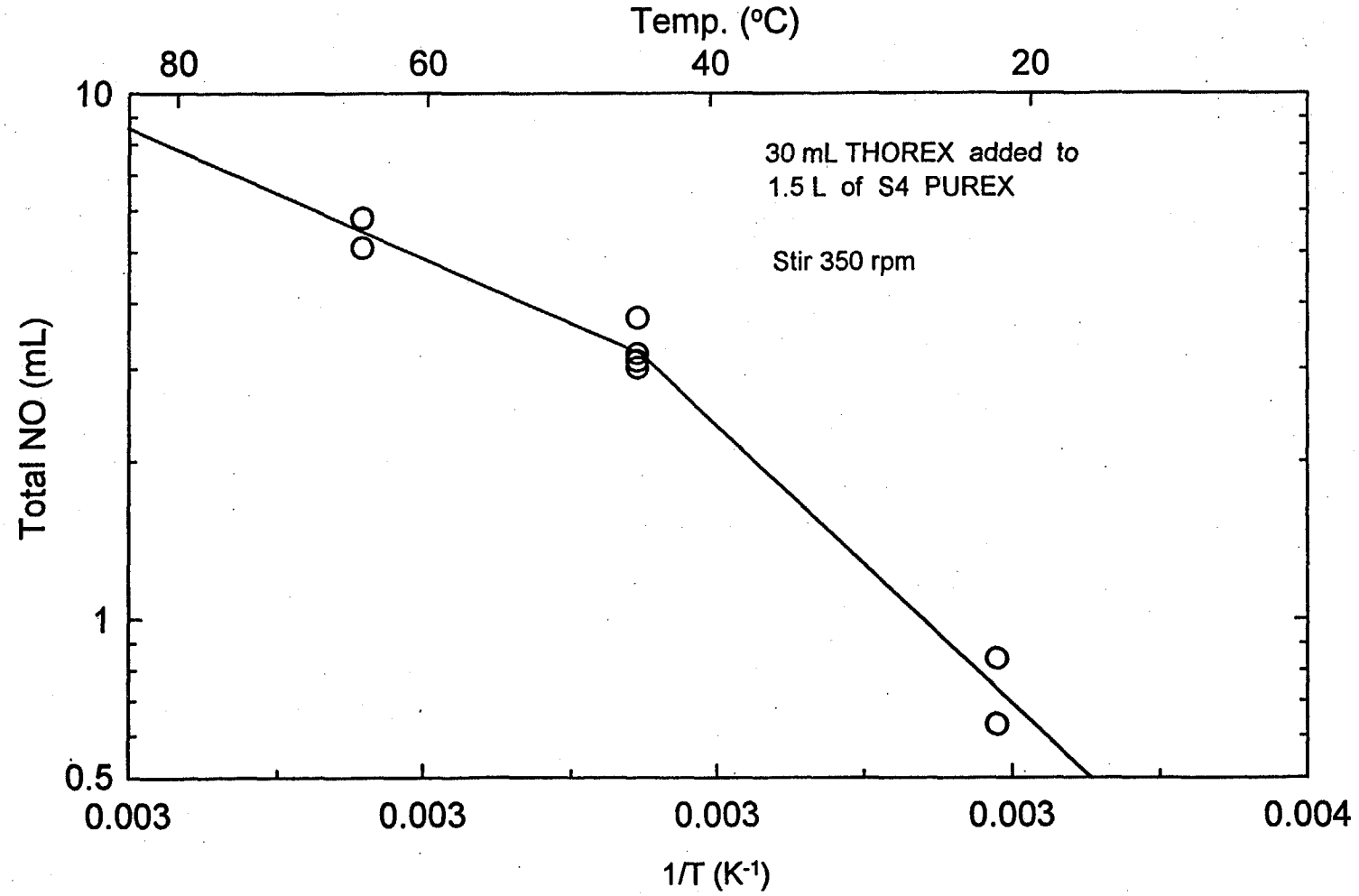

Figure C.35. Arrhenius Plot of Tests 14A to 14D and 20A to 21B

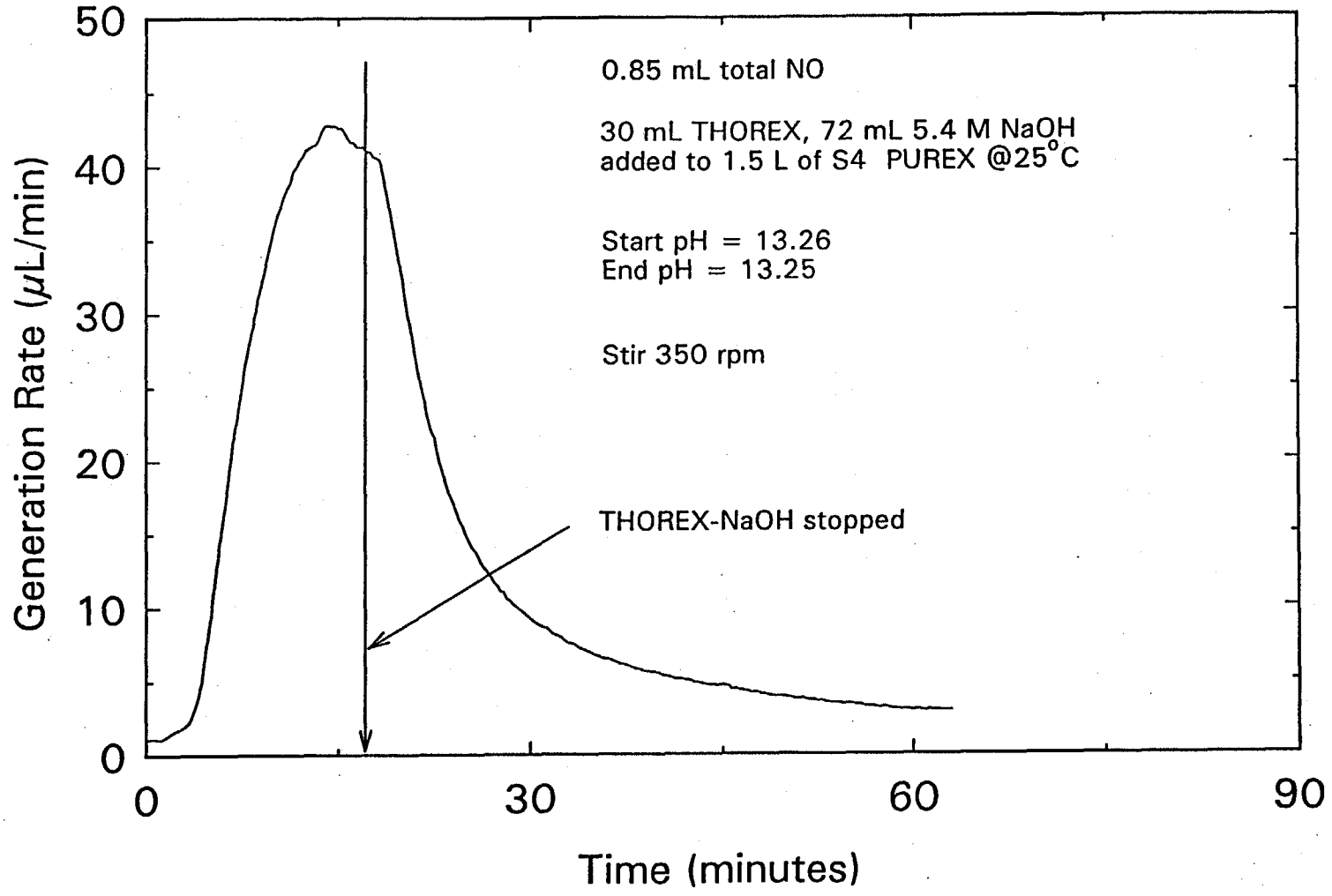

Figure C.36. Simultaneous Addition of THOREX and NaOH to PUREX at Relative Rates Intended to Maintain pH Constant at About 13.3

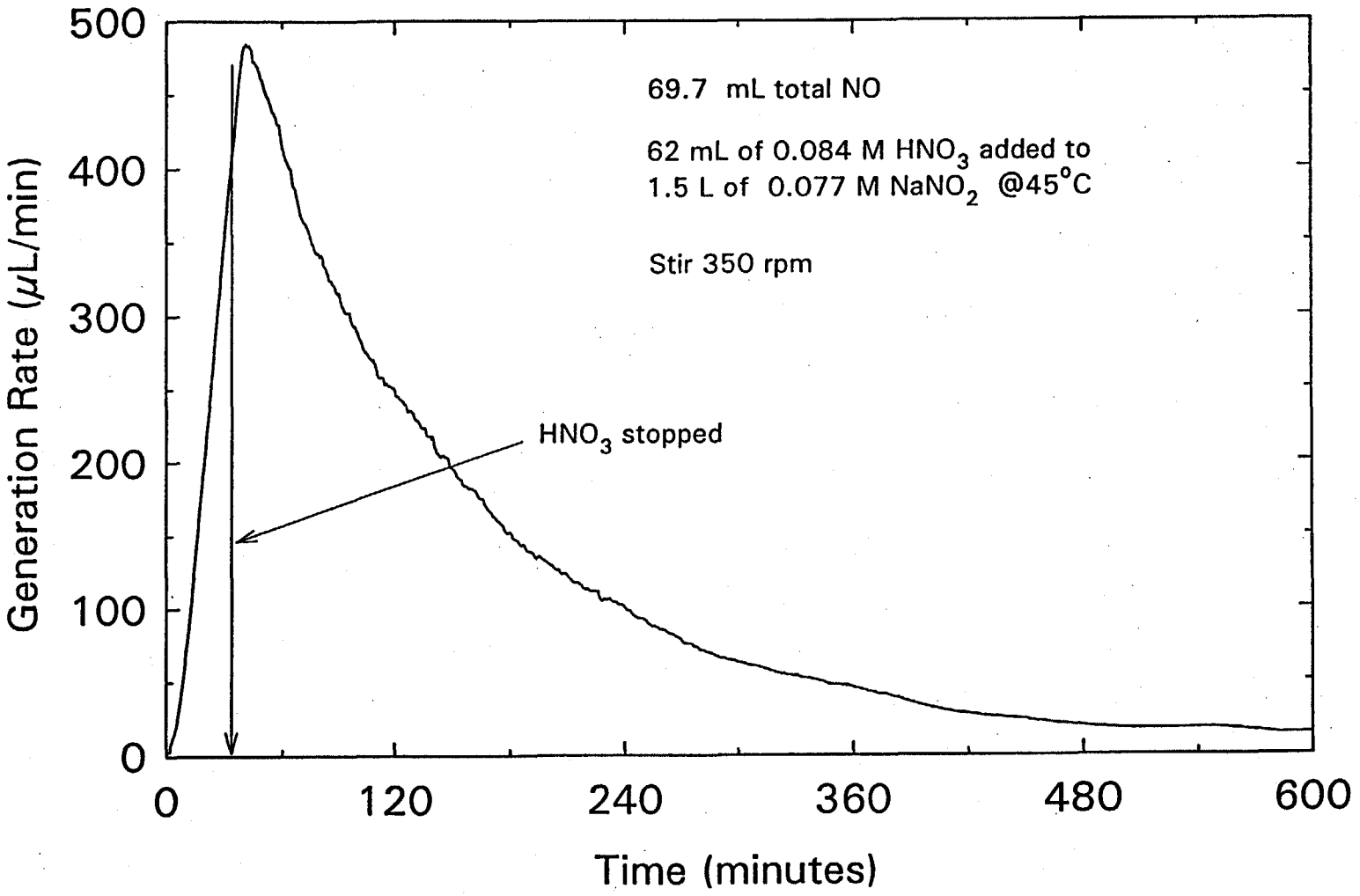

Figure C.37. Addition of Pure HNO_3 to Pure $NaNO_2$

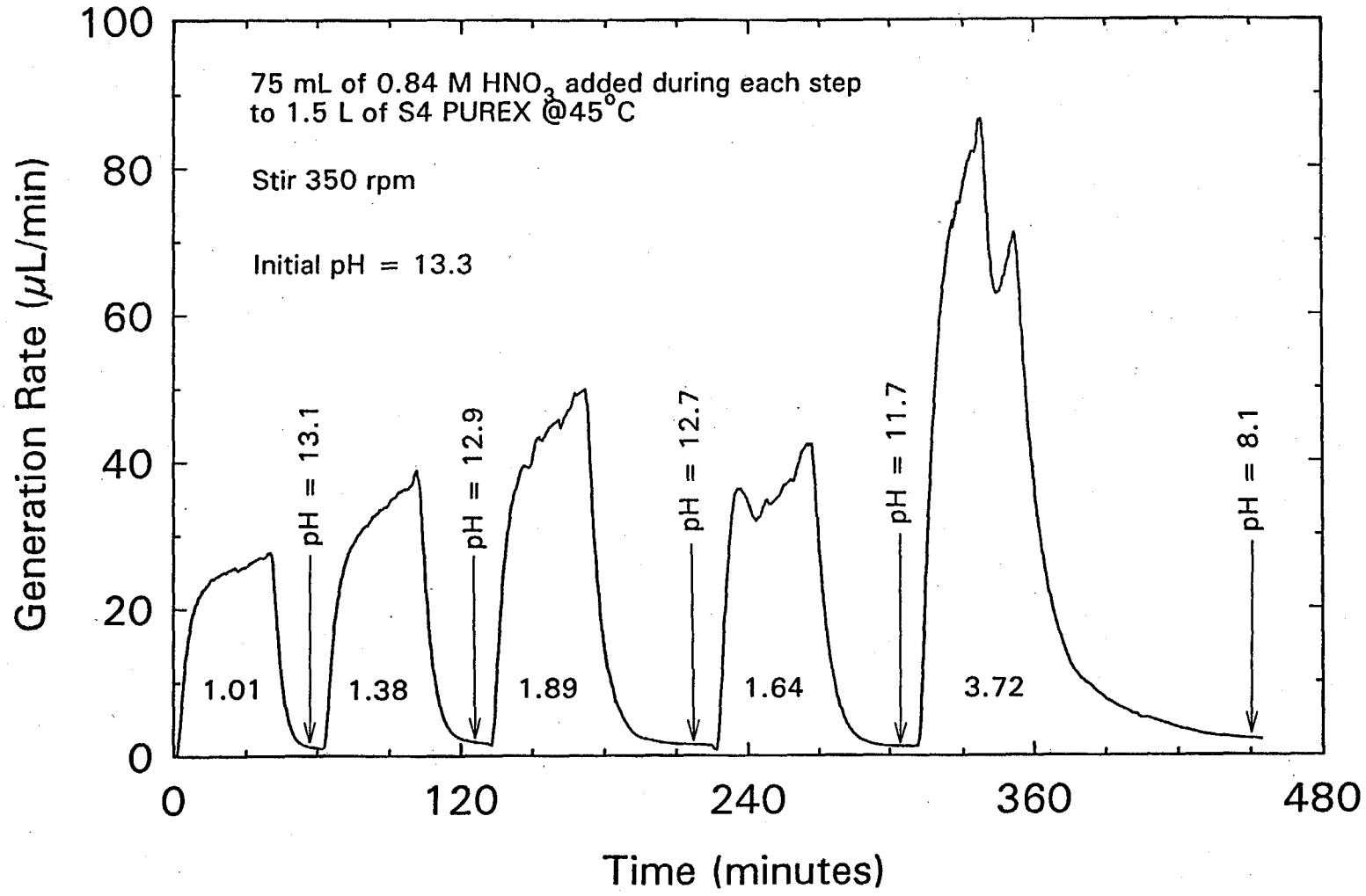

Figure C.38. Step-Wise Addition of Pure HNO_3 to S4 PUREX. First three steps were conducted one day and the last two steps the next day.

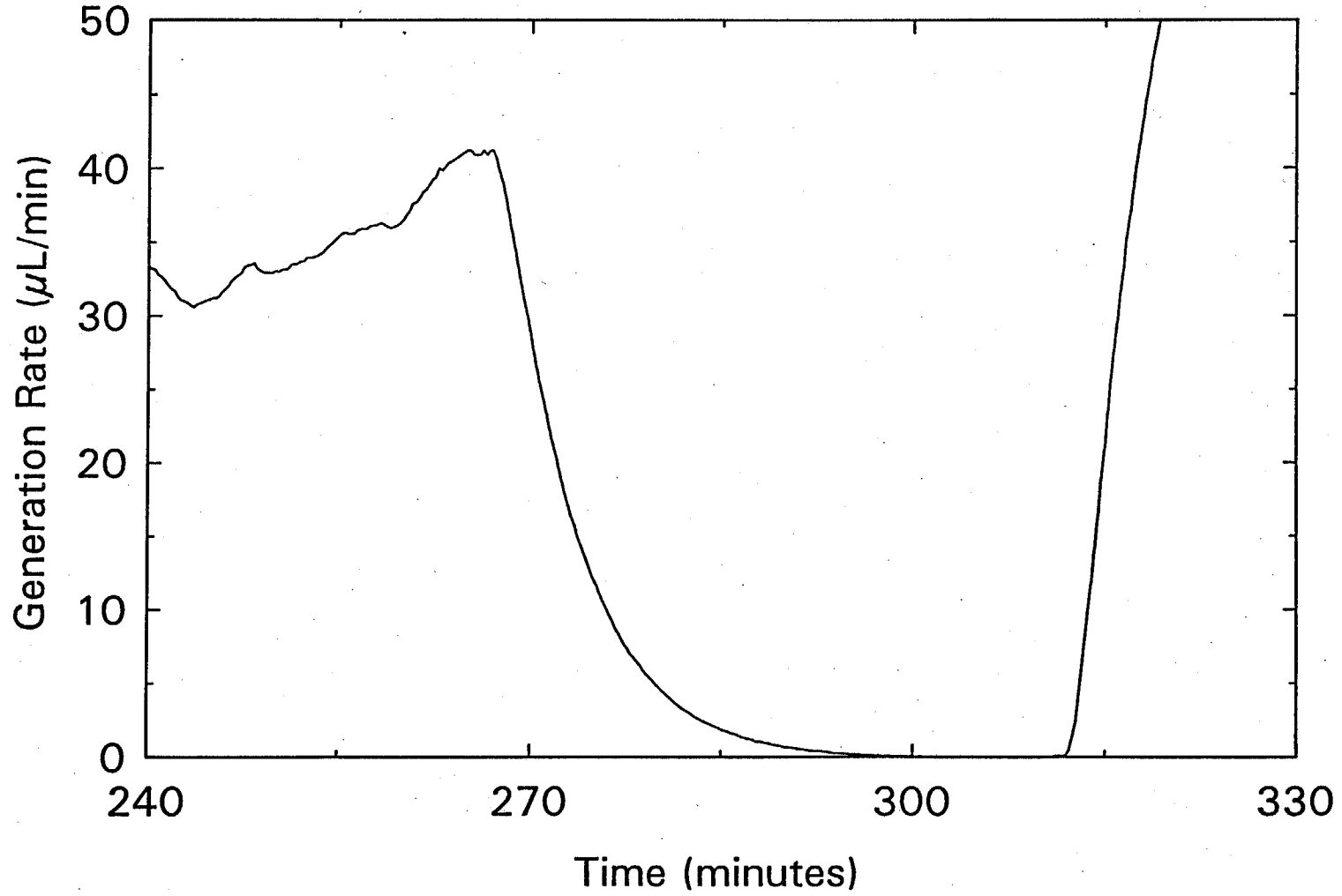

Figure C.39. Expansion of Figure C.38 Between 240 and 330 minutes. The baseline was normalized to zero near 300 minutes.

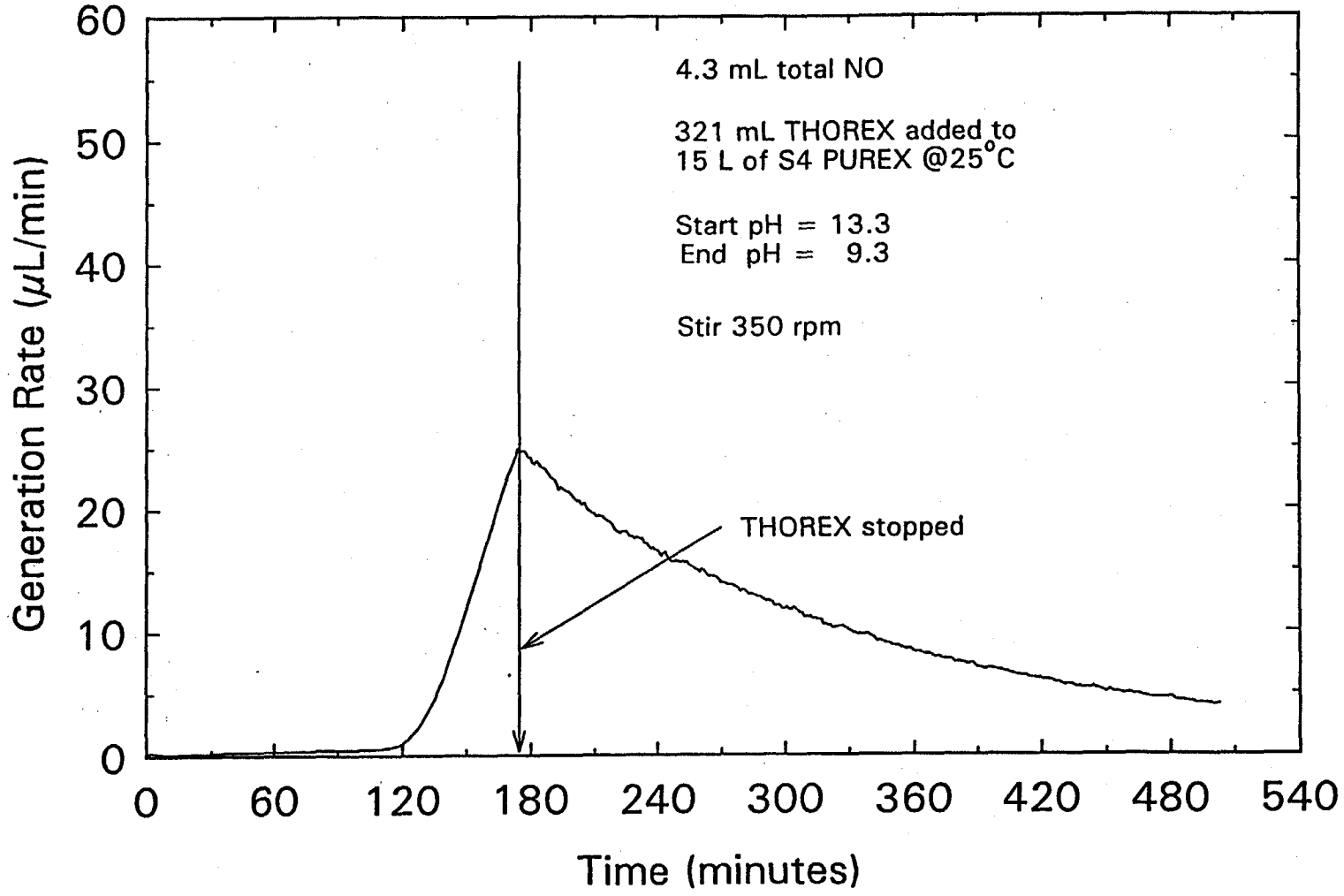

Figure C.40. Test 23A, First Large-Scale Test Using 17 L Reaction Vessel. Test was terminated before the NO generation rate returned to zero.

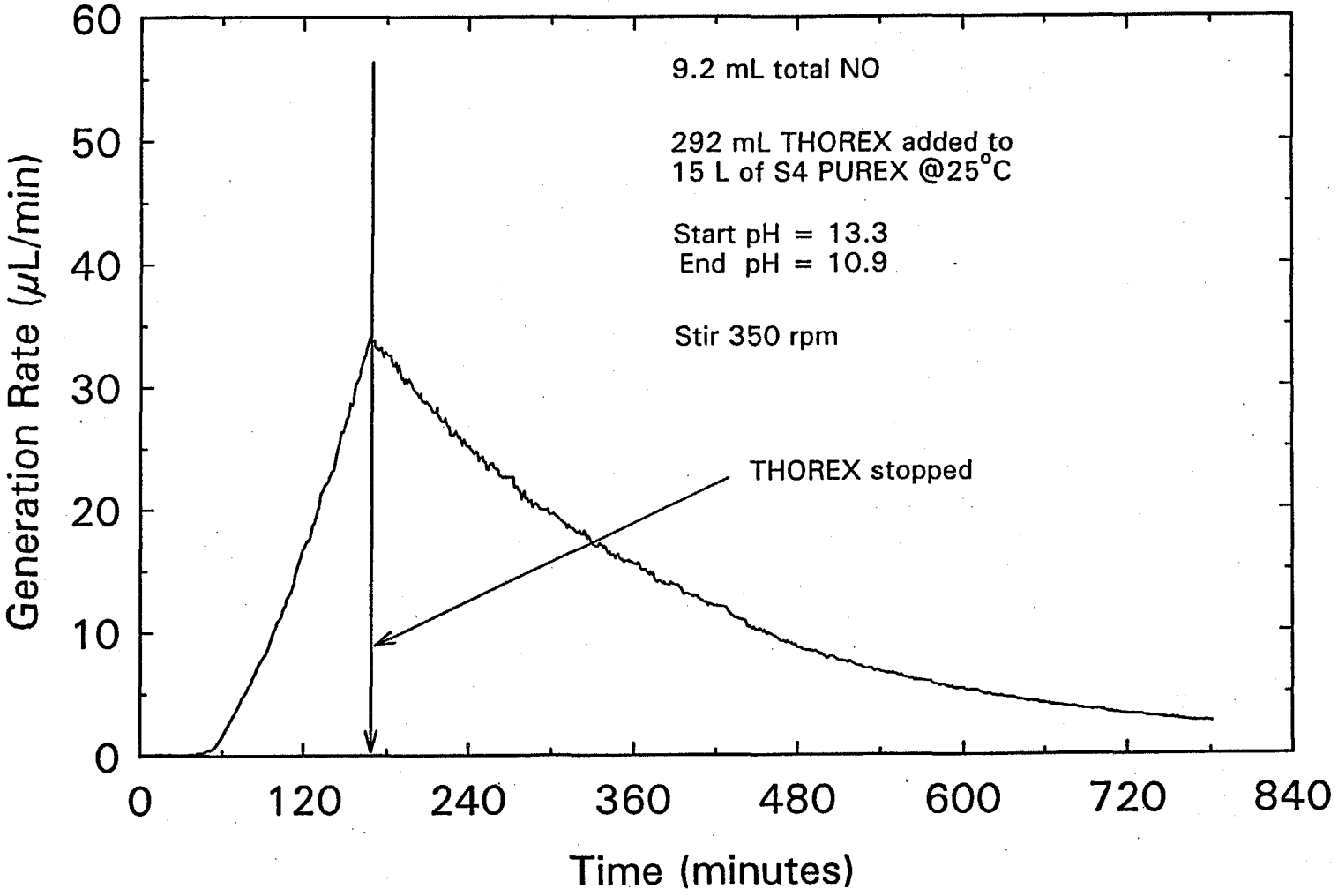

Figure C.41. Test 23B, Second Large-Scale Test Using 17 L Reaction Vessel. NO_X analyzer zero was verified at end of test. This confirmed that a small amount of NO was still being generated when the test was terminated.

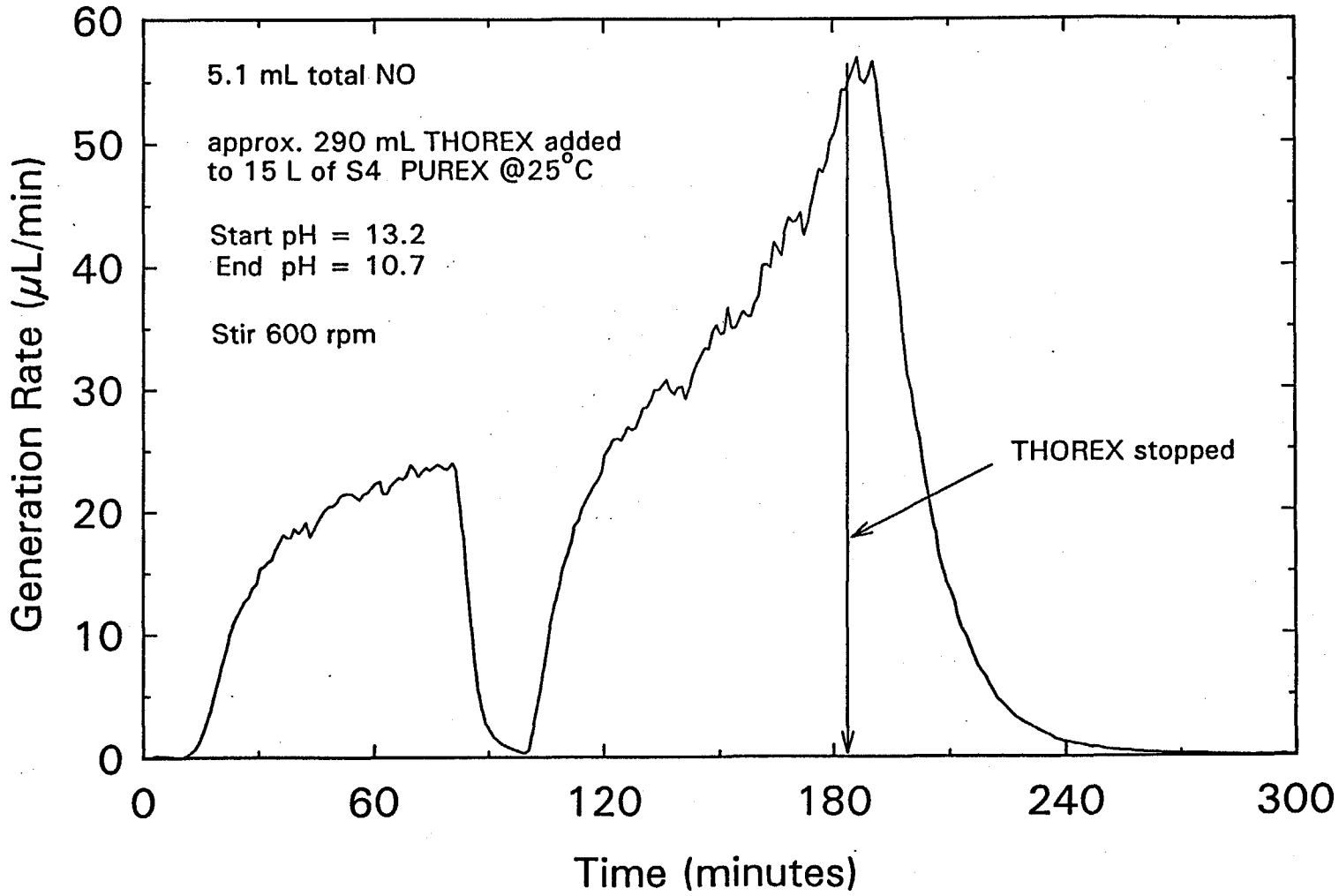

Figure C.42. Test 24, Large-Scale Test with Fast Stirring. Dip in curve happened when THOREX level was drawn down below the level of the pump intake line.

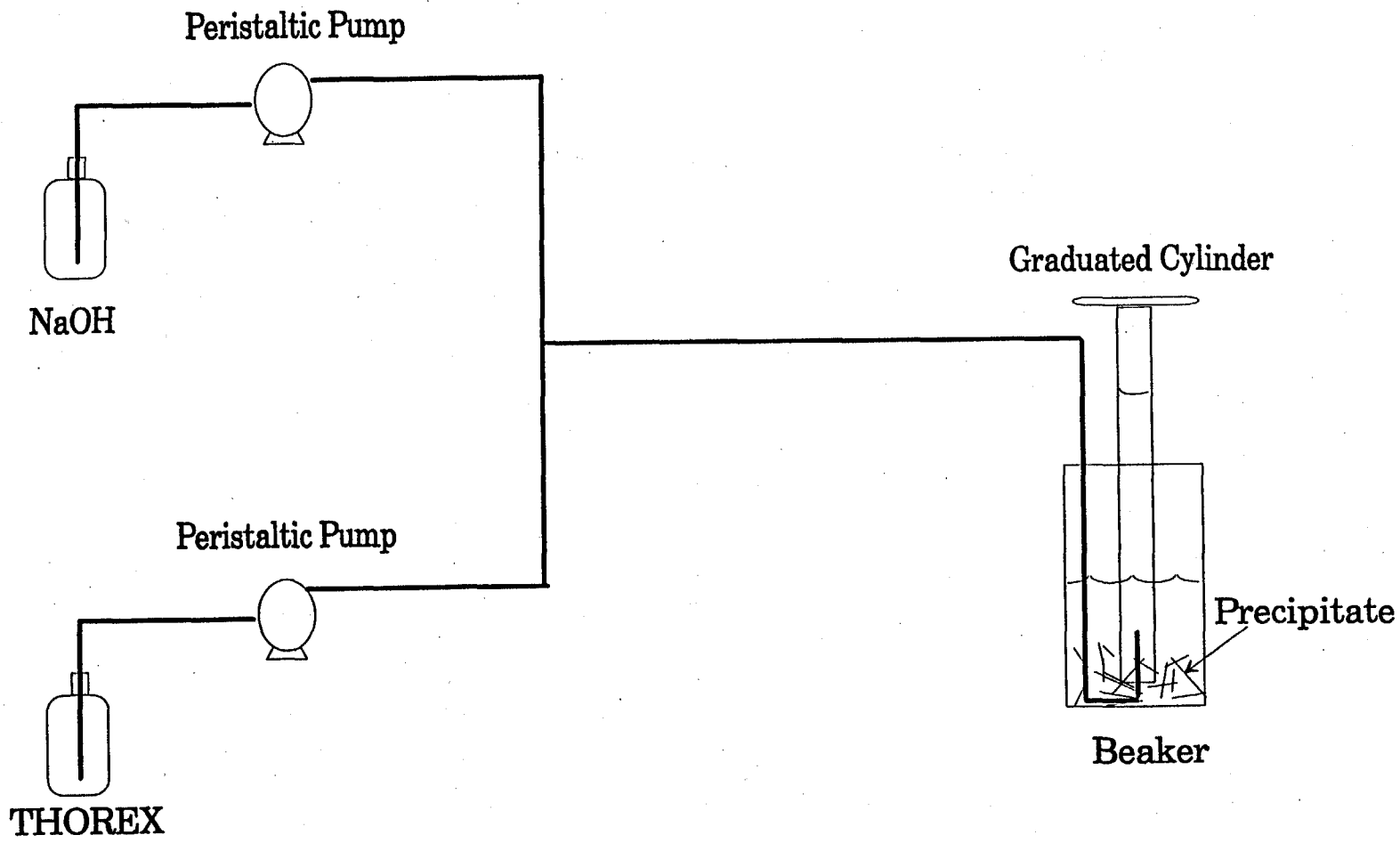

Figure C.43. Schematic Diagram of THOREX/NaOH Mixing Tests

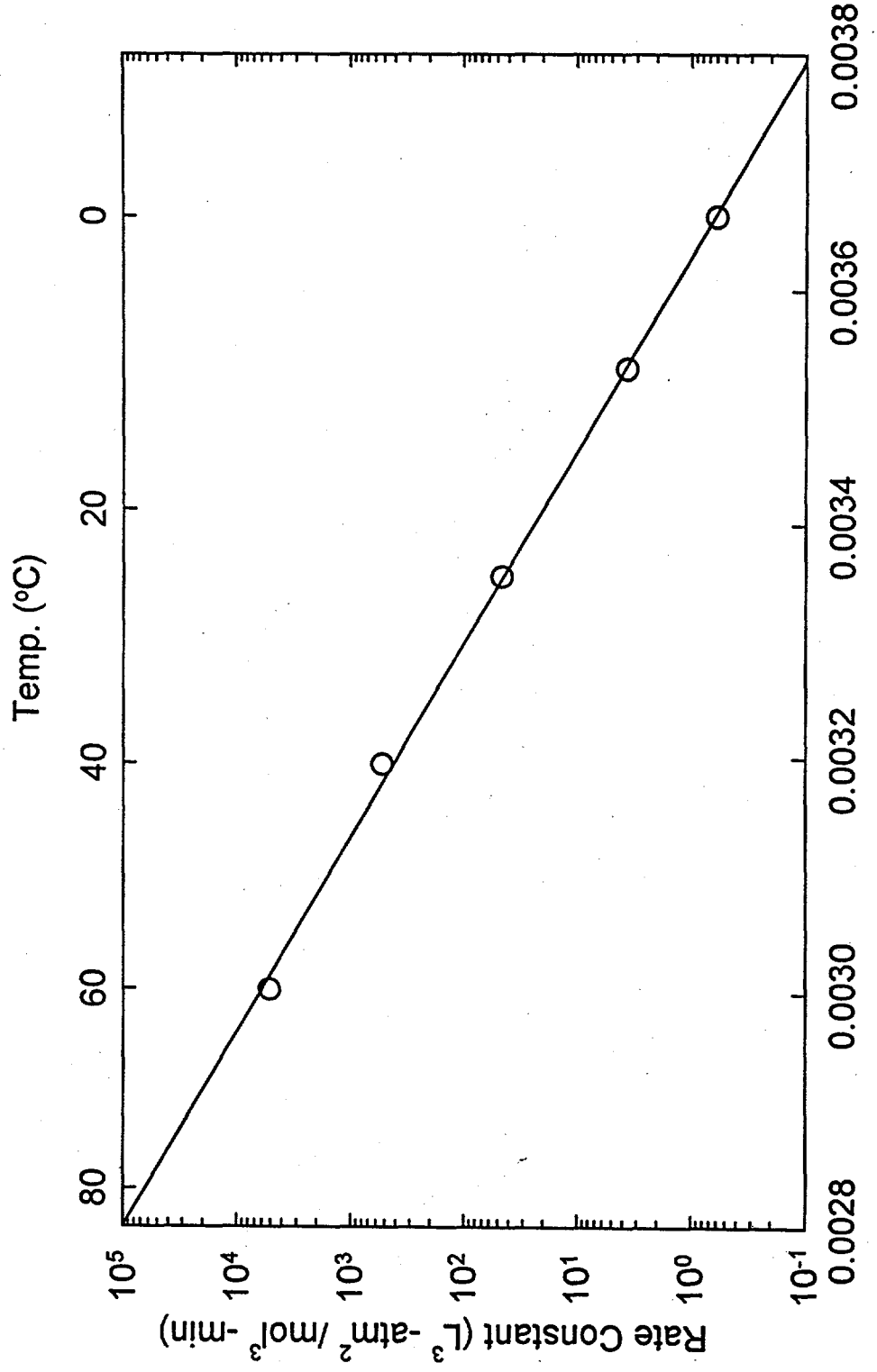

Figure C.44. Arrhenius Plot of HNO_2 Decomposition Rates, Equation 2.14

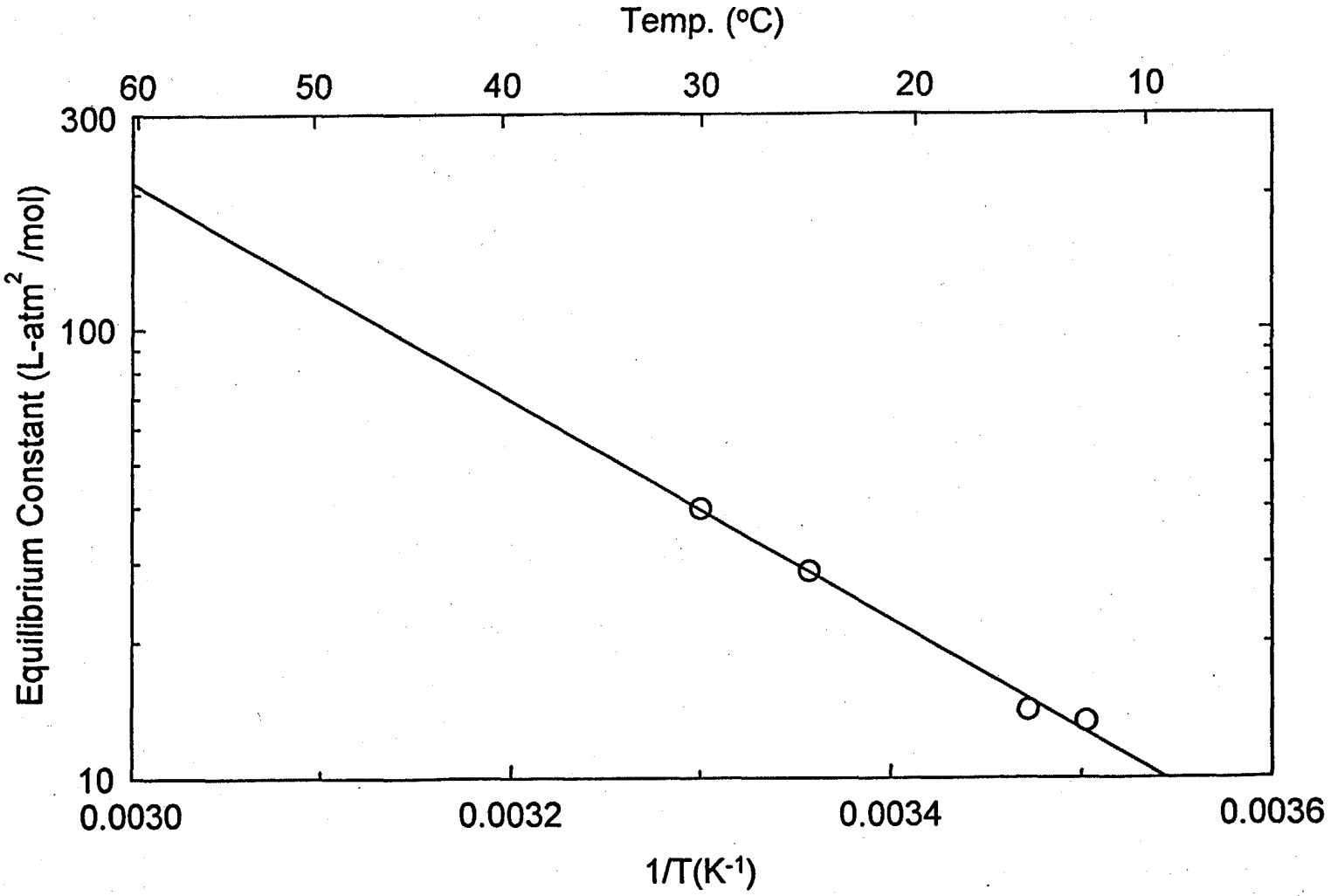

Figure C.45. Arrhenius Plot of Equilibrium Constant, Equation 2.15

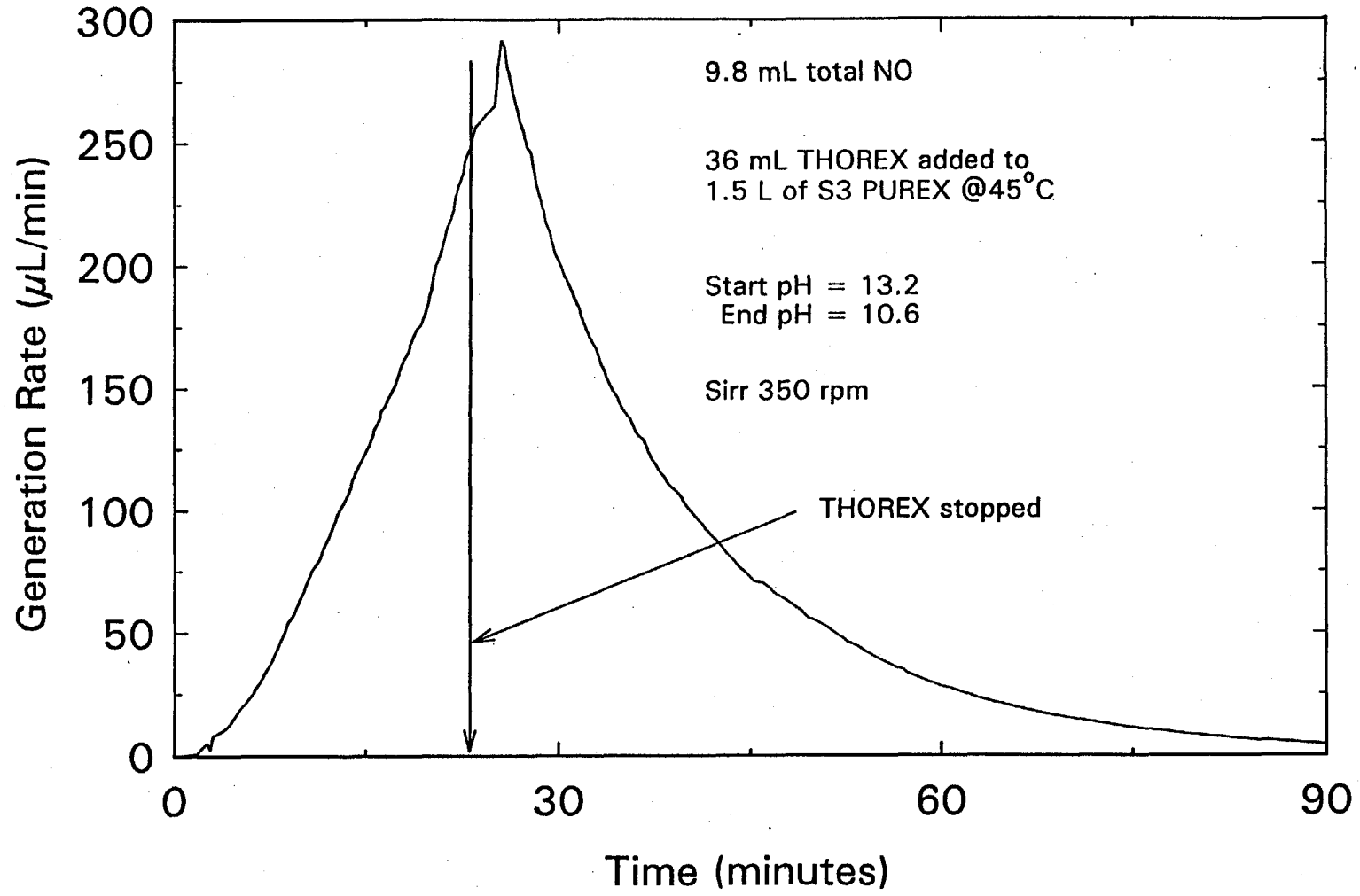

Figure C.46. Supplemental Test 25A. Duplicate run of Tests 7A/7B, Figures C.12 and C.13. See Figure C.47 for second duplicate run.

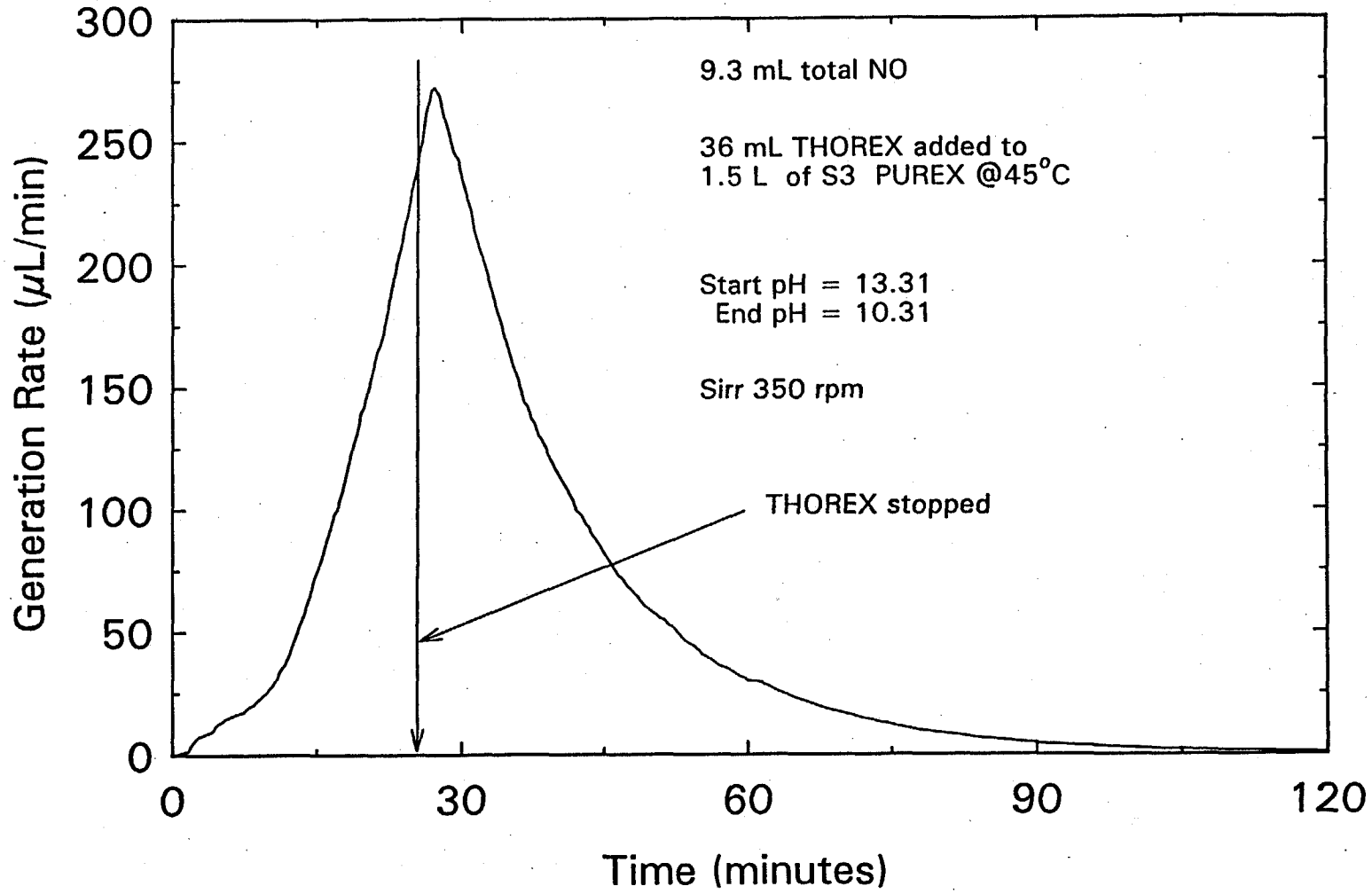

Figure C.47. Supplemental Test 25B. Duplicate run of Tests 7A/7B, Figures C.12 and C.13. See Figure C.46 for first duplicate run.

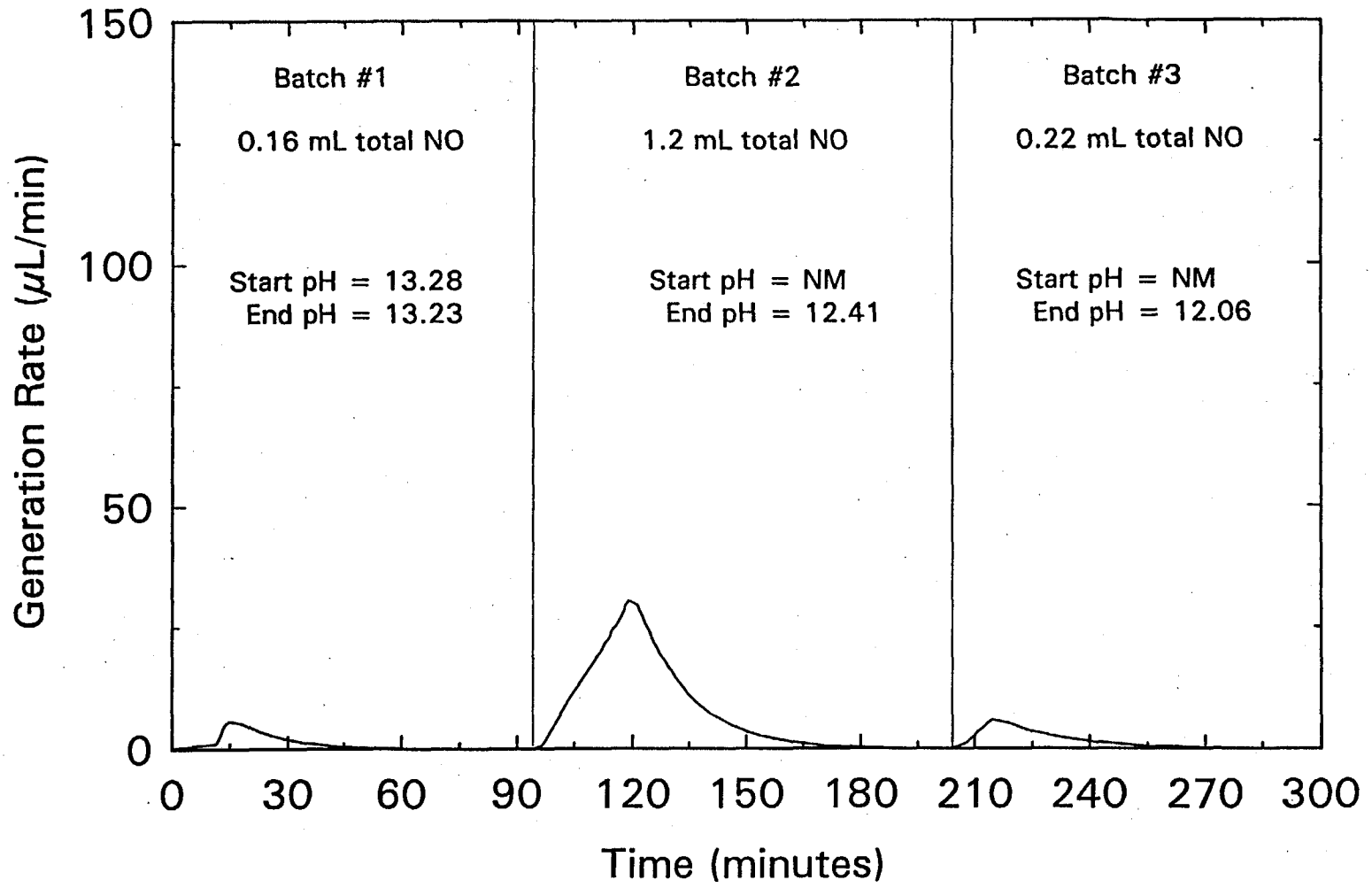

Figure C.48. Supplemental Test 26. No $NaNO_2$ added during this run. See Figures C.52 and C.53 for similar tests in which $NaNO_2$ was added at the beginnings of Batches #2 and #3.

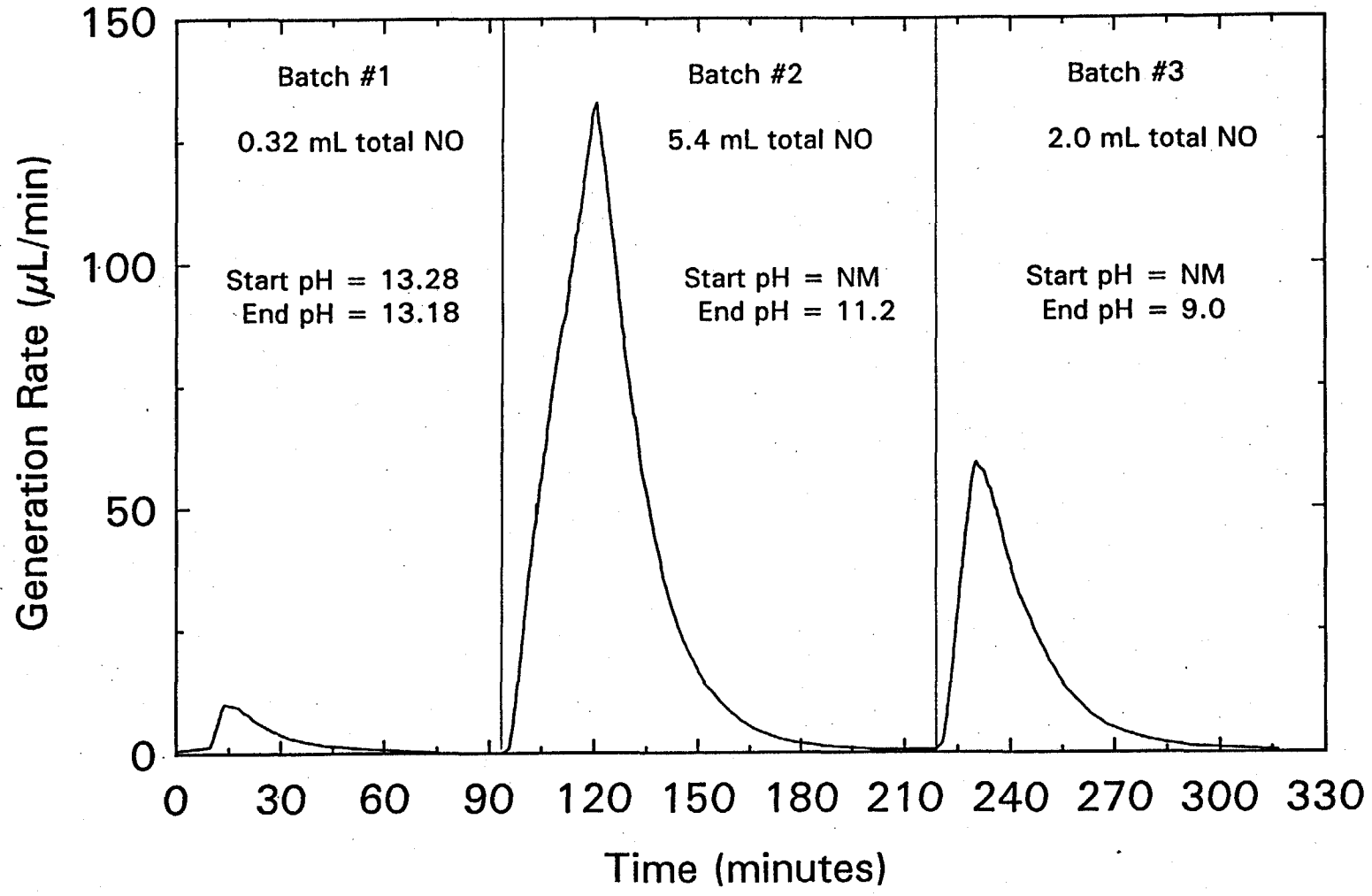

Figure C.49. Supplemental Test 27. Similar to Test 26, Figure C.48, except that $NaNO_2$ was added at the beginnings of Batches #2 and #3. However, due to low pH values, this test yielded atypically high quantities of NO gas. See Figures C.52 and C.53.

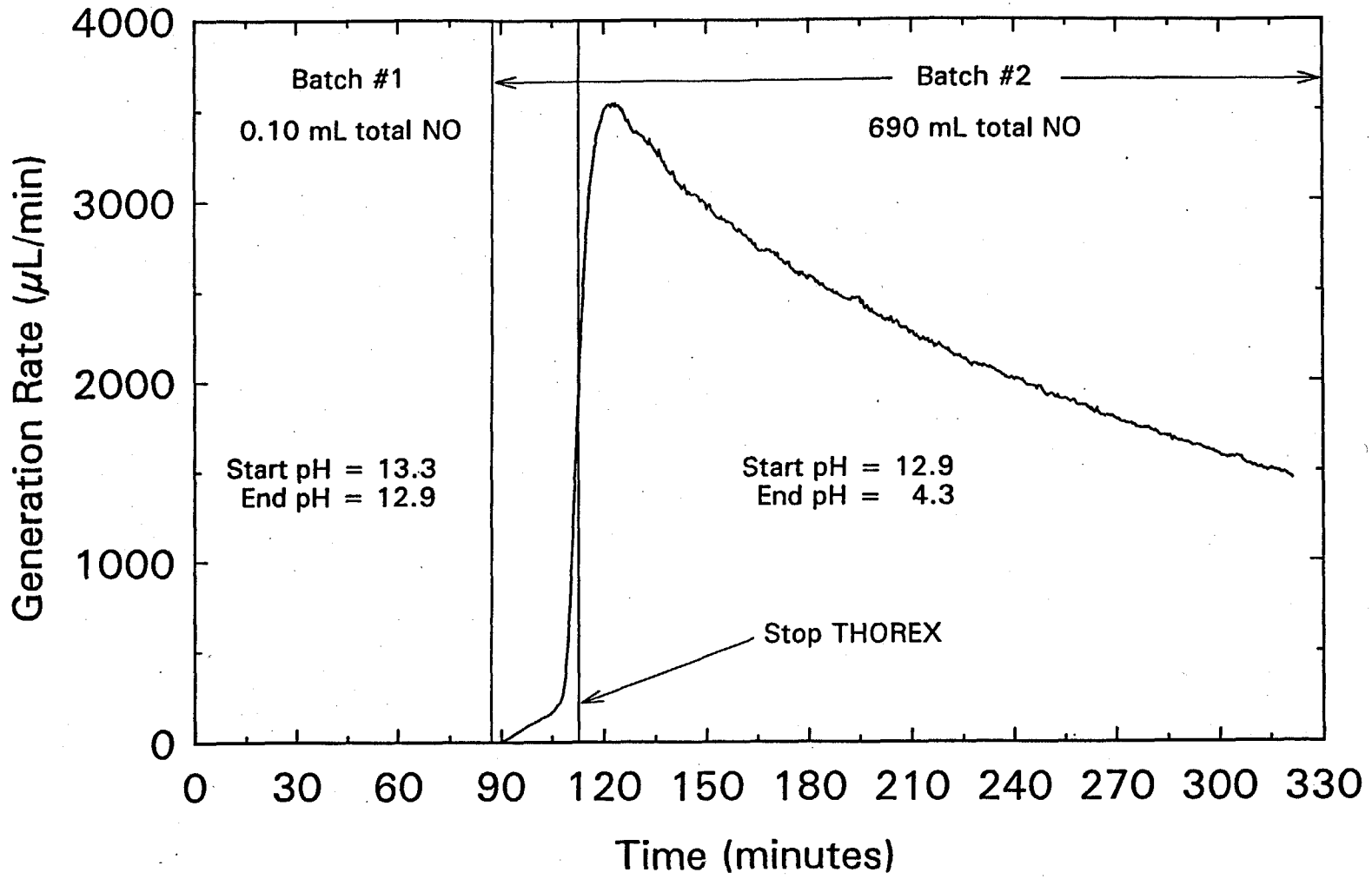

Figure C.50. Supplemental Test 28. Because no NaOH was added during Batch #1, the pH dropped far too low in Batch #2 giving rise to a very large amount of NO gas. See Figure C.51 for different plot of same data.

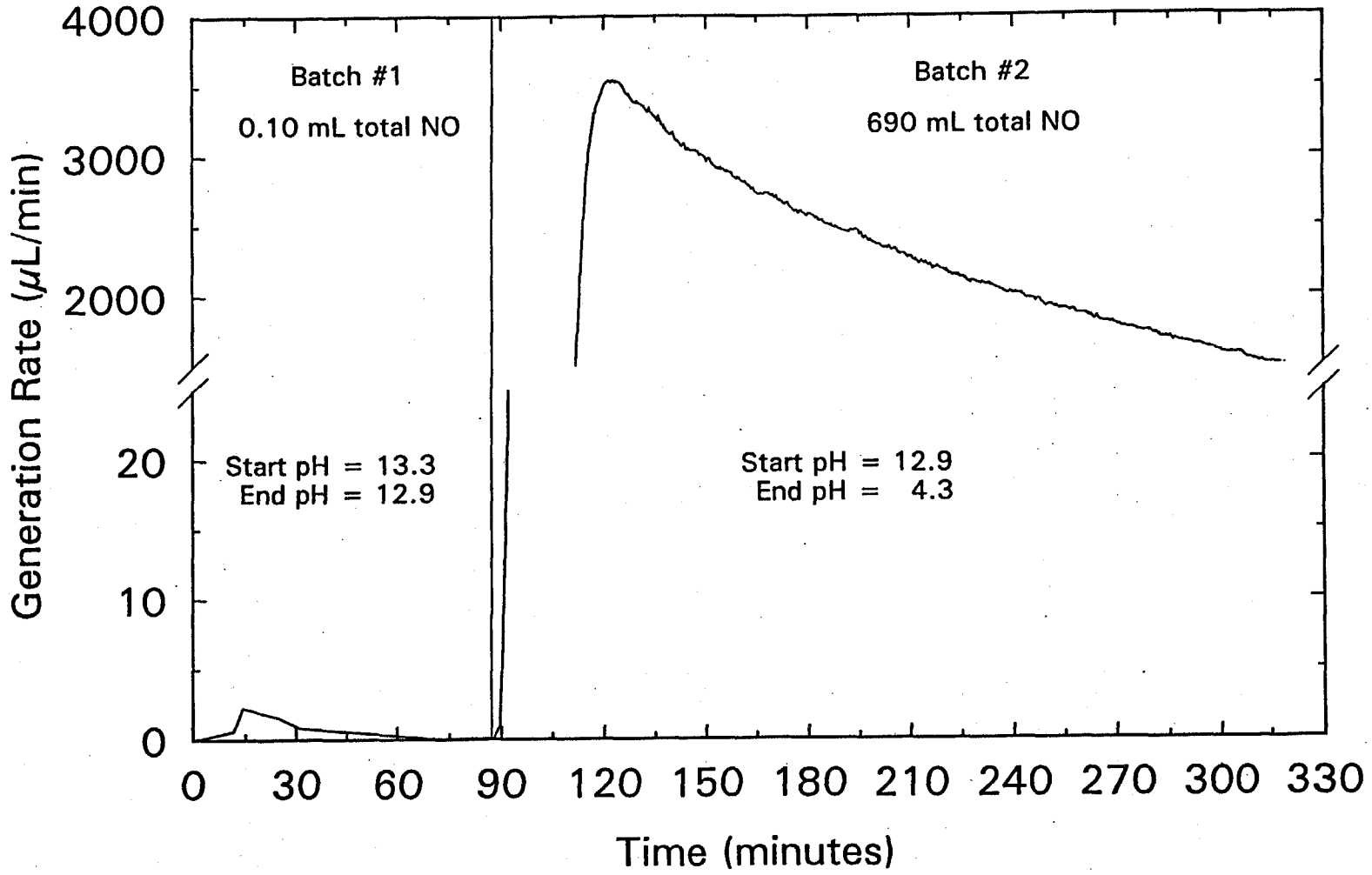

Figure C.51. Supplemental Test 28. Because no NaOH was added during Batch #1, the pH dropped far too low in Batch #2 giving rise to a very large amount of NO gas. See Figure C.50 for different plot of same data.

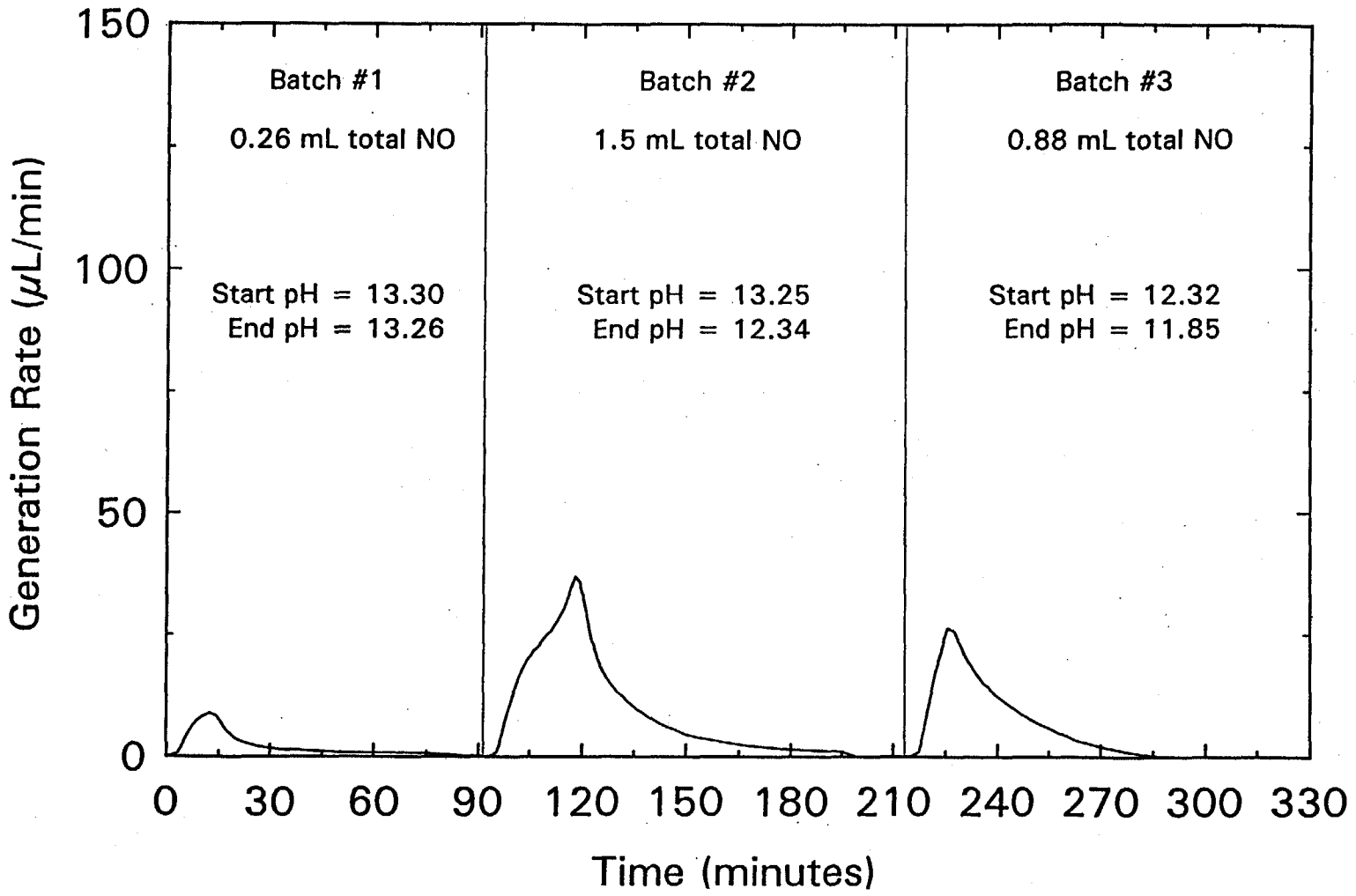

Figure C.52. Supplemental Test 26½. Similar to Tests 27 and 27A, Figures C.49 and C.53, except that only half the amount of $NaNO_2$ was added at the beginnings of Batches #2 and #3.

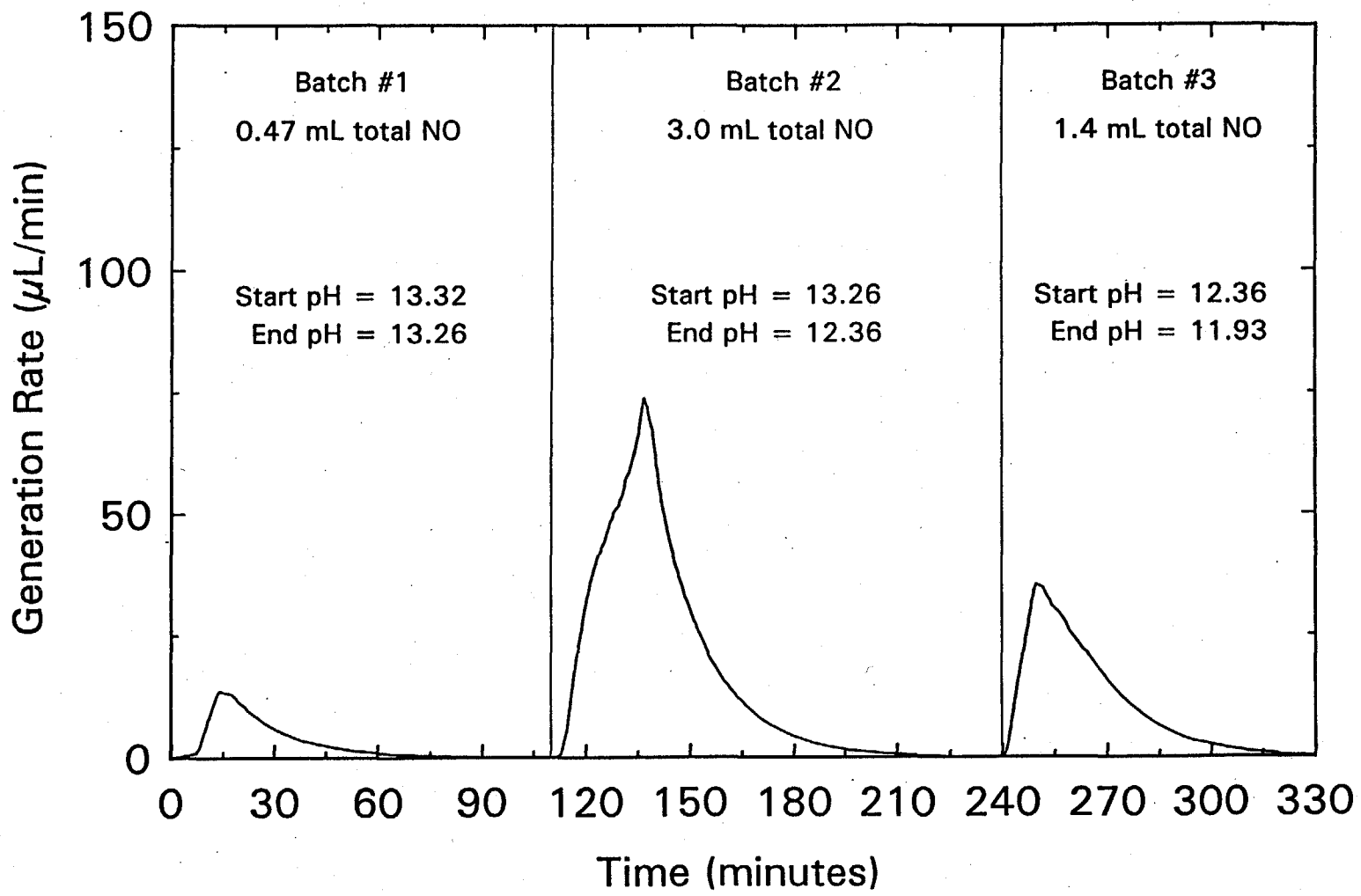

Figure C.53. Supplemental Test 27A. This was a duplicate of Test 27, Figure C.49. However, the pH didn't drop as low as in Test 27, and the amount of NO gas produced is thought to be more representative of this test condition.

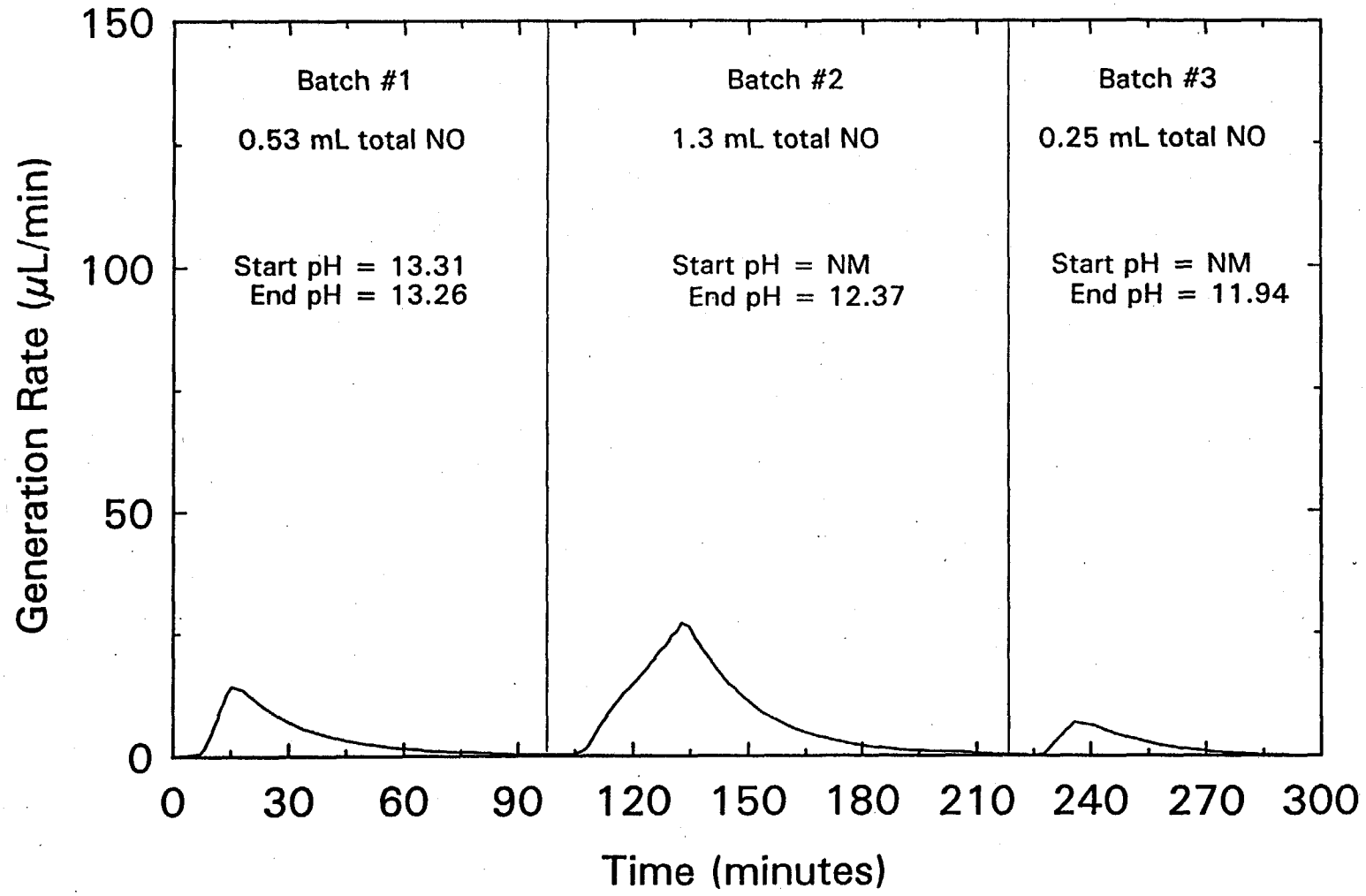

Figure C.54. Supplemental Test 29. This was essentially a duplicate of Test 26, Figure C.48, except that the starting NO_2^- concentration in the PUREX was slightly higher.

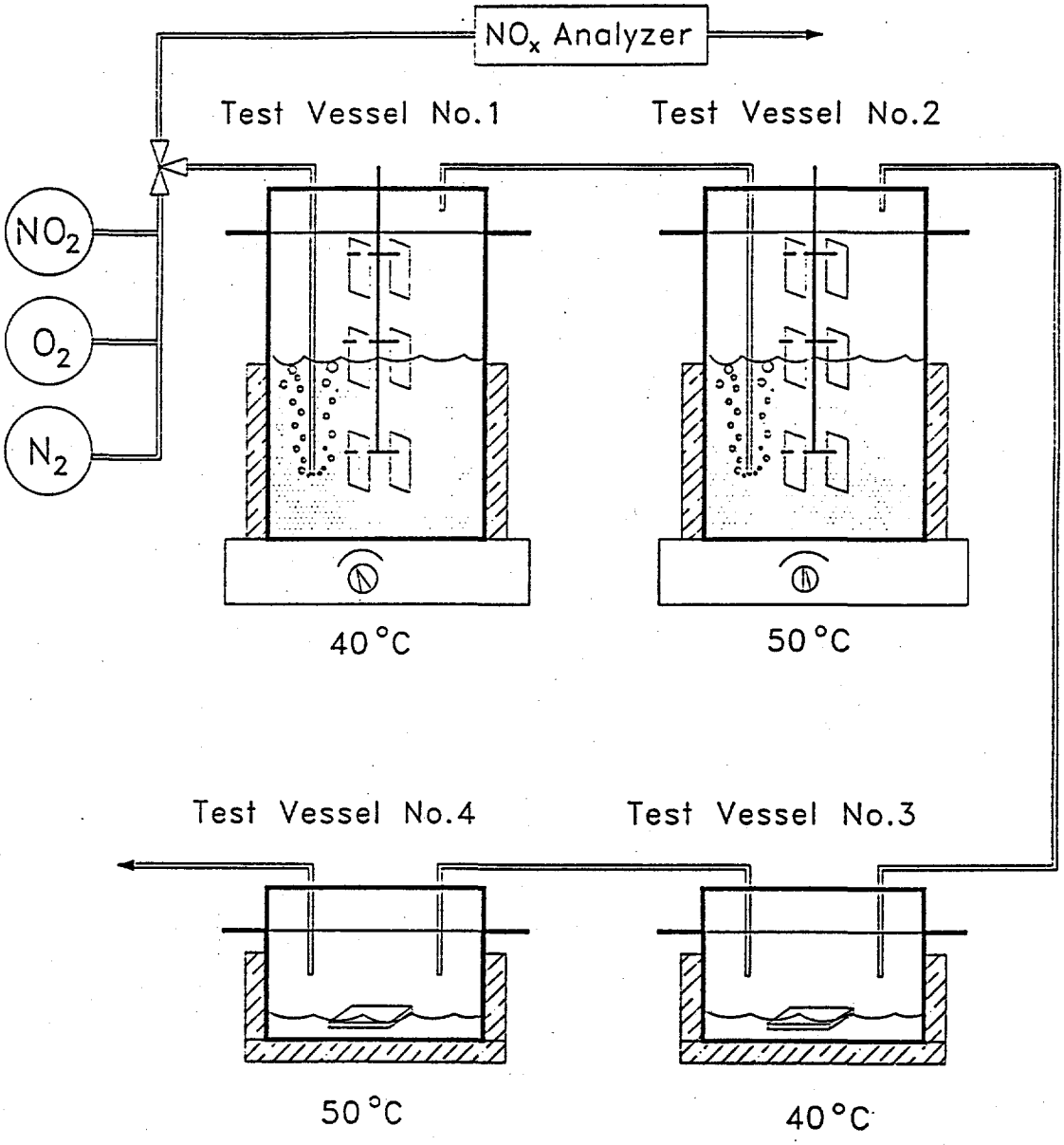

Figure C.55. Sketch of NO_X Corrosion Test System Configuration

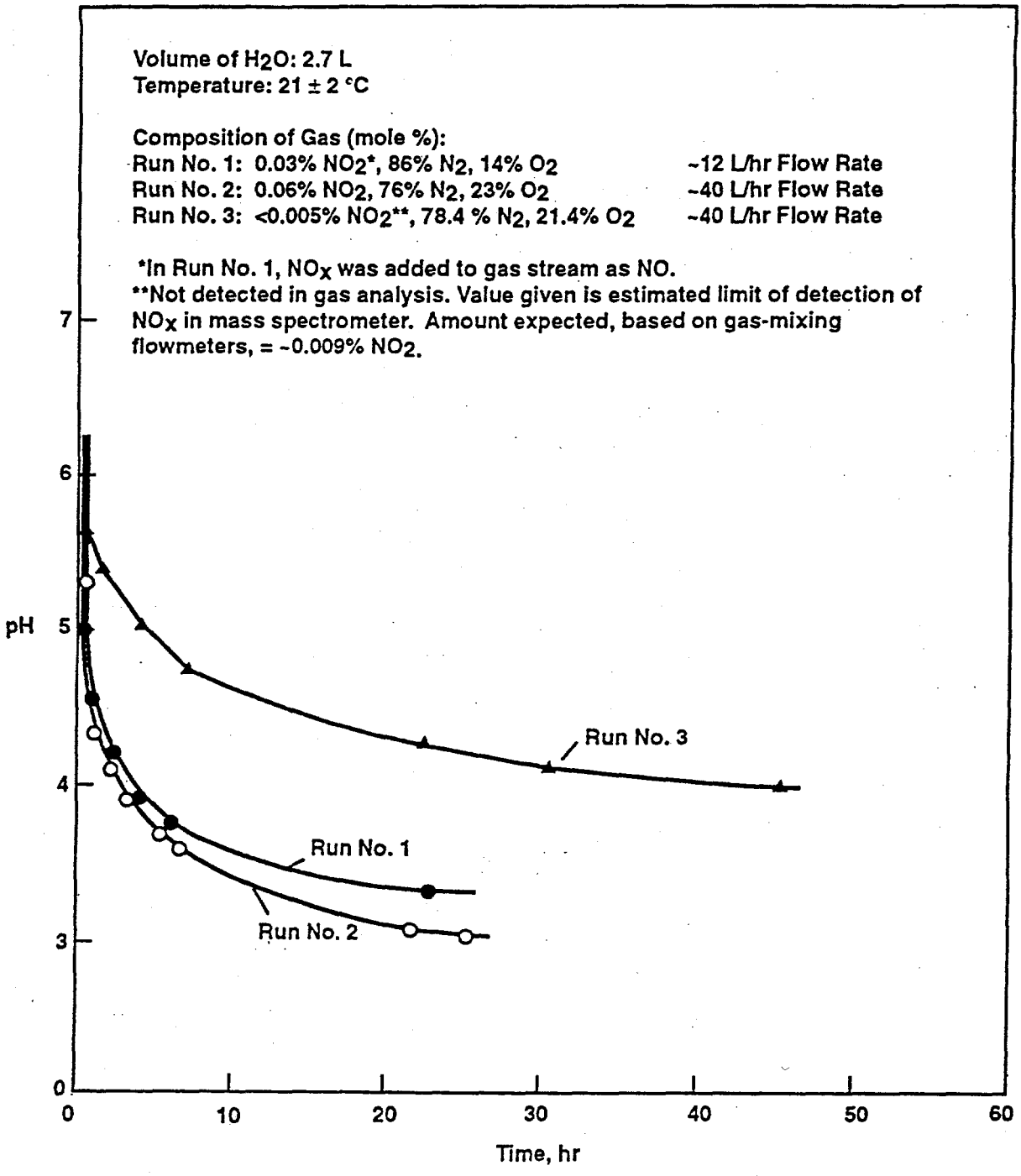

Figure 56. Solution pH as a function of NO_2 Purge Conditions

Distribution

No. of Copies

Offsite

12 **DOE/Office of Scientific and Technical Information**

T. Evans
U.S. Department of Energy (HQ),
EM-55
12800 Middlebrook Rd., SU400
Germantown, MD 20874

10 West Valley Nuclear Services Co., Inc.
P.O. Box 191
West Valley, NY 14171-0191
ATTN: S. M. Barnes (3)
R. E. Lawrence
J. L. Mahoney
D. C. Meess
M. A. Schiffhauer (3)

2 DOE/West Valley Area Office
P.O. Box 191
West Valley, NY 14171-0191
ATTN: J. J. May
W. F. Hamel

Onsite

3 **DOE Richland Field Office**

S. T. Burnum, S7-53
D. D. Button, S7-53
J. C. Peschong, S7-53

No. of Copies

4 **Westinghouse Hanford Company**

R. L. Gibby, H5-27
R. L. Gilchrist, L5-63
W. O. Greenhalgh, L5-31
R. W. Powell, G3-21

34 **Pacific Northwest Laboratory**

G. H. Beeman, S7-71
N. G. Colton, K3-75
J. M. Creer, K9-80
R. E. Einziger, P7-14
M. L. Elliott (3), P7-41
W. J. Gray (10), P7-14
B. M. Johnson, K9-70
L. A. Mahoney, K7-15
E. V. Morrey, P7-19
J. M. Perez, P7-41
H. D. Smith, P7-14
R. E. Westerman (5), P8-44
K. D. Wiemers, P7-14
Publishing Coordination
Technical Report Files (5)